University of Stavanger

FACULTY OF SCIENCE AND TECHNOLOGY

MASTER'S THESIS

Study programme / Specialization: Petroleum Engineering / Reservoir Engineering	Spring semester, 2018 Open access
Author: Bente Hetland	…… (signature of author)
Supervisor(s): Tina Puntervold and Skule Strand	
Title of master's thesis: Smart Water injection into sandstone reservoir for EOR – Optimal mineral sample preparation and influence of feldspar minerals.	
Credits: 30	
Keywords: Smart Water EOR in Sandstone reservoirs Feldspar Microcline Anorthite Optimal mineral preparation Wettability Adsorption	Number of pages: 95 + enclosure: 40 Stavanger, 15. June 2018

Acknowledgement

First, I would like to express my sincere gratitude to my supervisors Tina Puntervold and Skule Strand for letting me be a part of the Smart Water EOR team. For presenting me the thesis, and your guidance and motivation trough the progress. For sharing your professional knowledge and expertise. For always having an open door. It has been both inspiring and educational to cooperate with you and I feel truly honoured to have been a part of your team.

Then, I would like to thank PhD-student Alexandr Mamonov, for all hours you have spent assisting me and guiding me in the lab. For your incredible expertise and knowledge, and inspiring conversations. It has been a privilege to work with you. And student assistent Amalie Harestad, you are truly the best assistant one could ask for. Thank you for making every day fun and for sharing your expertise.

I would also like to thank all the students and all the people that has been working at the lab. For our great conversations, for your smiles, for your humour and for making the lab a great place to be.

An lastly, to my family, Thank you for your love, patience and encouragement during the writing of this thesis.

Abstract

Smart Water is an injection brine that has been modified and designed for inducing wettability alteration to increase oil recovery in a reservoir. It is an cost effective and environmentally friendly EOR method that can be easily implemented both in secondary and tertiary production phases. Smart Water EOR in sandstone reservoirs are highly complex due to chemical interactions in the crude oil-brine-rock system. Sandstones are a mixture of several minerals, each contributing with different reactivity and behaviour dependent on pH, salinity, temperature and pressure. To optimize the Smart Water design, great understanding of the initial wetting in the reservoir and the wettability alteration during a Smart Water flood is important. Feldspars have shown to influence pH in a reservoir system, which could impact both the initial wetting in a reservoir and the wettability alteration when Smart Water is injected. Polar organic components can be adsorbed to a clay surface and influence initial wetting.

To study the influence of feldspar minerals regarding initial wetting static adsorption tests were made. For a wettability alteration to take place, initially adsorbed polar organic components must be desorbed from the mineral surface. This adsorption / desorption is controlled by an increase in pH. Feldspars influence on pH and dependence on salinity were studied from static pH screening tests and IC analysis. Previous studies at the University of Stavanger have shown that the preparation of the feldspar mineral samples greatly can influence the adsorption results. To optimize the mineral samples new milling equipment has been used in the preparation process. Adsorption studies have been conducted on two feldspar minerals; microcline and anorthite, using both high salinity (HS) and low salinity (LS) brine at ambient temperature conditions. Static pH screening studies have been conducted at ambient temperature for the anorthite sample, using NaCl brines with different salinities.

The results from the adsorption studies are in line with previous findings. Feldspars are capable of adsorbing some polar components onto the surface, however it was not possible to quantify their adsorption behaviour or dependence on pH and salinity in detail due to varying results that did not show any trends. The only conclusion that can be made is that there is some adsorption and that the adsorption is generally low.

The optimized feldspar samples did not manage to provide representative adsorption results, but managed to produce stable results in the pH screening test. A major difference between the two tests is the addition of the organic phase in the adsorption tests. The combination of three phases (polar organic component-brine-mineral) made the system chemically complex and added extra uncertainty. This resulted in varying and unstable adsorption results. Static pH screening tests and IC analysis of anorthite verified that feldspar is influencing pH in a system through cation exchange at that this is dependent on salinity.

Further work is needed to optimize mineral samples, as they are an important part in continued analysis in understanding feldspars contribution both regarding initial wetting and in a Smart Water flooding for EOR. The preparation of minerals are the first of many steps in the adsorption studies, and have shown to be very important. Especially the PSD of the mineral sample will greatly influence the reactivity of the feldspars, and needs to be controlled. Bad preparation results in non representative static results which could cause misleading conclusions in dynamic studies.

List of Abbreviation

μ	Viscosity
ρ	Density
θ_c	Contact angle
C	Concentration
E_m	Microscopic sweep efficiency
E_{MA}	Macroscopic sweep efficiency
g	Gravitational constant
h	Height
I	Ionic Potential
k_{ro}	Relative permeability oil
k_{rw}	Relative permeability water
m	Mass
Mm	Molarity
n	mole
P_c	Capillary Pressure
r	radius
S_{wi}	Initial water saturation
t	Time
V	Volume
v	Velocity
Z	Ion Valency
ABS	Absorbance
AN	Acid Number
BET	Brunauer-Emmet-Teller
BN	Base Number
CBR	Crude oil-Brine-Rock
CEC	Cation exchange capacity
DI	Deionized water

EOR Enchanced Oil Recovery

FW Formation water

HS High Salinity

HSQ HS brine-quionline solution

HTHP High Temperature High Pressure

IC Ion Chromatography

IOR Improved Oil Recovery

LS Low Salinity

LSP Low salinity polymer

LSQ LS brine-quionline solution

LSS Low salinity surfactant

MIE Multi Ion Exchange

ppm Parts per million

PSD Particle Size Distribution

Q Quinoline

RDR Real dilution rate

rpm rounds per minute

RSD relative standard deviation

SEM Scanning Electron Microscope

TDS Total Dissolved Solids

USBM U.S. Bureau of Mines

Contents

List of Figures

List of Tables

1 Introduction

As global oil demand rises and the search for hydrocarbon reserves are moving into more inhospitable environments, the need for generating innovative enhanced oil recovery (EOR) techniques to keep the oil flowing increases. Sustainable and cost-effective EOR solutions that can extract between 30 to 60 % additional oil from a reservoir compared to primary or secondary recovery techniques are needed for producing oil that usually is left behind. This additional recovery will increase the oil flow substantially, as only about 35 % of the oil in place is extracted globally leaving huge natural sources untapped (Turner, 2012).

Water flooding of oil reservoirs has long been performed for pressure support and for oil displacement. The water is usually following the higher permeable zones, or fractures, from the injector to the producer, also influenced by the initial wetting preference of the rock surface. Introducing a water (e.g. Smart Water) that is different from the formation water into the reservoir will disturb the established chemical equilibrium and interactions will take place between the oil, water and rock. Research has shown that the injected water composition may be modified to alter the wettability of the rock towards a more water-wet state. thus creating positive capillary forces, and water can move into previously unswept pores and improve oil recovery due to improved sweep efficiency.

Sandstone is a very heterogeneous and complex material consisting of many different minerals which contribute with different reactions towards polar components. To understand how sandstones behave regarding initial wetting, it is important to identify the different roles of different minerals. Clay is considered the main wetting mineral in sandstone reservoirs (Austad et al., 2010). Feldspars could contribute both regarding initial wetting and wettability alterations, depending on the salinity of the formation water (Reinholdtsen et al., 2011; Strand et al., 2016). The Smart Water EOR group at the University of Stavanger, consisting of several researcher and students, are developing methods for confirming the chemical mechanism of wettability alteration in reservoirs as stated by Austad et al. (2010). Abdullah (2016) conducted adsorption tests of polar basic organic components onto feldspars to study the effect of feldspars on initial wetting in a reservoir. The results were unstable with large variations in adsorption values, figure 1. To identify the source for the unstable results she performed several error studies on the samples and it was concluded that the particle size distribution (PSD) was too heterogeneous and had to be improved. She managed to improve her results with a sedimentation procedure that removed small particles from the mineral sample.

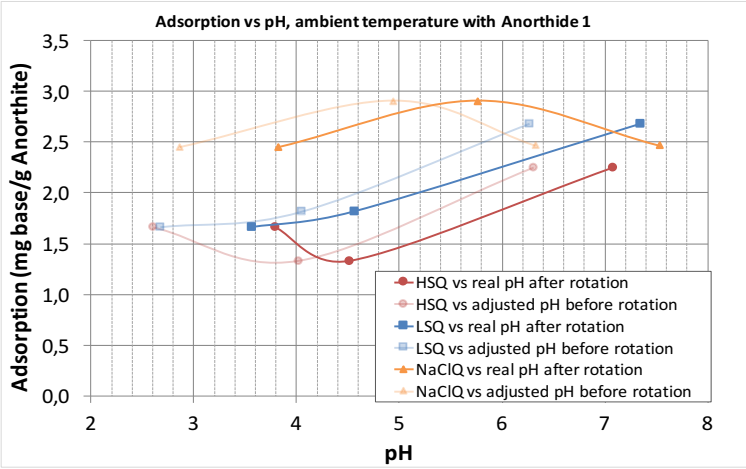

Figure 1: Adsorption of polar basic organic components onto anorthite, 24 hrs ripening (Abdullah, 2016)

Harestad (2017) and Tat (2017) continued the work done by Abdullah (2016) using the same milling equipment combined with a sedimentation procedure and included different ripening processes. Their results showed very little adsorption of polar components onto the feldspars, but still there were too large variations in the results to draw any conclusions, figure 2 and figure 3.

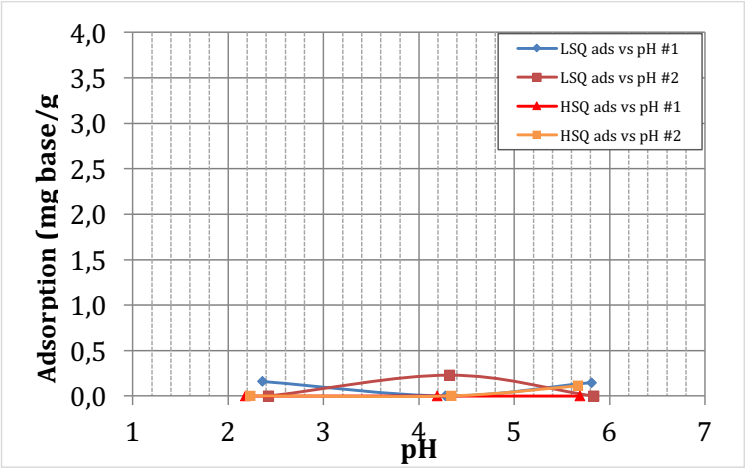

Figure 2: Adsorption of polar basic organic components onto microcline, 24 hrs ripening (Harestad, 2017)

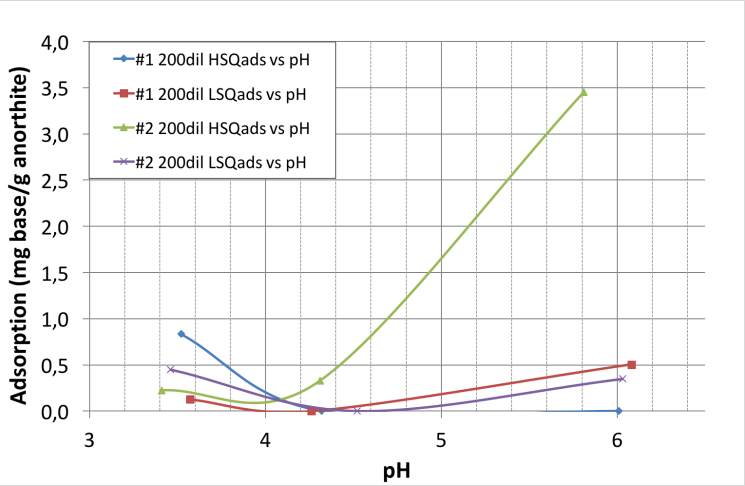

Figure 3: Adsorption of polar basic organic components onto anorthite, 24 hrs ripening (Tat, 2017)

Previous experiments have shown that the preparation of feldspar minerals are affecting the results (Andersen, 2015; Abdullah, 2016; Harestad, 2017; Tat, 2017; Algazban, 2017) . Adsorption tests showed large dependence on the preparation procedure. This was the motivation for improving the mineral preparation which has been done by introducing new milling equipment that are capable of preserving the crystal lattice of the minerals. It has been attempted to find a balance between particle sizes, surface area and homogeneity. The particles should not be too small or heterogeneous, and the surface area should not be too high. A long milling time will produce very small and homogeneous particles, but it will also increase the surface area of the sample. A shorter milling time produce a heterogeneous sample, with a larger range of particle sizes and a smaller surface

area. Optimal mineral samples generate representative and reliable results, which is crucial in understanding the contribution from feldspar minerals to Smart Water EOR in sandstone reservoirs.

1.1 Thesis objective

The objective of this thesis is to investigate how the feldspar minerals contribute to Smart Water EOR in sandstone reservoirs.

Several attempts have been performed at the University of Stavanger to study feldspars influence on initial wetting and wettability alterations. Static adsorption and pH screening tests have been conducted and all have shown the importance of proper mineral preparation in feldspar analysis. Feldspars are highly reactive in the presence of water, and the reactivity is dependent on the particle size distribution (PSD) of the mineral. Small particles react stronger than large particles and a heterogeneous PSD will give unreliable results.

Especially the adsorption studies have revealed large variations in the results, which is the main motivation for improving the mineral preparation. A representative mineral sample is crucial for getting representative results in further analysis, and has therefore been the main objective in this thesis. Second objective is to perform reliable static adsorption tests of quinoline onto feldspar minerals and static pH screening tests, which only will be possible if the mineral sample is properly prepared. In a proper preparation a balance between homogeneous PSD, BET surface area and preservation of crystal lattice is maintained. Optimal sample preparation is important for generating representative results, and new milling equipment will help achieve this.

Thesis objectives can be summarized:

1. Optimal mineral preparation on feldspar minerals by using new milling equipment.
2. Perform reliable static adsorption tests of polar basic organic components onto feldspars to study influence on initial wetting.
3. Perform reliable static pH tests on feldspar to study how feldspar affects pH at different salinities.
4. Study the contribution of feldspars in Smart Water EOR, both regarding initial wetting and wettability alteration.

2 Theory

2.1 Hydrocarbon Recovery Mechanisms

Most oil and gas reservoirs are under pressure and hydrocarbons will flow up through the well and to the surface when a well penetrates a reservoir. Such reservoirs are self producing for short period of time, only relying on the work done by the reservoir, but as oil is produced, the pressure will fall rapidly. This rapid decline is especially fast in oil reservoirs where oil and water are more or less incompressible. A gas reservoir can maintain pressure for a longer period due to the high compressibility of gas, creating a so called gas-drive. Large oil reservoirs can maintain pressure if there is an aquifer maintaining the pressure in the reservoir by water flowing into the reservoir replacing the produced oil. This is called water-drive. Production from a reservoir without any water-drive or gas drive is greatest at production start and then declines asymptotically towards zero. To maintain pressure and thus production, water or gas can be injected through injection wells. Such recovery mechanisms only relying on natural drive are called secondary recovery methods. Methods involving changes in the internal properties of the reservoir have historically been referred to as tertiary methods. However, since tertiary methods can be used prior to or instead of secondary, they are more often referred to as enhanced oil recovery methods (EOR). (Green, 1998)

2.1.1 Primary recovery

Primary recovery results from the use of natural energy present in a reservoir as the main source of energy for the displacement of oil to producing wells. Drive mechanisms for the natural energy sources are solution-gas drive, gas-cap drive, natural water drive, fluid and rock expansion, gravity drainage and a combination of these. Due to a rapid pressure decline in the reservoir only 10 - 30 % of the original oil in place (OOIP) is produced (Green, 1998).

2.1.2 Secondary recovery

Normally a secondary recovery by waterflooding is implemented at an early stage of primary production to avoid depletion of reservoir energy. Secondary recovery results from the augmentation of natural energy through injection of water or gas to displace oil toward producing wells. Gas can be injected into a gas cap for pressure maintenance and gas-cap expansion or into oil-columns. If the gas is injected into oil-columns, the oil is displaced immiscible. This immiscible displacement is inefficient compared to a waterflood and therefore used infrequently as a secondary recovery process. Today, most secondary recovery processes are synonymous to water injection. The main reasons for performing a water flood is (1) to give pressure support and (2) displace the oil by water by viscous forces. Although a waterflood are capable of mobilizing and displacing a certain amount of oil, most of the oil will remain in the reservoir. There could be several reason for this, amongst them are: (1) As water will follow the easiest path through a reservoir, a large part of the reservoir remains unswept by a waterflood. (2) The viscosity of water will be low compared to the viscosity of oil, creating an unfavourable mobility ratio. In both cases, water will break through before the oil, producing water and leaving the oil behind. (Green, 1998)

2.1.3 Tertiary recovery / EOR

Methods that involve changes in the internal properties of the reservoir by injection of miscible gases, chemicals, modified waters and/or thermal energy to displace additional oil are defined as tertiary recovery or enhanced oil recovery methods. The purpose of the injected agents is to induce

new mechanisms for displacing oil (Baviére, 1991). EOR methods are often implemented when a secondary recovery process has become uneconomical, but it can also be implemented prior to or instead of a secondary recovery process. Main EOR methods include (Bjørlykke, 1989):

1. Thermal processes. Injection of steam to increase temperature of the oil and thus lower the viscosity. Steam injection must be repeated at regular intervals to maintain low viscosity as the reservoir starts to cool off. Only used for highly viscous oils, i.e. heavy oils.
   (a) Steam injection
   (b) In situ combustion
2. Chemical processes. Injection of chemicals into the reservoir. For an oil to be mobile it must overcome the capillary forces involved in a two-phase flow. The capillary forces can be reduced by reducing the surface tension between the injected water and the oil in place.
   (a) Surfactants, reducing surface tension in water phase and thereby changing wettability. An oil wet system can be altered into a more water-wet system, which increases the mobility and the relative permeabilty of the oil. Drawback: chemicals can easily be adsorbed to the reservoir rock, particularly onto clay minerals due to its high ion exchange and adsorption capacity and its huge surface area. A pre-flush with other reactive chemicals are often injected to prior to injection of surfactants. These will react with the mineral surface and prevent surfactants from being adsorbed when they are injected.
   (b) Polymers, increase viscosity of the injected water creating a piston like displacement of the oil. Oil reservoirs with high relative water permeabilty tend to have low recovery percent as the oil is difficult to produce. Water have low viscosity compared to oil and will flow in the direction with least resistance, e.g. along cracks. By adding a polymer to the injection water, the mobility of the water is reduced and viscosity is increased. This creates a piston like displacement capable of pushing more oil droplets ahead. Drawback: polymers tend to adsorb onto the mineral surface and thus the effect decreases with the distance from the injection well.
   (c) Alkaline flooding, reducing surface tension of aqueous phases making the reservoir more water wet and thus increase oil production. This method is commonly used in sandstone reservoirs.
3. Injection of gas to increase miscibility of the hydrocarbon phases
   (a) CO_2 is gaseous at reservoir conditions and soluble in oil. By injecting CO_2 into the reservoir, the gas is dissolved into the oil, making it less dense and viscous and and also expanding the oil. This makes the oil more mobile and creates a gas drive.
   (b) N_2
   (c) Hydrocarbon gases

Several emerging EOR processes have been developed in recent years (Piñerez Torrijos, 2017):

- Smart Water
- Low salinity water flooding
- Carbonated waterflood

- Microbial EOR
- Enzymatic EOR
- Electromagnetic heating
- Surface mining and extraction
- Nano particles

2.2 Wettability

Wettability is defined as the tendency of one fluid to spread or adhere to a surface in the presence of another immiscible fluid. At reservoir conditions, the FW and crude oil interactions with the rock surface will dictate the initial rock wettability A reservoir rock can be roughly characterized in terms of its wetting conditions, preferential water-wet, oil-wet and neutral wet. At oil-wet conditions, the oil is more strongly bound to the mineral surface than water. At water-wet conditions the water is more strongly bound to the mineral surface. Wettability is a key factor in determining the success for waterflood. It influences the location, distribution and flow of fluids present in the reservoir in addition to dictating the capillary pressure, P_c, and relative permeability of oil and water, k_{ro} and k_{rw}, for a two phase flow (Green, 1998; Anderson, 1986; Puntervold, 2008; Austad, 2013).

For oil-water-solid systems in static equilibrium, the degree of wettability is expressed as a function of the angle measured through the denser phase (Piñerez Torrijos, 2017). Static equilibrium is defined by Young's equation 1:

$$\sigma_{os} = \sigma_{ws} + \sigma_{ow} cos\theta \tag{1}$$

where

θ is the contact angle measured through the denser phase

σ_{os} is the oil-solid interfacial tension

σ_{ow} is the oil-water interfacial tension

σ_{ws} is the water-solid interfacial tension

Contact angle θ_c separates the different phases into water-wet, neutral-wet and oil-wet systems, figure 4

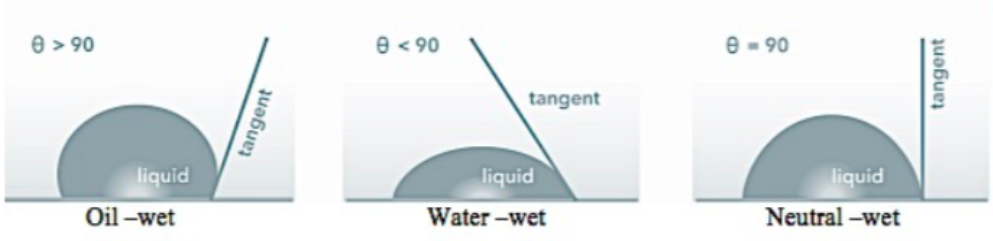

Figure 4: Contact angle for different wetting (Abdullah, 2016)

Classification of the wettability is a function of the contact angle measurements, table 1.

Table 1: Wettability in terms of contact angles

Contact angle [degrees]	Wettability preference
0-30	Strongly water-wet
30-90	Water-wet
90	Neutral wettability
90-150	Oil-wet
150-180	Strongly oil-wet

2.2.1 Wettability measurement

Wettability can be determined from both qualitative and quantitative methods. Quantitative methods involve direct methods where wettability is measured on a representative rock sample using reservoir fluid. Examples of quantitative methods are: contact angle measurements, Amott test (spontaneous imbibition and forced displacement) and U.S. Bureau of Mines (USBM) method. Qualitative methods include: imbibition rates, microscope examination, flotation, glass slide method, relative permeability curves, permeability/saturation relationships, capillary pressure curves, capillarimetric method, displacement capillary pressure, reservoir logs, nuclear magnetic resonance and dye adsorption (Anderson, 1986). Strand et al. (2006) developed a new method for measuring wettability in carbonates using chromatographic wettability test.

2.3 Displacement Forces

Different displacement forces are acting in a EOR process, and can be divided into different scales. In the macroscopic scale, reservoir heterogeneity and gravity forces influence the effectiveness of displacing the fluids in contacting the reservoir in a volumetric sense. At microscopic scale, the displacement efficiency is on pore scale, affected by parameters like wetting and interfacial tension.

2.3.1 Macroscopic and Microscopic sweep efficiency

Macroscopic sweep efficiency, (E_{MA}), relates the effectiveness of the displacing fluids in contacting the reservoir in a volumetric sense. It measure how efficient the displacing fluid sweeps out the oil of a reservoir, areal and vertical. Efficiency of displacement is affected by the mobility ratio of the fluids, permeability, geometry and communication between layers.

Microscopic sweep efficiency, (E_m) relates the displacement or mobilization of oil at pore scale. E_m is a measure of the effectiveness of the displacing fluid in mobilizing the oil at those places in the rock where the displacing fluid contacts the oil. It is a ratio between mobile and the oil present (Green, 1998).

2.3.2 Capillary Forces

Capillary forces are the major driving forces in fluid flow in a porous media. Capillary pressure is the difference in pressure between two immiscible fluids and is defined by equation 2 (Green, 1998)

$$P_c = P_{NW} - P_W = \frac{2\sigma cos\theta}{r} \tag{2}$$

where

P_c is the capillary pressure [Pa]

P_{NW} is pressure of non wetting fluid [Pa]

P_W is pressure of wetting fluid [Pa]

σ is the interfacial tension [N/m]

θ is the wetting angle [degree]

r is the radius [m]

2.4 Waterchemistry

Water (H_2O) consists of one oxygen atom and two hydrogens, which are held together by hydrogen bonding. This structure gives water a lot of great properties (Bjørlykke, 1989):

- Water is a great solvent for polar substances
- Water has high surface tension which enables transport of particles and organisms to its surface.
- The high surface tension makes it possible for capillary forces to draw water up through thin capillary pores.

2.4.1 Ionic potential

Ionic potential describes the distribution of the elements in sediments and aqueous systems. Ionic potential can be defined by equation 3

$$I = Z/r \tag{3}$$

where

Z is the valency of an ion in solution

r is the radius of the ion

Ionic potential gives an expression of the charge on the surface of an ion, i.e. its capacity for adsorbing ions. Large ions with small charge have a low ionic potential, while small ions with high charge have a high ionic potential. This means that in an aqueous solution with ions with small ionic potential, the O-H bonds in the water will not be broken, and the ions will remain in solution as hydrated cations surrounded by water molecules with negatively charged dipole towards the positive ion. If the cation - oxygen bond is approximately as strong as the hydrogenbond, the cation ion can replace a hydrogen atom and then hydroxides are formed. $Al(OH)_3$ is an example of an hydroxide formed by a metal ion replacing a hydrogen atom. Such hydroxides tend to have very low solubility. Ions with a high ionic potential form stronger bonds with oxygen than O-H bond, and form soluble anion complexes which releases H^+ into the solution. During weathering of minerals, the ions with small ionic strength remains in solution together with anionic complexes of metals and non-metals with high ionic potential. (Bjørlykke, 1989)

2.4.2 Hydrolysates

Hydrolysates are sediments that are rich in the least soluble weathering products, e.g. metal cations in the form of oxides or hydroxides. When a metal ion with low ionic potential is surrounded by water molecules, its chemical properties and the ability to form part of a crystal structure are strongly affected. Metals with intermediate ionic potential, $Mg^{2+}, Fe^{2+}, Mn^{2+}, Li^{+}, and\ Na^{+}$ are the ones that are most strongly hydrated. The surrounding water molecules will occupy a certain radius around the ions, called "hydrated radius", and thus prevent the ion from participate in other reactions. The hydration potential and hydration radius affects the solubility of different ions. As an example, Na^{+} is most soluble in seawater and therefore only slightly adsorbed by other minerals like clays. K^{+} has large ionic radius and will therefore not be attracted as strongly to adjacent water molecules. The surface charge of these ions will be more effective and they will be more easily adsorbed to a negatively charged surface. Therefore there are much more Na^{+} present in seawater compared to K^{+}, because more K^{+} will be adsorbed and involved in various reactions and thus removed from the solution. Larger ions with smaller ionic potential are least hydrated and can therefore more easily be adsorbed onto different surfaces. Mg^{2+} has a higher ionic potential than Ca^{2+}, and as a consequence Mg^{2+} will be more strongly hydrated. Thus Mg^{2+} is more likely to stay in solution than Ca^{2+}, which is more easily adsorbed to a surface. As a result there are 5 times as many Mg^{2+} ions in seawater than Ca^{2+}. Despite a higher ratio of Mg^{2+} in seawater, calcium carbonate is the first to precipitate. This is because of the Mg^{2+} is more strongly hydrated and thus prevented from participate in mineral forming reactions. Without the water molecules surrounding the ion, the story would be different. Mg^{2+} has a greater ionic potential and therefore would precipitate more easily. Temperature also affects the hydration. If the temperature increases the ions will be less hydrated. As a result magnesium carbonates are typically found at higher temperatures, $80 - 100°C$. (Bjørlykke, 1989)

2.4.3 Acid-Base behaviour

Brønsted defined acids and bases as species which can supply or accept a proton. Lewis defined acids and bases as species which can accept or donate an electron pair. Thus a proton from a surface hydroxyl can donate or accept a proton, and a transition metal with two accessible valence states can transfer electrons. Water can act as a Lewis base to a surface oxygen and thereby transferring a charge. (Smith, 1994)

2.4.4 pH

pH is defined as the negative logarithm of the hydrogen ion concentration and is a measure of the concentration of H^{+} in the solution. The activity of hydrogen ions are controlled by the acidity or alkalinity of the solution.

$$pH = -log_{10}[H^{+}] \tag{4}$$

The ionisation product of water is defined by equation 5

$$[H^{+}] \cdot [OH^{-}] = 10^{-14} \tag{5}$$

The ionisation product varies with temperature, which means that temperature should be considered when evaluating pH. Neutral water at 25°C has a proton and base concentration of 10^{-7}, which means it has a pH of 7. Solutions with more protons than base components are called acidic solutions, and have a pH between 1 and 7. While solutions with higher concentration of base components have pH 7-14. Acidic solutions provide hydrogen ions to replace cations in the mineral lattice and are effective agents of hydrolysis. (Bjørlykke, 1989; Prothero and Schwab, 2004)

2.4.5 Equilibrium constants

A chemical reaction can be described by equation 6

$$A + B = C + D \tag{6}$$

where the left hand side are referred to as the reactants (A and B) and the right hand side are the products (C and D). The equal sign suggests that the reaction proceeds in both directions with equal speed. Normally this is not the case, the reaction will occur at a higher rate in one direction compared to the other, it can also go completely in only on direction. The relative speed is shown by using arrows of different sizes pointing in different directions. To determine which way the reaction is more likely to go the equilibrium constants should be determined. If the reaction is going from left to right, the equilibrium constant are defined by equation 7

$$k_1 = \frac{[C][D]}{[A][B]} \tag{7}$$

If the reaction is going in the reverse direction a second equilibrium constant can be determined from equation 8

$$k_2 = \frac{[A][B]}{[C][D]} \tag{8}$$

The two reactions occur simultaneously but at different rates. If $k_1 > k_2$ the reaction will proceed from left to right, while it will proceed in the opposite direction if $k_1 < k_2$. An overall equilibrium constant k, are defined by equation 9

$$k = \frac{k_1}{k_2} \tag{9}$$

(Prothero and Schwab, 2004)

2.4.6 Precipitation and dissolution

Dissolution of minerals affects the chemical composition of natural waters. Precipitation of minerals and the subsequent sedimentation of these solids from supersaturated solutions alter the chemical composition of natural waters. Solubility of a mineral depends on the particle size and the degree of crystallinity. Ions that are dissolved into solution from solid may undergo further reactions in solution (Prothero and Schwab, 2004).

2.5 Reservoir Rock

A profitable reservoir rock is a rock where hydrocarbons have accumulated. These rocks are usually sandstones or carbonates. (Prothero and Schwab, 2004) A good reservoir rock has high porosity and permeability, and a thickness and volume sufficiently to hold large quantities of oil. The primary porosity of the reservoir rock must be well preserved prior to oil migration for the rock to hold any oil and the reservoir rock must be within reach for the hydrocarbons migrating from the mature source rock. To prevent the hydrocarbons escaping the reservoir, a cap rock must overlay the reservoir rock providing a non permeable seal. (Bjørlykke, 1989; Zolotuchin, 2000) A reservoir rock can be divided into two main rocks; carbonates and sandstones. The different rocks have different properties, and depending on the type of reservoir, one expect different behaviour.

2.5.1 Porosity

Porosity is the ratio between void volume to the total rock volume. The volume unoccupied by grains and minerals can hold and transport fluids like water, gas and oil. One distinguish between effective porosity and total porosity. Effective porosity accounts for connected pore space in the rock, and total porosity is a measure of the total pore space in the rock. Porosity is controlled by several factors, amongst them are :

- rock type
- grain size
- grain packing
- orientation of grains
- cementation
- weathering

Porosity can be classified according to its origin from geological processes; (1) primary porosity and (2) secondary porosity. Primary porosity is porosity initially developed during sedimentary deposition while secondary porosity is the resulting porosity after primary porosity have been altered through processes such as fracturing, dolomitization and dissolution (Zolotuchin, 2000).

2.5.2 Permeability

Permeability is the ability of a rock to transmit fluid. A rock with high permeability represents better transmission of fluid through a rock than for a rock with poor permeability (Zolotuchin, 2000).

2.6 Mineralogy of Sandstone Reservoirs

Sandstone is an important reservoir rock, making up 80 % of global reservoirs and 50 % of the global reserves. Sandstones are siliciclastic sedimentary rocks. They are termed siliciclastic because they are almost exclusively silica-bearing rocks, either by quartz or other silicate minerals. Clastic sediments consist of fragments and minerals from older rocks and authigenically formed minerals.

The diameter of the sand grains are typically in the size range of 0.0625 mm to 2 mm. In this range the sand grains are small enough to be transported by fluvial, ice, gravity or eolian forces. Initially the sand grains are loosely packed, but as the sediments are buried deeper they undergo a lithification process called diagenesis (compaction, cementation (new minerals precipitate into the pore spaces as groundwater flows through) and authigenisis (new minerals grow from old recycled chemicals, e.g. clay minerals growing in sedimentary environments due to chemical breakdown of feldspars, or montmorillonite turning into illite) and turn into sedimentary rocks.) This process lowers the porosity and the permeability of the rock, and can make the rock impermeable. As permeability affects fluid flow, this will determine whether the rocks allows migration or accumulation of hydrocarbons.

The framework of sandstone are built of sand grains and are composed mainly of quartz, feldspar and other lithic rock fragments. Pore spaces between the framework can be empty or filled with finer grained material, cement or fluids such as gas, air, oil and FW (Prothero and Schwab, 2004).

Chemical reactivity of the sandstone minerals are different, some measured BET surface area and cation exchange capacity (CEC) values are listed in table 2 (Mamonov et al., 2017).

Table 2: Measured BET surface area for the typical sandstone minerals and average CEC values (Mamonov et al., 2017)

Mineral	CEC, $meq/100g$		BET surface area, m^2/g
Quartz	0.01-1	Depending on particle sizes	0.1-0.2 (fine grained, avg particle size 30 μm
Feldspars (ex. Albite)	0.2-2		2-3 (average particle size 20 μm)
Kaolinite	1-15		10-12 μm
Illite	20-30		20-25 μm
Montmorillonite	70-100		25-30 μm

Minerals weather at different rates due to difference in their chemical stability in the presence of water at certain temperatures. Chemical stability is a measure of a substance's tendency to retain a chemical identity rather than reacting spontaneously to become a different chemical substance. For example, feldspars are stable in the deep of the Earth's crust, where there are high temperature and negligible amount of water, but becomes unstable at the surface where the temperature is lower and water is abundant (Grotzinger and Jordan, 2010). Relative stabilities of common sandstone minerals are listed in figure 5, redrawn after Grotzinger and Jordan (2010).

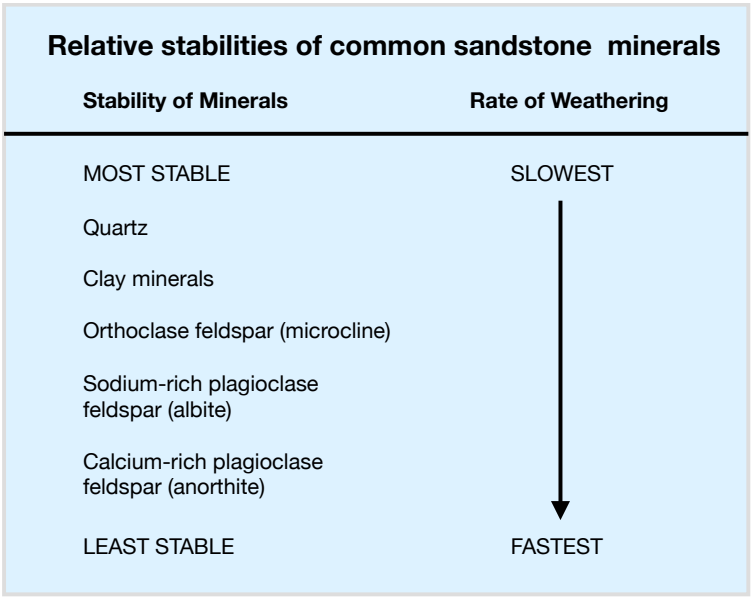

Figure 5: Relative stabilities of common sandstone minerals, redrawn after Grotzinger and Jordan (2010)

2.6.1 Quartz

Quartz (SiO_2) is the most abundant type of sandstone mineral grains, and a sandstone typically consists of 60-70% (or more) quartz. This is linked to the low solubility of quartz which resists disintegration and decomposition during weathering processes. Quartz is a relatively stable mineral with a solubility of 5 ppm at surface temperature and pH 7-8. At higher pH the solubility increases, and a basic water speeds up the solution of quartz (Bjørlykke, 1989). Weathering reaction of quartz

can be expressed by equation 10

$$SiO_2 + 2H_2O \rightarrow H_4SiO_4 \tag{10}$$

which shows how quartz in contact with water dissolves silica in solution as hydrosilicic acid. (Prothero and Schwab, 2004)

Quartz crystals are constructed from one silica ion located at the center surrounded by four oxygen ions at the corners, making a SiO_4 tetrahedron.

The reactivity of quartz is affected by the particle size. Carroll (1959) found that depending on the particle size of quartz, the CEC would be different. A silt fraction of quartz with size range $2-6\mu m$ had a CEC of $0.6 cmol kg^{-1}$. Compared to a clay fraction of quartz with particles less than $2\mu m$ had a higher CEC, $5.3 cmol kg^{-1}$.

2.6.2 Feldspars

Feldspars make up around 60% of the earth's crust by weight and is the most abundant of all minerals. Still, it is more easily decomposed than quartz and therefore make up only $10-15\%$ of the sandstone composition. A high feldspar content in sandstones implies that chemical weathering has not been extensive. Important feldspars are K-feldspars (microcline), $K[AlSi_3O_8]$, Na-feldspars (albite), $Na[AlSi_3O_8]$ and Ca-feldspars (anorthite), $Ca[Al_2Si_2O_8]$. The feldspars minerals have an infinite three-dimensional lattice made up of $[(Al, Si)O_4]$ tetrahedra joined at their vertices. (Holleman, 2001; Prothero and Schwab, 2004; Greenwood, 1984)

Feldspars have a structure similar to quartz except an Al^{3+} will exchange within the tetrahedron and require an additional electron to satisfy the valency. Ca^{2+}, Na^+ and K^+ are non-framework cations that provide charge balance, these can be exchanged with H^+ from water by hydrolysis. (Greenwood, 1984). The exchange is instantaneous and reversible and is accompanied by an increase in pH, equation 11:

fast reaction

$$NaAlSi_3O_8 + H_2O \rightleftharpoons HAlSi_3O_8 + Na^+ + OH^- \tag{11}$$

Similar exchange reaction also occurs for Ca-feldspars and K-feldspars, equation 12 and equation 13 (Parsons, 1994):

fast reaction

$$CaAl_2Si_2O_8 + H_2O \rightleftharpoons HAl_2Si_2O_8 + Ca^{2+} + OH^- \tag{12}$$

fast reaction

$$KAlSi_3O_8 + H_2O \rightleftharpoons HAlSi_3O_8 + K^+ + OH^- \tag{13}$$

Most feldspars are classified chemically in a ternary phase diagram, figure 6, where orthoclase, anorthite and albite are end phases. Composition between Na-feldspar and K-feldspar are commonly referred to as alkali feldspar. Composition of Na-feldspar and Ca-feldspar are referred to as Plagioclase feldspars. Alkali feldspars are not homogeneous but contain separate K-rich and Na-rich phases unless they have crystallized rapidly from solid solutions at high temperatures ($> 660\,^{\circ}C$) (Greenwood, 1984)

2.6.2.1 Surface chemistry

If an anorthite crystal is in contact with an aqueous solution of NaCl, ionic exchange between Ca and Na might occur in the outer layer of anorthite. This will be similar for all feldspars in acidic

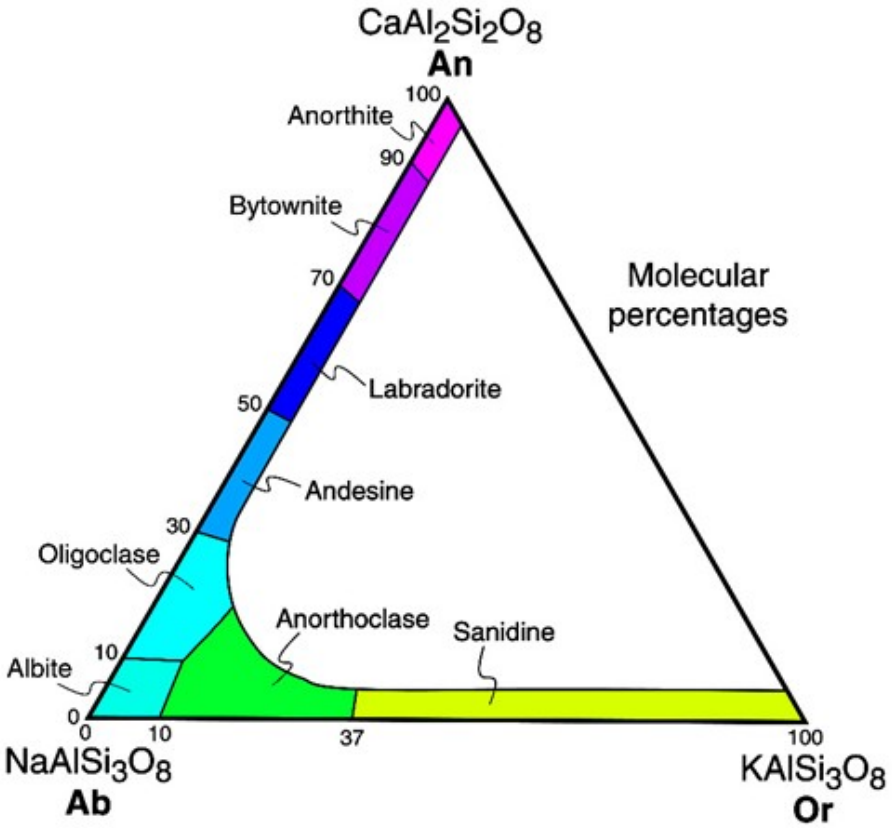

Figure 6: Ternary phase diagram for feldspars (Northern Arizona Meteorite Laboratory, 2014)

solutions. A proton exchange occurs in the outer layers for all feldspars in acidic solutions. There are strong interaction of oxygens and cations in the framework, which gives large variations in cell dimensions and atomic positions from the regular K-feldspars to the irregular twisted structure of Ca-feldspars. Cell dimensions are impacted by temperature and pressure, which can give changes in the cell dimension and atomic positions. At high temperature atomic movements will be greater than at low temperature. Atomic movement will be larger for a surface in which one phase is mobile (liquid or gas) than for a surface between two dense phases. A cluster of linked silica tetrahedra can be terminated by hydrogen atoms to maintain charge balance.

Feldspar surfaces are in contact with inorganic ions and complexes. If organic cations are present, they will compete with the inorganic cations and interact ionically with a charged aluminiosilicate surface. Organic cations can fit into the feldspar cages and thus be adsorbed to the feldpsar surface. Saturated organic compounds are hydrophobic, and can be adsorbed on an aluminosilicate surface if the hydrogen bonding is weaker than in water. A surface with low polarity (high Si/Al ratio) has greater preference of adsorption of a hydrophobic organic compound than a surface with high polarity (Smith, 1994).

2.6.2.2 Weathering

Feldspars are chemically stable at high temperature with negligible water present. At lower temperature in the presence of water it becomes highly unstable (Grotzinger and Jordan, 2010). Feldspar solubility is dependent on pH under both acidic and basic conditions, but at neutral pH or near-neutral pH (pH 5.7 - 7.5) it is independent. Dissolved cations in solution affect the kinetics of feldspars and quartz very significantly The dissolution rate of feldspar decreases when dissolved ions such as Na^+ and K^+ are added to solution due to the competition of ions with protons on the surface. (Gülgönül et al., 2012)

Feldspars weathers via dissolution of all components into solution, where a secondary mineral can precipitate from solution. Some feldspars are more easily dissolved than others, depending on composition. Calcium-rich plagioclase has the lowest stability while albite and potassium feldspars are more stable, figure 5. As a result the prevalence of K-feldspar is higher.

Dissolution of feldspar is the rate determining step of feldspar weathering. The rate is controlled by kinetics of surface reactions at the mineral-water interface. The experimental dissolution rate of feldspars increases with increasing H^+ activity at pH < 6, and increasing OH^- activity for pH > 8.5. Depending on the pH, feldspars have two different dissolution rate mechanisms. A proton promoted mechanism in the acidic region (pH < 5) and a hydroxyl promoted mechanism in the basic region (pH > 7.5) The effect of pH on dissolving feldspar is indirect, controlling the equilibrium concentration of surface species through an adsorption process.

The weathering process of feldspars involve two independent processes: First, the initial dissolution of feldspar into solution and secondly the subsequent precipitation of kaolinite and clay minerals from solution. The overall process can be summarized to a breakdown of feldspars that causes alteration of feldspars to common clay minerals (Blum, 1994; Bjørlykke, 1989). The alteration of K-feldspar to kaolinite can be described by equation 14

$$2KAlSi_3O_8 + 2H^+ + 9H_2O \rightarrow Al_2Si_2O_3(OH)_4 + 4H_4SiO_4 + 2K^+ \tag{14}$$

2.6.3 Clay minerals

Clay minerals have many properties which distinguish them from other minerals. At the relevant pH-range the surface of clays are permanently negatively charged, making them great cation ex-

changers and adsorbants for polar components in the crude oil. Clay minerals have a very large surface area giving them great adsorbing capacity. The very large surface area of clays are an essential background for its cation exchange capacity (Carroll, 1959). Relative affinity of cations towards the clay surface are regarded to be (Bjørlykke, 1989; Austad, 2013):

$$Li^+ < Na^+ < K^+ < Mg^{2+} < Ca^{2+} << H^+$$

Clay minerals can be produced by the weathering of igneous, metamorphic or sedimentary rocks. Clay minerals are phyllosilicates. These sheet silicate minerals consists of oxygen, silicon, aluminium, magnesium, iron and water. They occur as metamorphic and eruptive minerals and as clastic minerals in clay sediments. Clay minerals are also a product from the weathering reactions between minerals and porewater during the breakdown of feldspars and mica. Clay minerals that are formed in sediments after deposition are called autigenic clay minerals. (Bjørlykke, 1989)

The structure of sheet silicates consists of sheets of SiO_4^{-4} tetrahedra and octahedra alternating with layers of Al^{3+}, Fe^{2+} and Mg^{2+} cations. In the tetrahedra layers the cation is surrounded by six oxygen or hydroxyl ions. The octahedral layer can be filled with both bi- and trivalent ions. If the sheet silicates contain trivalent ions only 2/3 of the positions are filled. If there are bivalent ions, all positions are filled. Depending on the structure, the different clay minerals exhibit different properties.(Bjørlykke, 1989) A great variety of clay minerals are constructed from the tetrahedra and octahedral sheets (plus additional cations and anions). Sandwiches made of repeating layers of tetrahedral and octahedral sheets constitutes most clays.(Prothero and Schwab, 2004)

Some of the main clay minerals are illite, montmorillonite, and kaolinite.

2.6.3.1 Illite

Illite is the most abundant clay mineral with its stable 2:1 structure. The structure consists of sheets of tetrahedra and one octahedra which are bonded together by potassium. The potassium ion provide strong ionic bonding to the structure, preventing layers from expanding readily. The ionic bonding between potassium and oxygen in the two sheets are weak and thus the mineral are easily cleaved along this plane. The tetrahedra and octahedra layers are stronger bonded, and not as easily broken. (Bjørlykke, 1989)

2.6.3.2 Montmorillonite

Montmorillonite has a similar 2:1 structure as illite, but most of the potassium is replaced by hydrogen and water, other cations or organic compounds. Montmorillonite has a small net negative charge that is balanced by filling the interlayers with Na^+, K^+ and Ca^{2+} cations. Montmorillonite is known for its swelling when in contact with water and it also has a very high ion-exchange capacity. Montmorillonite is converted to illite at increasing temperature. (Bjørlykke, 1989)

2.6.3.3 Kaolinite

Kaolinite $Al_2(OH)_4[Si_2O_5]$ is a water-containing clay which may form under high temperature and high pressure (HTHP) conditions. Kaolinite has a polysilicate layered structure, which contain silicate layers of formula $[Si_2O_5^{2-}]_x$. (Holleman, 2001) The structure of kaolinite consists of a tetrahedra layer and an octahedra layer. The ion exchange capacity is smaller for kaolinite than montmorillonite due to the 1:1 structure. This structure makes no room for water or larger cations between the layers, which makes them chemically and mineralogically simple compared to other clays. Kaolinite sheets are neutral and are held together by hydrogen bonding. Kaolinites attracts

external cations only by negative charges on the edges of the sheets. Because of this, grain size affects the CEC (Carroll, 1959). Kaolinite are stable at low temperatures. At higher temperatures kaolinite becomes unstable and will be altered to illite at $120 - 130°C$ if K^+ is available. If there is no available K^+ kaolinite will remain stable at high temperatures. (Bjørlykke, 1989; Prothero and Schwab, 2004)

2.6.4 Other important sandstone minerals

In addition to the siliclastic minerals, some can be generated in-situ by chemical processes at high temperature in sandstone reservoirs with high FW salinity. Anhydrite ($CaSO_4$), calcite ($CaCO_3$) and gypsum ($CaSO_4{\cdot}2H_2O$) are important sandstone minerals that can affect the chemical reactions during a wettability alteration process (Strand et al., 2016).

2.7 Ion Exchange

An ion held by a negative charge near a mineral surface can exchange place with another that is present in a solution in contact with the mineral, this phenomena is called ion exchange and is a reversible process governed by physiochemical laws. Ion exchange occur with substances like organic matter, minerals, finely crushed rocks and amorphous material. Clay minerals have noticeable exchange reactions due to their broken bonds at the edges and the particle size of the mineral plates. Adsorption onto these unsatisfied edges are considered as part of an ion exchange. Cation exchange in clay minerals can be simply stated by equation 15 (Carroll, 1959):

$$Na\ clay + H^+ \rightleftarrows H\ clay + Na^+ \tag{15}$$

Ion exchange is affected by several factors

- type of mineral
- nature of the replacing ion
- pH in the solution
- concentration in the solution of the replacing ion
- cations already in the exchange positions of the clay minerals

2.7.1 Cation Exchange Capacity

Cation exchange capacity (CEC) is defined as the amount of exchangeable cations, in milliequivalents per gram or per 100 grams of clay (soil or mineral) determined under experimental conditions at pH 7.

Variation in exchange capacity for the individual minerals is caused by differences in availability of exchange sites and by the chemical composition that causes the negative charges to develop. Irregularities in the lattice structure and variation in particle size increases the ion-exchange capacity by providing a greater number of unsatisfied bonds at the edges. The exchange capacity increases as the particle size of a mineral decreases due to a larger surface area with more broken bonds.

Cation exchange capacity depends on a number of factors (Carroll, 1959):

1. Quantity of clay and silt fractions. The clay fraction has higher CEC than the silt fraction.
2. Type of clay mineral - illite and montmorillonite will give a greater exchange capacity than a considerably larger amount of kaolinite.

2.7.1.1 Mechanisms of Cation Exchange

Ion exchange takes place when a solution containing cations and anions comes in contact with a mineral surface. The reactions are due to the structure and chemical composition of the mineral and to the chemical elements in the solution in contact with the mineral.

Structural causes of cation exchange (Carroll, 1959):

1. Unsatisfied valences produced by broken bonds at surfaces and edges of particles. Broken bonds are the most important cause of cation exchange in clays and in fine particles of minerals.

2. Unbalanced charges caused by isomorphous substitution of cations- for example, Al^{+3} substituted for Si^{+4}.

2.8 Preparation of Minerals

2.8.1 Homogeneous and Heterogeneous Systems

For a given material, the chemical properties are nearly independent of its shape and size, except when the particle size is very small. Objects which differ only in size and shape, but otherwise have the same specific properties, e.g solubility, density, chemical reactivity, etc. can be applied a collective concept; substance. Substances which appear to have uniform composition are called homogeneous substances, or homogeneous systems. While a non-uniform substance, like granite, is a heterogeneous substance. (Holleman, 2001)

2.8.2 Separation of Heterogeneous Systems

Heterogeneous systems have difference in physical properties of their homogeneous components, and are therefore easily separated by mechanical methods. Difference in density and particle shape are properties that can be used to separate the systems.

2.8.2.1 Sedimentation

One of the simplest way to separate a solid-liquid mixture is to let the solid suspended in the liquid settle to the bottom. The clear liquid above can then be poured off (decanted). This procedure is called sedimentation, and is gravity driven. The same principle can be used to separate solid-solid mixtures. By placing the mixture in a liquid, the difference in the rate of sedimentation can be used. If the particle size is the same, the denser particles will sink more rapidly than the lighter ones. The lighter particles can then be removed (eluted) with the liquid. For mixtures with same density, the particle size will determine how quickly the particle will sink; larger particles will sink more rapidly than smaller ones.
(Holleman, 2001)

2.8.2.2 Sieving

Another method for separating solid-solid mixtures with different particle sizes is sieving. Depending on the mesh size, particles with smaller size than the mesh will go through, and larger ones will be held back.

2.8.2.3 Ultrasonication

Particles that have been milled are highly reactive and the problem of agglomeration is always there as long as the particles are in dry powder form. Ultrasonication can disaggregate and deagglomerate particle agglomerated particles by cavitation phenomena (Mani et al., 2011). A ultrasonic bath or an ultrasonic probe is usually used when applying ultrasonication to break up aggregates of micron-sized colloidal particles.

Mani et al. (2011) used ultrasonication combined with ball milling to produce nano-sized clay particles. Their goal was to increase the BET surface area of the clay samples as much as possible. In this process, the particles were highly reduced in size and got highly reactive. The problem of agglomeration arises when powder is in dry form, making particles cluster and agglomerate. They were using Laser diffraction to analyse the particle size distribution (PSD) of the samples and the high reactivity of the particles were influencing the analysis. By treating their minerals in a ultraconication process they managed to disaggregate and deagglomarate particles that were clustering, obtaining a more representative PSD of the samples.

2.8.2.4 Wet sieving

Multiple fractions of a mineral sample can be obtained by vacuum filtration technique. Wolfe et al. (2007) used a porcelain Bücher funnel with a fixed perforated filter combined with brass sieves with fitted mesh sizes according to pre defined PSD range. A filter paper was used to trap particles below a certain micron size. A vacuum pump ensured sufficiently rapid sieving. Prior to the wet sieving, the sample was ultrasonicated.

2.8.3 Size reduction of minerals

Solids can be reduced from one average particle size to a smaller average particle size by crushing, grinding, cutting, vibrating or other processes. The technique for size reduction could affect the mineral properties. A important rule of thumb of size reduction is to only grind the sample as fine as necessary and not as fine as possible.

2.8.3.1 Size reduction tools

Reproducible sample preparation is important to obtain reliable and accurate analysis. Representative samples should have homogeneous and analytical fineness which is only obtained by proper size reduction tools. Examples of milling tool are: Jaw rushers, Rotor mills, Knife mills, Cutting mills, Mortar grinder / Disc mills and Ball mills. To determine what is the best suited mill several properties should be considered: characteristics of sample (dry, abrasive, brittle, hard, soft etc), required final fineness, sample volume and subsequent analysis. Depending on the quality of the material different size reduction principles should be applied to obtain required fineness. Hard-brittle materials are best comminuted with impact and friction and should be milled in ball mills. Soft and elastic materials should be handled in knife or cutting mills (RETSCH GmbH, 2017).

2.8.4 Particle size distribution

The particle size distribution (PSD) of a mineral can be important in understanding its physical and chemical properties. It affects both the reactivity of solids participating in chemical reactions as well as the strength and load-bearing properties of rocks and soils, table 3. The particle size distribution can be broken down into size classes: Cobbles ($20 - 2000mm$), Gravel ($2 - 20mm$), Sand ($20\mu m - 2mm$), Silt ($2 - 20\mu m$), Clay ($< 2\mu m$), figure 7 (TerraGIS, 2007)

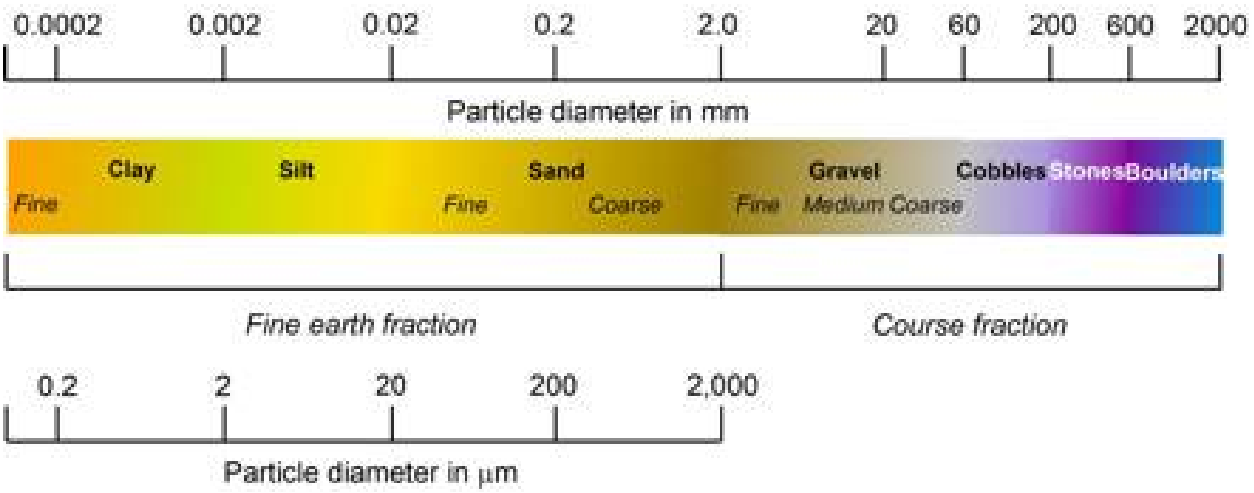

Figure 7: Particle size fraction, (TerraGIS, 2007)

Table 3: Properties and behaviour of particle size fractions, redrawn after (TerraGIS, 2007)

Property	Clay	Silt	Sand
Size range (mm)	<0.002	0.002-0.02	0.02-2
Observation	Electron microscope	Light microscope	Naked eye
Attraction of particles	High	Intermediate	Low
Surface area	High-very high	Low-medium	Very low

Particle size influence properties of particulate materials and is a valuable indicator of quality and performance. It is therefore important to measure and control the particle size distribution for the mineral. The PSD of a sample can be expressed as a range analysis, in which the amount of size ranges is listed in order. Range analysis is suitable when a particular ideal mid range particle size is being sought. If the amount of under-size or over-size particles are being determined, it is usually presented in cumulative form. Here the total of all sizes retained by a mesh size is given for a range of sizes, normally resulting in a S shaped curve. D10, D50 and D90 are values commonly used to define distribution width. D50 is the median. D90 means that 90 percent of the distribution is below this value and D10 means that 10 percent of the population is below this value. Other values that are used to analyse particle sizes are mean, median, mode, standard deviation and variation.

Mean is a calculated value giving an average value. Depending on the basis for the distribution calculation a volume mean, surface mean, number mean can be used to define the central point.

Median is defined as the value where half of the population resides above this point and the other half below. In PSD median is referred to as D50. Volume median is commonly referred to as D50, while a number distribution should use Dn50 instead, to distinguish between them.

The highest peak of a frequency distribution is called the mode and represents the most commonly found particle size in the distribution.

Standard deviation and variance are commonly used to describe the width of the PSD. Standard deviation can also be normalized by diving by the mean and are then called relative standard deviation (RSD).

PSD is usually defined by the method by which it is determined. One method frequently in use is sieve analysis. Dynamic light scattering, Laser diffraction and Image analysis are other commonly used techniques for determining PSD (HORIBA Instruments Inc, 2012).

2.8.4.1 Sieving

The material is separated on sieves of different sizes and the PSD is determined in terms of discrete size ranges. E.g. % of sample between $45\mu m$ and $53\mu m$, when sieves of this sizes are used. Normally the PSD is determined over a list of size ranges that covers nearly all sizes present in the sample.

2.8.4.2 Image Analysis

Particles are inspected visually one at a time, and usually reported as a number distribution. In many cases the number distribution is converted to another basis, i.e. volume. This conversion is generally accepted and does not introduce unknown errors into the result as long as a sufficiently number of particles have been inspected to fully define the distribution. Many techniques make the general assumption that every particle is a sphere and the value is reported as an equivalent diameter. The only method that can describe particle sizes using multiple values for particles with larger aspect ratios is a microscope. A scanning electron microscope can be used to produce images for image analysis. Here the images can be analysed manually, identifying size and shape. Depending on the shape of the particles, the longest and shortest diameter, perimeter, projected area, equivalent diameter, or the length is used to determine PSD. SEM will provide images that give reliable and correct information about the particles shapes and sizes, and is considered a great (but time consuming) option when analysing PSD for different minerals (HORIBA Instruments Inc, 2012).

2.8.4.3 Laser Diffraction Technique

This technique uses the particles ability to scatter light at an angle depending on the particle size to determine the PSD. Larger particles scatter at smaller angles, while smaller particles at wider angles. A collection of particles produce a pattern of scattered light defined by intensity and angle that then can be transformed into a particle size distribution. A bench-top laser diffraction instrument can be used to perform this analysis, and is a fast, flexible method with high accuracy when identifying PSD, thus it has displaced other popular techniques such as sieving, sedimentation and manual microscopy. This method assumes that the particles are spherical (HORIBA Instruments Inc, 2012).

2.8.5 Ripening

Ripening is a phenomena where the crystal size of a precipitate increases. In a mixed particle system, large particles become larger and small particles dissolve due to surface energies (Snoeyink, 1980). Thus reducing the reactivity of the broken bonds after a milling process.

3 Smart Water in Sandstones

Smart Water is an injection water that is different in composition compared to the initial formation water (FW) and can induce wettability alteration to improve oil recovery. Unlike conventional waterflooding that is used for secondary recovery, a Smart Water may change the wetting properties and are therefore considered as an EOR method (Austad, 2013).

Smart Water is made by modifying the ion composition

- no expensive chemicals are added
- it is environmentally friendly
- easy to implement
- can be combined with other chemical if needed. If Smart Water is combined with other chemical they are called hybrid methods, e.g. Low salinity surfactant (LSS) and low salinity polymer (LSP).

When a Smart Water is injected to a reservoir of mixed-wet conditions, it can induce a wettability alteration towards more water wet. Capillary forces, P_c, increases and water imbibe into the previously unswept pores increasing microscopic sweep efficiency, figure 8. A new bank of oil is mobilized and can be displaced by the water. The imbibition process is not fast, and therefore an increase in recovery is not observed instantaneously.

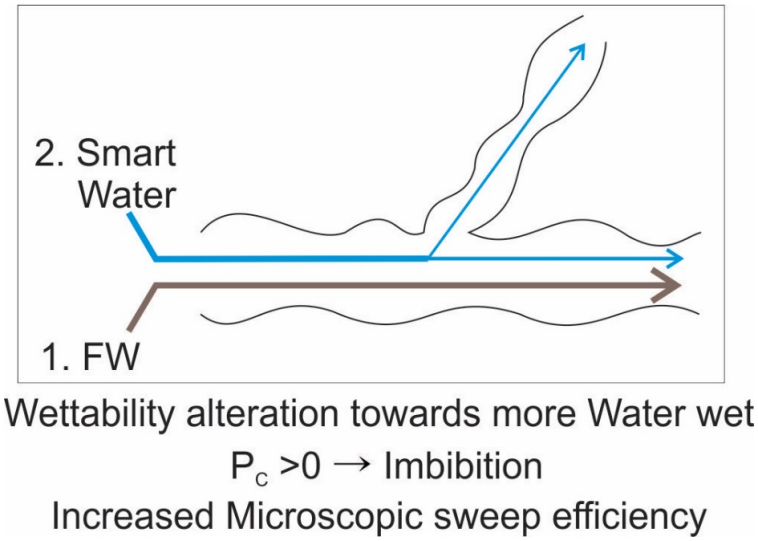

Figure 8: Scheme of how wettability alteration with Smart Water increases sweep efficiency due to increased capillary forces

A chemical equilibrium between the crude oil, brine and rock (CBR) in a reservoir has been established during million of years creating initial wetting properties. When a water that is different in composition than the initial FW is injected to the reservoir, the chemical equilibrium of the CBR system is disturbed. The CBR system will try to establish a new equilibrium and in this process changing the wetting conditions in the reservoir which could result in improved oil recovery. Chemically, the CBR-interaction is completely different in carbonates and sandstones.

3.1 Important Wetting Parameters

3.1.1 Formation water (FW)

Formation water influences the initial wetting of a reservoir. Salinity and types of salt are important factors and will affect initial wetting as well as pH in the FW. The salinity of the FW varies, ranging from 10,000 - 250,000 ppm. Common ions in FW is Na^+, K^+, Mg^{2+}, Ca^{2+}, Sr^{2+} and Ba^{2+}. The pH in the FW is very often acidic due to presence of acidic gases like CO_2 and H_2S. If feldspars are present, and the salinity of FW is reasonably low, alkaline conditions can be observed (Reinholdtsen et al., 2011; Strand et al., 2016).

3.1.2 Crude Oil

Crude oil is a non homogeneous phase containing polar organic acids and polar organic bases. The individual polar organic components contribute as anchor molecules towards rock surface and are important for creating wetting in reservoirs. These organic components can be quantified in terms of acid number (AN) and base number (BN). AN and BN are measured in mg KOH/g. Carboxylic group, $-COOH$ represents the acidic organic components, while R_3N : represents the basic organic components. The organic components can undergo fast proton exchange reactions as the pH of a system changes, equation 16 and equation 17:

Organic bases:

$$R_3NH^+ + OH^- \rightleftharpoons R_3N : + H_2O \tag{16}$$

Carboxylic acids:

$$R - COOH + H_2O \rightleftharpoons R - COO^- + H^+ \tag{17}$$

The reacticity of the polar organic components changes with pH. At acidic conditions, organic bases are positively charged while carboxylic acids are neutrally charged, as seen at left hand side of equation 16 and equation 17. At alkaline conditions the organic bases are neutrally charged while carboxylic acids are negatively charged, right hand side of equation 16 and equation 17. The pK_a is ~ 5 for both carboxylic acids and organic bases thus protonated bases and acids have the same variation with pH. Both acidic and basic organic components can adsorb onto a negatively charged mineral surface (Strand et al., 2016).

3.1.3 Rock

Sandstones are composed of many different materials which make the chemical understanding of the CBR-system complex. (Austad, 2013). Reservoir rocks are highly heterogeneous having variation in permeability, porosity, wettability and mineralogy. Depending on the mineral, the initial wetting and potential for LS EOR effect are affected. The most common sandstone minerals are quartz, clay and feldspar. Surface area is an important property regarding wetting, a higher surface area provide great adsorption capacity. Quartz is the main mineral in sandstones, however due to small surface area ad low CEC they do not affect the chemical CBR interactions in sandstone reservoirs very much. Clays are unique due to their permanently negative charge, high CEC and very large surface area, which are adsorbed by polar organic compound of crude oil and are considered the main wetting mineral in sandstone (Austad et al., 2010). Feldspar is another important mineral regarding initial wetting due to its influence on pH (Mamonov et al., 2017).

3.1.4 Reservoir temperature

Temperature is an important parameter to consider when evaluating wetting conditions in a reservoir. Chemical reactions may speed up as the temperature increases, establishing a chemical equilibrium faster. Temperature affects ion reactivity; dehydration of divalent ions and increased adsorption. Solubility of compounds in water increases or decreases depending on temperature (Strand et al., 2016).

3.2 Chemical Mechanism for Low Salinity Waterflooding in Sandstone Reservoirs

Low salinity (LS) waterflooding with salinity in the range 1000-2000 ppm has been used as a tertiary EOR method, and its effect has been documented both on laboratory and field scale (Tang and Morrow, 1999; Lager et al., 2007). The chemical mechanism behind LS effect in sandstone reservoirs are much more complex to study than for a carbonate reservoir. The reason for this is that the LS effect is a result of several different mechanism that are acting together, where each also is contributing on its own. A lot of research has been done to identify the mechanism behind the observed tertiary low salinity EOR effect. It has been generally accepted that the LS effect is caused by a wettability alteration, but other physical mechanisms have also been proposed (Austad et al., 2010).

- Migration of fines (Tang and Morrow, 1999)
- Fluid flow due to osmotic pressure caused by salinity gradients (Sandengen et al., 2016)
- Wettability change at rock surface due to local pH increase (Austad et al., 2010)
- Multi-ion exchange (MIE) (Lager et al., 2008a,b)
- Double layer effects (Ligthelm et al., 2009)

3.2.1 Wettability alteration due to local change in pH

Austad et al. (2010) published an article discussing the chemical mechanism for LS waterflooding in sandstone reservoirs. They stated that to better understand the chemical mechanisms one should look at all parameters involved. In sandstone reservoirs there are complex crude oil-brine-rock (CBR) interactions, which makes it difficult to evaluate the potential for increased oil recovery by LS waterflood. They proposed a local pH increase as the mechanism behind the LS EOR effect, which has been well-founded in experimental observations and are commonly referred to as the Smart Water EOR (Austad et al., 2010; Piñerez Torrijos, 2017; Mamonov et al., 2017; Aksulu et al., 2012; Piñerez Torrijos et al., 2017; Strand et al., 2014; Aghaeifar et al., 2015; RezaeiDoust et al., 2011; Reinholdtsen et al., 2011).

At reservoir conditions the pH of formation water is around 5 due to dissolved acidic gases like CO_2 and H_2S. Clay minerals act as cation exchangers at this pH, and protonated acidic and basic components from crude oil and cations from formation water (FW) can be adsorbed. Especially divalent cations like Ca^{2+} are important adsorbing cations. When a LS brine is injected Ca^{2+} is desorbed from the clay surface which gives a local increase in pH close to the clay-brine interface. This increase is caused by the decrease in H^+ in the FW because of Ca^{2+} is substituted by $H+$ from the brine, equation 18. This is an effect of disturbing the chemical equilibrium initially at place before the LS brine is injected. When the LS brine is injected, the equilibrium is disturbed,

and the clay mineral tries to stabilize by adsorbing protons onto the surface. Fast reaction between OH^- and the adsorbed acidic and protonated basic material which desorbs the organic material from the clay surface, equation 19 and equation 20. The surface gets more water wet, and thus an increase in recovery may be observed. The chemical wettability alteration mechanism can be expressed by following chemical equations 18 - 20:

slow reaction

$$clay - Ca^{2+} + H_2O \rightleftharpoons clay - H^+ + Ca^{2+} + OH^- + heat \tag{18}$$

fast reaction

$$clay - R_3NH^+ + OH^- \rightleftharpoons clay + R_3N : + H_2O \tag{19}$$

fast reaction

$$clay - RCOOH + OH^- \rightleftharpoons clay + RCOO^- + H_2O \tag{20}$$

The process of desorbing the polar organic components from the clay surface are described in figure 9. Acidic and basic material that are adsorbed onto negatively charged clay minerals are removed by Smart Water at alkaline conditions caused by desorption of Ca^{2+} from the clay surface resulting in a local pH increase (Austad et al., 2010).

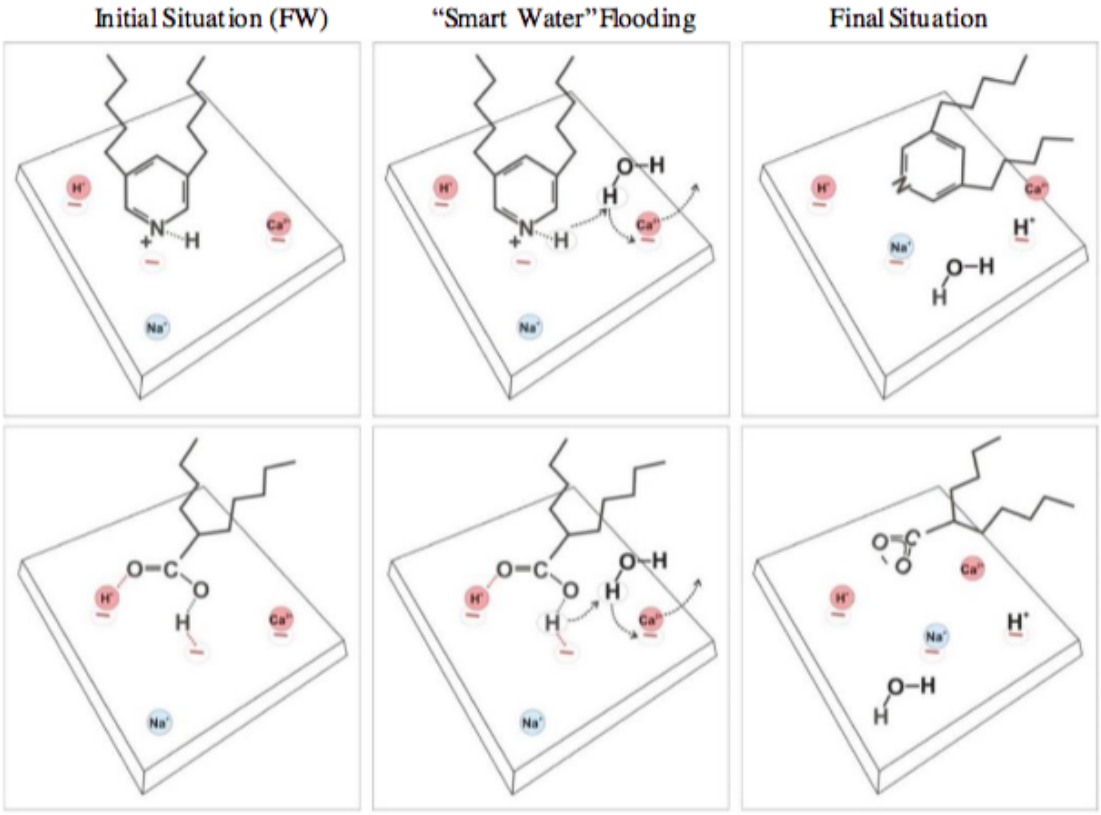

Figure 9: Illustration of the proposed LS Smart Water EOR mechanism in sandstone reservoirs. (Austad et al., 2010).

3.3 Conditions for Low Salinity EOR effect

To observe any effect of LS EOR flooding in a sandstone reservoir, there are some conditions that must be present. These conditions have been determined through experimental work by Tang and Morrow (1999) and researches at BP (Lager et al., 2007) and was stated to be (Austad et al., 2010):

- Porous medium
  - Clay must be present
- Oil
  - Polar components must be present (acids and bases)
- Formation water, FW
  - Divalent cations must be present, i.e Ca^{2+}, Mg^{2+}.
  - Initial FW must be present
  - Initial water saturation, S_{wi}, affects efficiency
- LS injection fluid
  - Salinity range should be 1000 - 2000 ppm, but there has also been observed effects at 5000 ppm.
  - Ion composition matters. i.e Ca^{2+} vs Na^{+}
- Produced water
  - pH of the effluent increases 1-3 pH units when injecting the LS fluid

Ca^{2+} and organic components should initially be adsorbed to the clay surface. Different clay minerals have different adsorption capacity and adsorption/desorption pH window. It is therefore important to understand the chemical mechanism behind the LS EOR process, together with information about FW brine composition, oil properties and type of clay mineral present. Evaluating all these properties gives rise for the potential for increasing oil recovery. (Austad et al., 2010)

Parameters/factors that could influence the main LS EOR process are: (1) Temperature, (2) combination of reservoir minerals, (3) composition and salinity of the FW. These parameters could have great impact on the EOR process by affecting the initial wetting conditions and the wettability alteration process. Aghaeifar et al. (2015) studied the effect of a FW with high temperature and high salinity and concluded that adsorption of active polar components onto clay minerals decreases as temperature and salinity of FW increases. At these conditions desorption of Ca^{2+} from the clay surface is reduced due to dehydration and common ion effect by dissolution of anhydrite. At high temperature and high salinity adsorption of organic polar components decrease.

3.4 Contribution of Feldspars

Austad et al. (2010) argued that a local increase in pH is a key factor for observing low salinity EOR effects, and this increase in pH is mainly caused by the desorption of Ca^{2+} from the clay surface when a LS brine is injected into a reservoir containing HS FW. Both clays and feldspar minerals have permanent negative sites that needs to be charge-balanced by cations. When a LS brine is injected into a HS FW the established equilibrium is disturbed and the minerals will try to establish balance by taking reactive protons from the brine, resulting in a local pH increase.

Aksulu et al. (2012) argued that a decrease in salinity itself could not be responsible for the observed LS EOR effect, but was mainly controlled by pH. Feldspars are important both regarding initial wetting and wettability alteration.

Reinholdtsen et al. (2011) studied sandstone cores from the Snorre field in the North Sea and how Smart Water EOR could affect the recovery. Analysis of the reservoir showed high clay content, polar organic components in the crude oil and divalent cations in the FW which are great conditions for observing Smart Water EOR effects, still only a minor increase in recovery was observed. An analysis of the mineralogy confirmed 30 wt% of feldspars in the reservoir. The combination of high feldspar content and low salinity FW probably made the initial wetting too water wet to observe any Smart Water EOR effect.

Strand et al. (2014) suggested that presence of plagioclase minerals in sandstones, which influence initial pH of the formation water (FW), could affect LS EOR potential in both a positive and a negative way depending on the salinity of the FW. They concluded that presence of plagioclase in reservoir rock could raise the initial pH > 7 in a moderate saline FW thus creating a basic environment which was too water wet to observe any LS EOR effect. While in a high salinity FW the plagioclase would be less reactive, resulting in a pH below 7. This acidic environment would promote mixed-wet conditions where significant LS EOR effects could be obtained. In such reservoirs feldspars could also contribute with increase in pH when a low salinity brine is injected, thus contribute positively in a wettability alteration.

Piñerez Torrijos et al. (2017) argued that presence of reactive plagioclase in high temperature sandstone reservoirs could be favourable for observing LS EOR effects, as long as the initial pH of the FW was low enough to make the rock mixed wet.

Mamonov et al. (2017) conducted both static and dynamic studies to evaluate sandstone minerals influence on initial wetting and how they affected wettability alteration during a Smart Water flood. He concluded that reactive feldspar are one of the most important factors in controlling reservoir pH.

3.5 Contribution of Clays

Clays are the main wetting mineral in sandstone reservoirs and play an important role in the initial wettability and the LS EOR effect. Due to its large surface area and permanently negative charge, cations and organic components can adsorb/desorb on the clay surface as a function of pH in the solution. Adsorption of polar components onto the clay surface creates initial mixed wet condition which can be altered toward more water-wet conditions as LS brine is injected into HS FW reservoir desorbing the organic components from the surface, and thus inducing a tertiary EOR effect. The adsorption of the organic components onto clay minerals are dependent on pH, temperature, ion composition and salinity of the FW (Aghaeifar et al., 2015).

4 Experimental

The objective in this thesis is to evaluate feldspar and their influence on initial wetting and wettability alterations. To achieve this, an optimal mineral preparation is essential. The main objective of this thesis is therefore to perform optimal mineral preparation by using new milling equipment which will help in getting representative adsorption and pH screening results.

Several steps have been done to produce mineral samples that will give reliable and repeatable results. Different apparatus and advanced analysis instruments have been used to analyse the mineral samples after different procedures. To verify stability and reproducibility of the prepared mineral samples adsorption and pH screening tests have been done and compared with results that have been obtained at the University of Stavanger by other students. (Andersen, 2015; Frafjord, 2015; Abdullah, 2016; Harestad, 2017; Tat, 2017; Algazban, 2017). The equipment, brines, minerals and procedures that are used will be described in detail in this section. Some of the procedures are performed identical to the procedures done earlier, and some have been improved.

4.1 Equipment

4.1.1 XRD - Mill McCrone

The XRD Mill McCrone is a small, compact bench top ball mill used for size reduction and homogenization of rocks, figure 10. This mill has a very specific application area and is primarily used for preparation of samples of materials that are going to be analysed by XRD. A key point is the preservation of the crystal lattice structure. Other ball mills have an aggressive modus operandi which will destroy the crystal lattice and therefore they will not be detected in a XRD analysis. The McCrone Mill however, employ very gentle modus operandi which will preserve the crystal lattice and is therefore available to analysis. Inside the grinding vessel there are 48 cylindrical grinding elements made of zirconium oxide. Zirconium oxide (ZrO_2) is a stabilized oxide which inhibit disruptive transformation to other crystalline forms. (Greenwood, 1984) A unique grinding motion grinds the samples gently via friction. Minerals can be grinded both dry or combined with a fluid. Wet grinding in airtight containers reduces crystal lattice deformation and oxidation. Grinding time can be adjusted to obtain optimum particle size distribution. Samples are grinded from $< 0.5mm$ to a low μm range. According to the manufacture, this process preserves the crystal lattice, gives almost no sample loss and produce a narrow particle size distribution. The preservation and gentle handling aim to ensure perfectly homogenized and contamination-free samples for reliable and accurate analysis to give reproducible sample preparation.

A sample preparation kit came as accessory to the ball mill consisting of a percussion mortar, sieve and sieve brush, figure 11. It was designed to rapidly and easily reduce large particles to suitable sizes for the ball mill. (Retsch, 2018)

Figure 10: XRD Mill McCrone (Retsch, 2018)

Figure 11: XRD milling equipment (Retsch, 2018)

4.1.2 Micromeritics TriStar II

Micromeritics TriStar II was used to determine the surface area of the minerals. BET method is the basis for the calculations. The apparatus uses nitrogen and helium gases to determine the surface area, by measuring the adsorption of gas molecules on to the surface of the sample at a given pressure. VacPrep 061 was used to prepare the samples for surface area measurement. Contaminants, like water vapor and adsorbed gas at surface and pores of the sample, are removed by vacuum and heat. Vacuum was turned on slowly to prevent fluidization of samples. (micromeritics, 2018)

4.1.3 Scanning Electron Microscope

To analyse the feldspars particles a scanning electron microscope (SEM) Zeiss Gemini Supra 35VP was used. SEM is an electron microscope employing a beam of electrons directed to a specimen to obtain an electronic image of the specimen's surface structure. The beam position is controlled digitally onto the sample, and the resultant image is displayed on a computer screen. The image formation in the SEM is built up sequentially during the scan, giving high pixel resolution and therefore good spatial resolution with a large depth of field. (Goodhew et al., 2000) All of which makes it possible to study the feldspars surfaces, sizes and shapes, and visualize how the particles were affected by the milling.

Emitech K550 was used to prepare the samples prior to the SEM analysis.

4.1.4 Mettler Toledo AB104-S analytical balance

Analytical balancer used to weight experimental materials.

4.1.5 Anton Paar DMA-4500 Density meter

Density meter used for measuring density of the brines.

4.1.6 Mettler Toledo pH meter

pH meter used to measure pH when analysing and adjusting the samples.

4.1.7 Gilson GX-271 Liquid handler

A Gilson GX-271 Liquid handler was used to dilute the NaCl-brines that had been in contact with anorthite for the static pH screening test. All salinity brines must be diluted before ion composition analysis. Gilson GX-271 Liquid handler provide precise and automate sample preparation, minimizing error in final results (Gilson, 2015).

4.1.8 Dionex ICS-5000+ DP

The Dionex ICS-5000 was used to determine ion composition for the brines that has been in contact with anorthite used in the pH screening tests. The samples are transported with the help of an elute through an ion exchange column where the ions are separated in contact with a resin, the stationary phase. Then the ions together with the eluent passes through a suppressor where the conductivity of the eluent is reduced and increased for the ions, before entering the conductivity detector (Fanali et al., 2013). In the conductivity detector each ion is found based on its conductivity measured in μS.

4.1.9 Stuart SB3 rotater

Rotator used to rotate samples at ambient temperature.

4.1.10 Hettich Universal 1200 centrifuge

Centrifuge used to separate mineral from water

4.1.11 Thermo Scientific Genesys 10S UV-VIS spectrophotometer

The Thermo Scientific Genesys spectrophotometer was used to determine the adsorption of quinoline onto the minerals.

4.2 Materials

4.2.1 Feldspars

Anorthite and microcline used for the experiments were provided by WARD's Natural science and was originally delivered as a 1 kg bulk pack. The origin of the minerals can be found in table 4. Both feldspars were crushed, sieved and milled as described in the pre milling preparation- and milling procedures.

Table 4: Vendor, origin and formula of feldspars

Feldspar	Formula	Origin	Vendor
Anorthite	$CaAl_2Si_2O_8(An_{90-100}/Ab_{0-10})$	Grass valley, California, USA	Ward's Science
Microcline (pink)	$KAlSi_3O_8$	Madawaska, Ontario, Canada	Ward's Science

4.2.2 Quinoline

For the adsorption tests quinoline (Q) ($> 97\%$) was used as polar basic component and was delivered by Merck. Q is a heterocyclic aromatic compound with a favourable solubility in water and can easily be detected by its absorption spectrum in UV light. Q is a basic compound present in crude oils and will act as a model compound for a basic crude oil.

The molecular formula for Q is C_6H_7N. Nitrogen can be protonated in acidic conditions thus pH strongly affects the solubility of Q in water. With a pKa = 4.87 Q will be highly protonated around this pH.

A 0.07 M Q solution was used in the experiments, this had been prepared previously by Abdullah (2016) by adding 9 grams of Q and 600 ml deionized water in a 1000 ml volumetric flask. pH was adjusted to 5 to dissolve the Q into water. Fraction of protonated base increases as the pH of the Q solution decreases below the pKa value. The fraction reaches 100% around pH 3.5. The solution was then put for 24 hours stirring. The flask was then filled up to 1000 ml with deionized water, shaken and stored in a dark bottle. This resulting a Q stock solution with a concentration of 0.07 M. Density for the 0.07 M Q was measured three times using a Anton Paar DMA-4500 density meter. Average density was used for further calculations, table 7

4.2.3 HS and LS brine

Brines used in the experiments were constructed by dissolving a certain amount of salts in deionized (DI) water, table 5. All salts were delivered by Merck Schuchardt OHG. Low salinity (LS) and high salinity (HS) brines were made, with salinities close to 1150 ppm and 30 000 ppm. Ion composition of the LS and HS brines are given in table 6 and average densities in table 7. The salts were weighed on a digital scale. Salts were put into 1000 ml volumetric flasks together with approximately 600 ml DI water. A magnetic stirrer was used to mix each brine for 24 hrs until the salts were dissolved and the solutions were clear. The magnetic stirrer was removed and DI water was added to the 1000 ml line of each flask. Any dissolved gas or particles were removed from the brines by vacuum and a 0.22 μm filter, figure 12. Density was measured with a Anton Paar DMA-4500 density meter, average density given in table 7.

Table 5: Composition of brines

	LS brine		HS brine	
Salt	$g/mole$	$mole/l$	$g/mole$	$mole/l$
$NaCl$	0.798	0.0137	20.750	0.355
$MgCl_2x6H_2O$	0.348	0.0017	9.050	0.045
$CaCl_2x2H_2O$	0.255	0.0017	6.620	0.045

Table 6: Ion composition of brines

Ion	LS brine	HS brine
$Ca^{2+}(mole/l)$	0.0017	0.0450
$Mg^{2+}(mole/l)$	0.0017	0.0445
$Na^{+}(mole/l)$	0.0137	0.3551
$Cl^{-}(mole/l)$	0.0205	0.5342
TDS (g/l)	1.15	29.99
Ionic strength	0.024	0.624

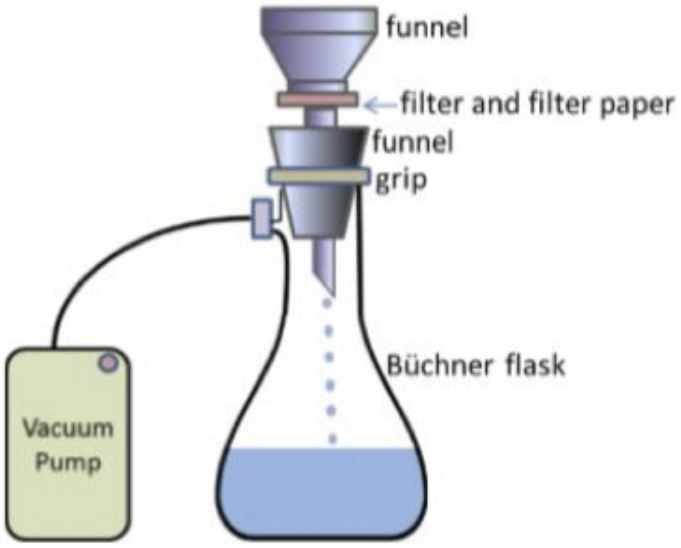

Figure 12: Filtration setup, (Abdullah, 2016)

4.2.4 Brine-quinoline solutions

Solutions of 0.01 M HSQ and 0.01 M LSQ were made to construct the calibration curve. HS and LS brines were mixed with 0.07 M Q to make brine-quinoline solutions, which hereafter are called HSQ and LSQ solutions. A scale was used to weight the mass of the added brines. Mass was determined from calculations using average density that had been measured , table 7. Preparation data for the 0.01 M HSQ and 0.01 M LSQ brines are listed in table A3

Table 7: Average densities of brines, DI water and quinoline

Solution	Average density (g/cm^3)
DI water, pH = 3	0.9977
HS brine	1.0199
LS brine	0.9986
0.07 M Quinoline	0.9994
0.01 M HSQ brine	1.0165
0.01 M LSQ brine	0.9985

4.2.5 NaCl brine

NaCl brines used in the pH screening experiments were constructed by dissolving NaCl in deionized (DI) water, table 8. The salt was delivered by Merck Schuchardt OHG. Different salinities were made, 5000 ppm, 30 000 ppm, 50 000 ppm and 100 000 ppm. Exact amount of NaCl was weighed on a digital scale and put into 100 ml volumetric flasks together with approximately 70 ml DI water. A magnetic stirrer was used to mix each brine for 24 hrs until the salts were dissolved and the solutions were clear. The magnetic stirrer was removed and DI water was added to the 100 ml line of each flask. The brines were not filtrated.

Table 8: Composition of NaCl-brines

Salinity (ppm)	NaCl (g)	DI water (ml)
0	0	100
5000	0.5	100
30000	3.0	100
50000	5.0	100
100000	10.0	100

4.3 Procedures and Analyses

The main experimental and analytical methods used in the experimental work are described as follows.

4.3.1 Milling the mineral samples

A large part of this thesis has been to prepare the minerals in a representative way, to get repeatable and reliable results. In previous experiments done at the University of Stavanger, the minerals were milled using a grinding machine called Retsch PM100 (Andersen, 2015; Abdullah, 2016; Harestad, 2017; Tat, 2017), which is a ball mill where the minerals are milled until almost powder. This very destructive milling gave a large range in the particle size distribution with irregularities in the crystal lattice giving varying and unreliable results. This is the motivation for using a new mill to prepare the minerals for this thesis; the XRD Mill McCrone. The XRD Mill McCrone provide a controlled milling procedure, that preserves the crystal lattice of the minerals, and also produces a much more narrow range of particle sizes. Sample preparation of the feldspar minerals were carried out in two steps: a preliminary crushing of the minerals followed by milling of the sample to analytical fineness. All minerals have been through the same preparation procedure. Crushing, grinding, sieving, milling, sieving, settling. A BET analysis to determine BET Surface Area, SEM to identify particle sizes and PSD.

4.3.1.1 Pre milling preparation

First step in the milling preparation was to perform a preliminary crushing of the minerals to a proper size of $\leq 0.5mm$. The McCrone sample preparation kit was used, which is designed to rapidly and easily reduce large particles to suitable sizes for the XRD Mill McCrone. The preparation kit consisted of a percussion mortar, sieve brush and a 0.5 mm sieve. The feldspar minerals were initially as solid rock and had to be prepared before it could be milled in the XRD mill. Small bits were chopped off the solid rock mineral by using a hammer. These pieces were then put into a mortar with associated pestle that came as accessory preparation set to the XRD Mill McCrone, and ground into a mixture of crushed minerals, figure 13. The crushed minerals were sieved through a $0.5mm$ mesh separating particles $\leq 0.5mm$. These crushed $\leq 0.5mm$ particles were then used for milling.

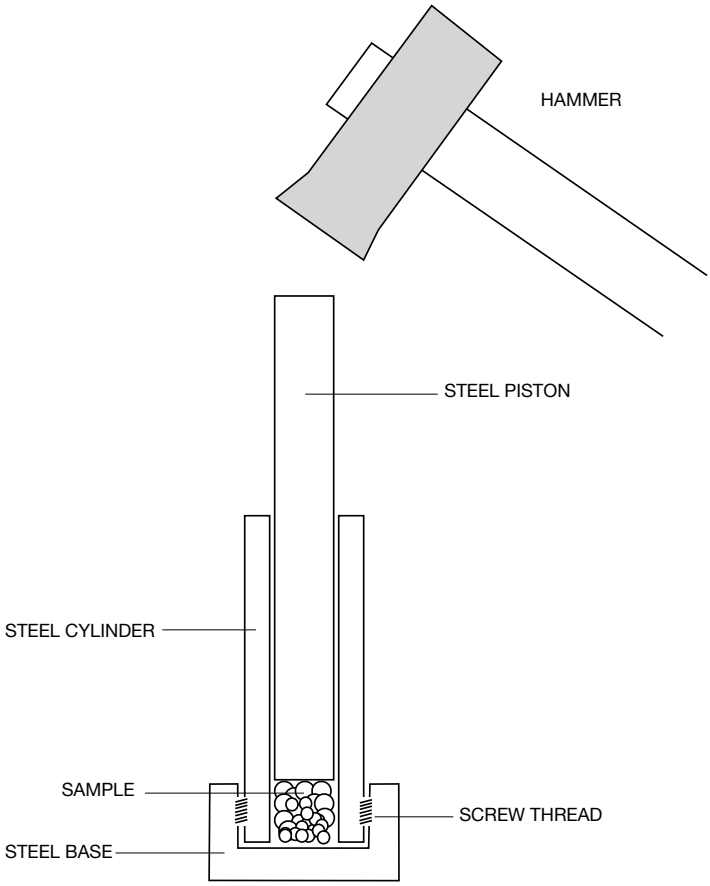

Figure 13: Pre milling preparation setup

4.3.1.2 Milling

The XRD Mill McCrone was used for milling the crushed $\leq 0.5mm$ minerals. A 125 ml polypropolyne grinding jar was filled with 48 grinding elements. A loading device was used to ensure correct position of the grinding elements inside the grinding jar. The grinding elements were packed in an ordered array of 8 layers, 6 elements in each. The loading device was removed after the grinding elements were in place.

A batch size of 4 g of the sieved $\leq 0.5mm$ mineral particles were put into the center of the grinding elements inside the grinding jar. 10 ml DI water was poured on top of the minerals, flushing them gently down into the center of the jar. A lid was put on top and screwed tightly on the grinding jar, before placing and securing it in the milling machine. A noise reduction cap was placed outside.

The grinding speed was increased from min speed to max speed in 4 steps. Each step consisted of approximately 10 seconds of milling, stop the mill and increase the speed and start again.

Several different milling times were tested. In the initial tests 1, 2, 3 and 5 minutes were chosen, and based on analysis (BET and SEM) of these a final milling time of 7 minutes were chosen for all minerals.

After milling, the mixture of DI water and particles were gently poured into plastic beakers using a lid with holes. For maximum recovery of wet ground samples, DI water was used to wash

particles from the grinding jar and grinding elements until the fluid poured off was clear. The wet ground sample was set to dry for 24 hrs in an oven at 60 degrees. After drying the samples, they were carefully scratched from the surface of the beaker, and sieved once again through the $0.5mm$ mesh sieve. The milled minerals were put into sample cups with cap and stored at room temperature. The preparation data for the minerals are listed in table 9 and a scheme of the different steps in the grinding process in figure 14.

Table 9: Preparation for milling minerals

Mineral ($\leq 0.5mm$)	Mass mineral (g)	DI water (ml)	Milling time ($minutes$)	Speed
Anorthite	4	10	1	Max
Anorthite	4	10	2	Max
Anorthite	4	10	3	Max
Anorthite	4	10	5	Max
Anorthite	4	10	7	Max
Microcline	4	10	1	Max
Microcline	4	10	2	Max
Microcline	4	10	3	Max
Microcline	4	10	5	Max
Microcline	4	10	7	Max

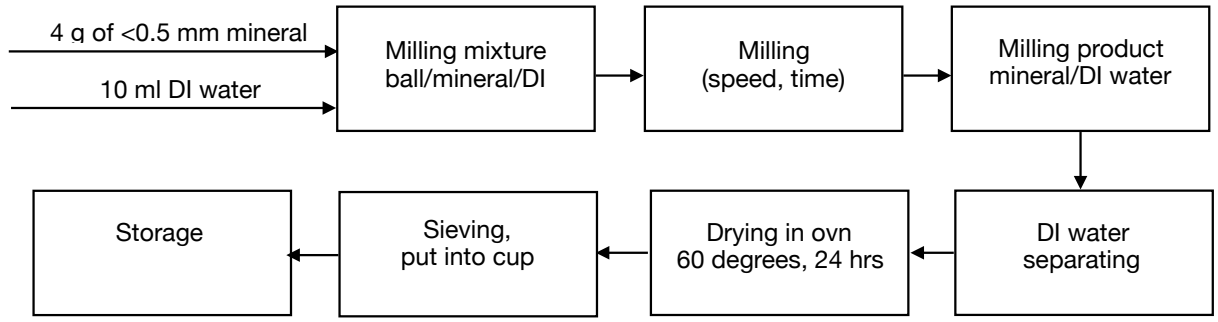

Figure 14: Scheme showing the steps in the mechanical grinding process to prepare the minerals

4.3.2 Sedimentation process

Sedimentation is a simple way to separate solid-solid mixtures. By suspending the solids in a liquid and let them settle to the bottom, gravity will separate them, and the liquid containing small particles can be removed (eluted) with the liquid. For the minerals, density will be the same, but particle sizes will be different. This means that the larger particles will settle at a higher rate than the smaller ones. The settling velocity can be calculated from Stokes law which can be written as equation 21 (McCabe et al., 2005)

$$v = \frac{2 \cdot r^2 \cdot g \cdot (\rho_p - \rho_f)}{9 \cdot \mu} \tag{21}$$

where

r is the radius of the spherical particle, m

g is the gravitational acceleration constant, m/s^2

ρ_p is the density of particles, kg/m^3

ρ_f is the density of fluid, kg/m^3

μ is the dynamic viscosity of the fluid, $kg/(m \cdot s)$

v is the settling (or thermal) velocity of the particle, m/s

Stokes law apply under the following assumptions (LLC, 2018):

- There is no other particle nearby that would affect the flow pattern
- The motion of the particles are constant
- The particle is spherical and rigid
- The air velocity right at the particle surface is zero
- The fluid is incompressible

After finding the settling velocity of the particle, it is possible to determine the settling time for the particle size in question. By using the equation 22

$$t = \frac{h}{v} \tag{22}$$

where

t is the settling time for the particle to reach bottom, s

h is the height of water column, m

v is the settling velocity of the particle, m/s

To remove the smallest particles from the mineral sample, a sedimentation procedure was performed identical as done by Abdullah (2016), figure 15. Settling velocity can be calculated from Stokes law, equation 21. The milled mineral sample was put inside settling bottles, filling up with approximately 600 ml of DI water, shake and let gravity separate the smaller particles from the larger ones for 1 hr. The smallest particles were eluted from the settling bottles, and then DI water was used to refill the bottle. The procedure was repeated 3 times. The settled particles at the bottom, along with the remaining liquid, were carefully put into glasses and set in oven to dry for 48 hrs at 60°C.

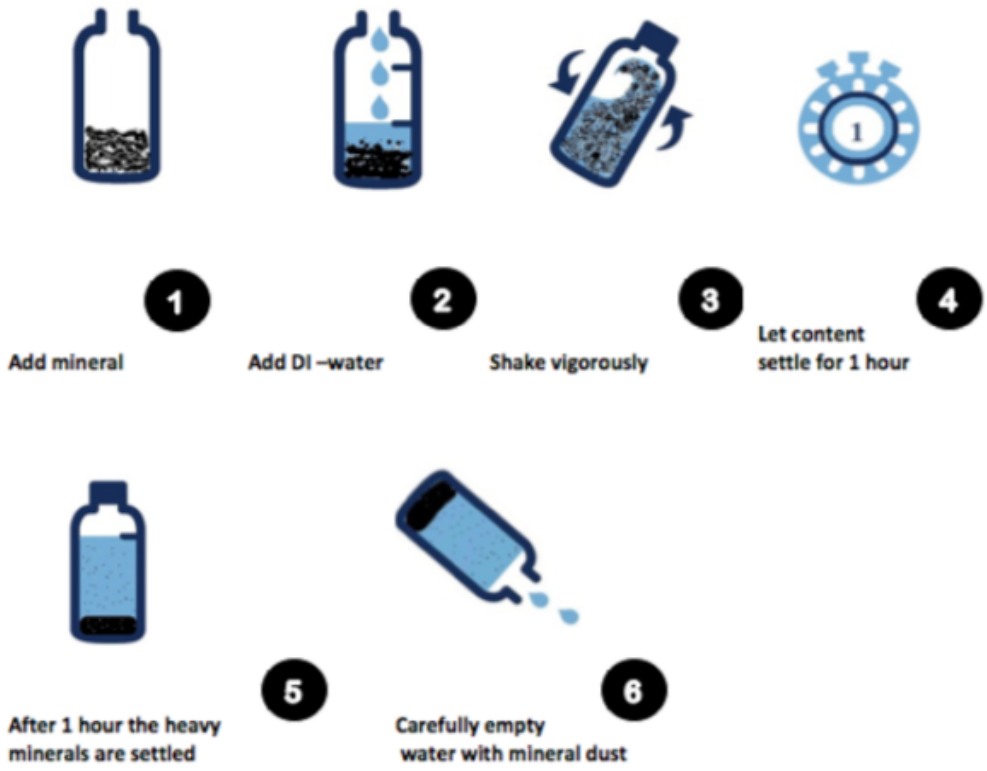

Figure 15: Illustration of sedimentation procedure (Abdullah, 2016)

4.3.3 Density measurements

The density of the brines was quantified using a density meter DMA-4500 from Anton Paar. Each sample was measured three times, and an average density was calculated. Between each measurement the apparatus was flushed with acetone and white spirit and any bubbles were removed.

4.3.4 pH measurements

Mettler Toledo pH meter was used to measure pH for all brines and solutions. All pH measurements were done at ambient temperature. Repeatability ± 0.01 pH units.

4.3.5 SEM analysis

The prepared feldspar minerals were analysed by a scanning electron microscope (SEM). All samples were coated with palladium in the Emitech K550 prior to the SEM analysis. The palladium prevent erosion of the samples and create the electronic conductivity necessary to observe the samples in the SEM. Several images were produced for each sample, and particle distribution and sizes were evaluated. The SEM was crucial in deciding milling time, determining PSD range and hence a proper mineral preparation for adsorption testing.

4.3.5.1 Determining PSD from SEM

By measuring the particles in the SEM pictures, small and large particles were identified, figure 16. Then a PSD range could be determined from several SEM images with a total of approximately 80 measurements. Both vol% and % count was considered for making a PSD plot. Since only a small amount of the total particles were measured, % count was used to picture the PSD range. Also, for the sample preparation, the volume is not important, only the amount of particles for a given size. Therefore a PSD by frequency was considered the best presentation method. The goal was to have a normal distribution of particles, with as small range as possible, thus measuring the largest and smallest particles would give a good estimate of the PSD range.

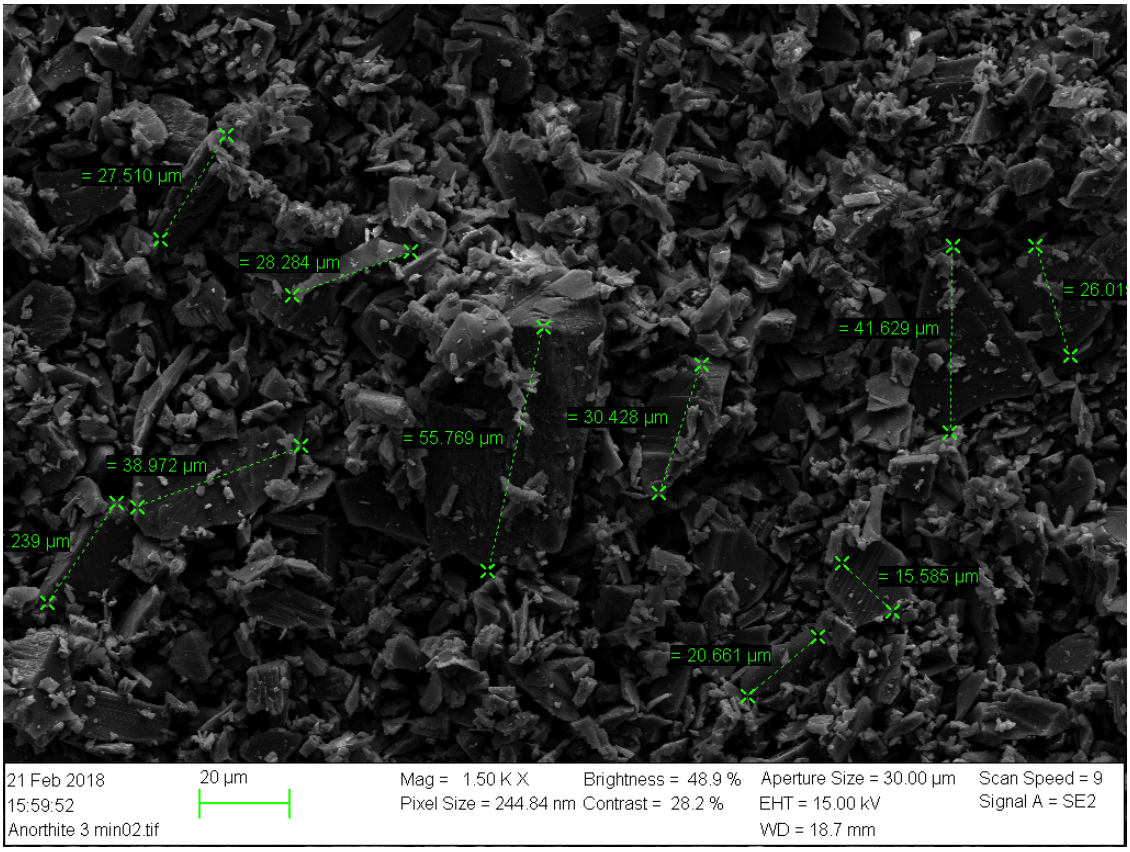

Figure 16: SEM measurement of large particles. Current image is of anorthite sample, milled 3 minutes.

After analysing the particle range of the different milling times, a final milling time was chosen, and a more precise PSD was constructed for this. The SEM images were analysed, measuring one particle at a time by drawing a line, figure 17. This was then converted to its actual length by equation 23

$$length = \frac{relative\ length \cdot unit\ value}{unit\ length} \tag{23}$$

where

relative length = measured length in image, cm

unit value = length of the scale, μm

unit length = measured length of the scale, cm

length = length of the particle, μm

Each value was noted, and used to determine PSD by number distribution. The largest diameter or length was chosen to measure each particle. Only particles where both ends were visible were measured. A total of approximately 400 - 500 particles were measured and used to describe the PSD for the optimal mineral sample that was used in further testing.

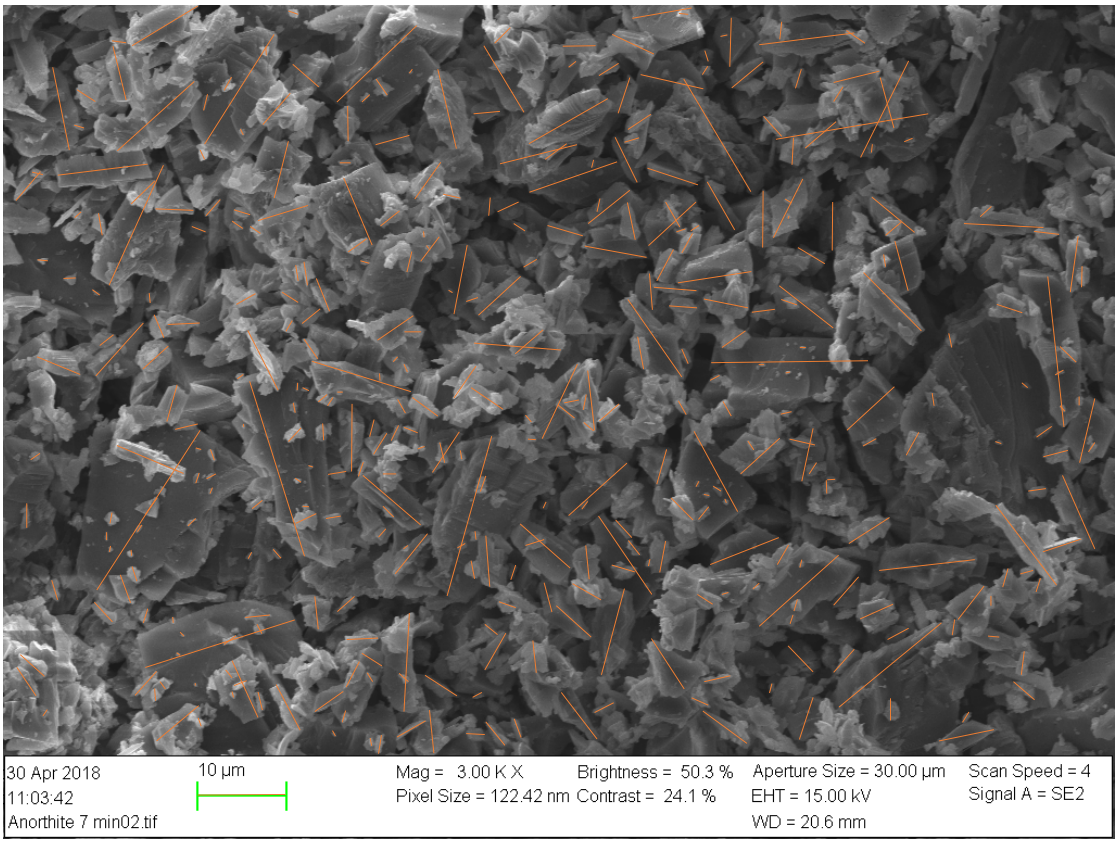

Figure 17: A SEM image was used to measure each particle with a orange line. Here a section of a sample of anorthite, milled 7 minutes, is visualized.

4.3.6 Adsorption

Adsorption is defined as the enrichments of material or increase in the density of the fluid in the vicinity of an interface. Whenever a solid surface is exposed to gas or liquid, adsorption occurs. One or more components in a liquid or gas is adsorbed to an available surface of an adsorbent (solid) and thus separated from the rest of the mixture. How much adsorption that occurs depends on the extent of the interfacial area. Minerals with a large specific surface area, e.g. clays, are highly porous or composed of very fine particles which will be great adsorbents. An important use of adsorption techniques is to characterize surface properties and textures of different materials. In particular, gas adsorption is a widely used procedure for determining the surface area and pore size distribution of porous minerals. In 1938, Brunauer and Emmet published the Brunauer-Emmet-Teller (BET)

theory, which involves adsorption of nitrogen onto a mineral to determine the surface area. They found that adsorption isotherms of several gases were S shaped at, or near, their respective boiling points. Today, the BET theory has become a standard procedure for determining the surface area of porous materials. (Rouquerol et al., 2013).

4.3.7 BET surface area measurement

Micromeritics TriStar II was used to determine the surface area of the minerals. Prior to the BET analysis, contaminations and fluids were removed in the VacPrep 061 preperation machine. Glass tubes were cleaned with acetone and DI water and dried in oven. Approximately 1 g of each mineral sample was put into glass tubes. Exact weight was measured. Samples were heated and vacuumed in the VacPrep machine. The temperature increase effectively evaporated any water and moisture in the samples. Dry samples were weighed. Finally, BET surface area was determined using Micromeritics TriStar II, table A1.

4.3.8 Absorbance

In chemistry absorption refers to the physical process of absorbing light, or the penetration of a fluid into a solid phase (Rouquerol et al., 2013), while absorbance measures the attenuation of transmitted radiant power caused by adsorption, reflection, scattering and other physical processes. Each line in the line spectra can be considered as monochromatic radiation. Because of the wave character of light, each line in the spectrum is characterized in terms of its wavelength, λ, defined by equation 24:

$$\lambda = \frac{c}{v} \tag{24}$$

where

λ is the wavelength, nm

c is the velocity of light in a vacuum, ms^{-1}

v is the frequency, Hz

The visible region for the spectrum extends from about 770 nm (red) to 380 nm (violet). In atomic spectrometry the spectral region extends from 190 nm (ultraviolet) to 850 nm (infrared).

Absorbance is typically measured using absorption spectroscopy. A source of light is then emitted through a solution and a detector records how much light and what wavelengths were transmitted. From this information, the absorbed wavelength can be determined (Lajunen and Peramaki, 2004) .

The measured absorbance can be related to Lambert-Beer law which is a relation used in spectroscopy concerning the absorption of radiant energy by an absorbing medium. The law states that the absorptive capacity of a dissolved substance is proportional to its concentration in a solution. The Lambert-Beer law is normally written as equation 25 (Rafferty, 2018):

$$A = \mathcal{E} \cdot l \cdot C \tag{25}$$

where

$\mathcal{E}$ is the absorption (molar extinction) coefficient. (A constant that is characteristic for the chemical and the wavelength of the light used)

A is the measured absorbance (or $log(\frac{I_0}{I})$)

l is the length of the path the light must travel in the solution, cm

C is the concentration of the absorbing spieces

Lambert-Beers law can be used to measure the concentration of the chemical compound in a sample. This concentration can then be used to calculate the adsorbed concentration.

4.3.9 Adsorption of quinoline onto feldspars

To determine if the polar components of oil adsorb onto the feldspar a Thermo Scientific Genesys spectrophotometer was used to quantify absorbance wavelength. Peak absorbance was measured for the 0.01 M HSQ and was found to be 312.5 μm

4.3.9.1 Calibration curve

By plotting the calibration curve, an ideal plot where the absorbent obeys the Lambert-Beers law in the whole concentration region and creates a straight line. Four diluted samples were prepared for both HSQ and LSQ for the calibration, data is given in table A5. The samples were diluted 100, 200, 500 and 1000 times respectively using DI water pH ~ 3.

Four diluted reference HS and four diluted reference LS samples were made, data is given in table A4. Samples were diluted 100, 200, 500 and 1000 times with DI water pH ~ 3.

A 5 ml syringe was used to add the DI water into the sample glass, using a digital scale to quantify. Accuracy $\pm 0.0005g$. Then a manual pipette was used to add 5, 10, 25 and 50 μl of the HSQ or LSQ brine into the glass. Weight was noted.

The samples were put into Thermo Scientific Genesys 10S UV-VIS spectrophotometer measuring absorbance using peak absorbance wavelength (312.5 μm), to make a calibration curve. Reference LS and LSQ with same dilution rate was put into the machine, reference LS as blank. The spectrophotometer was zeroed according to reference and then absorbance was measured for the LSQ sample. This was done similar for all samples, and data was transferred into excel to make a calibration curve, figure 18. .

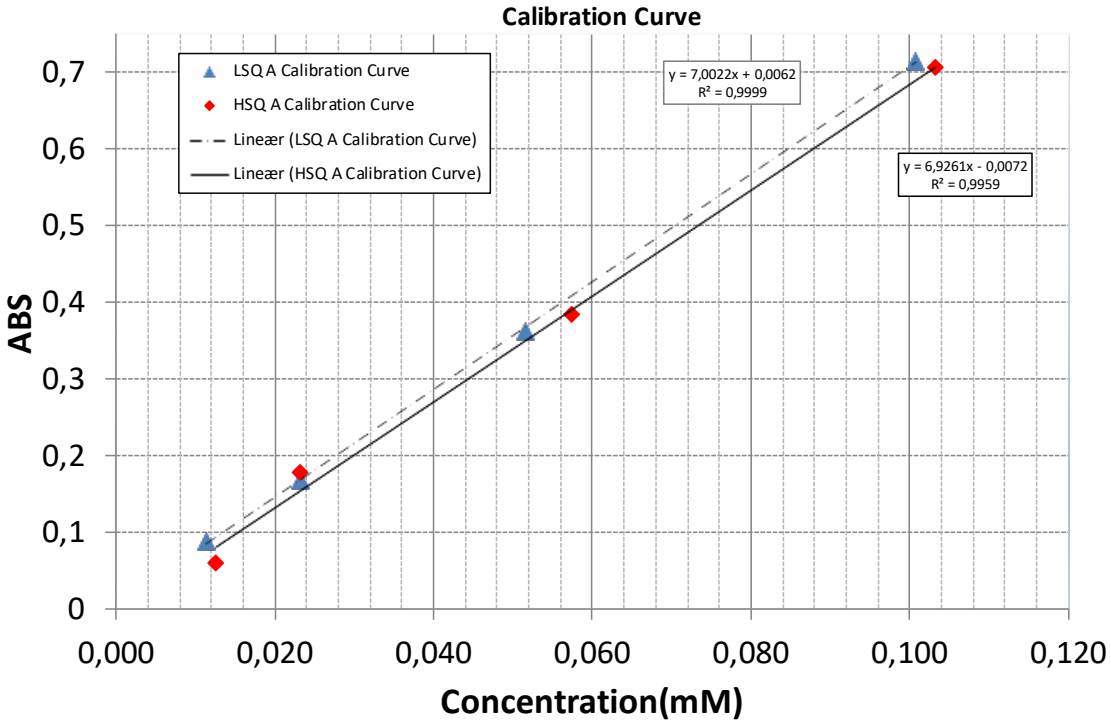

Figure 18: Calibration curve

The absorbance varied with the concentration of quinoline in the solution. Four absorbance readings for both HSQ and LSQ were plotted against the known concentration and formed two linear lines within measured area $R^2 = 0.9959$ and $R^2 = 0.9999$. The resulting equations (26 and 27) were used to calculate quinoline concentration in a sample based on its measured absorbance.

Calibration curve HSQ, equation 26

$$y = 6.9261x - 0.0072 \tag{26}$$

Calibration curve LSQ, equation 27

$$y = 7.0022x + 0.0062 \tag{27}$$

4.3.9.2 Sample preparation

Samples were prepared using 10 wt% of prepared mineral together with 90 wt% 0.01 M HS or LS brines. The brines were added into the sample glass, which was placed on a scale, with syringe to control the amount added with an accuracy $\pm 0.0005g$. Three parallel samples were prepared for each brine and each mineral. pH was adjusted using HCl and NaOH getting a pH from $2 - 7$. 1.000 gram of mineral was added into each sample. All samples were put for 24 hrs ripening at ambient temperature using a Stuart SB3 rotater at 40 rpm speed. The ripening was conducted to establish an equilibrium between the feldspar minerals and the ions in the bulk water. After ripening a known amount of 0.07M quinoline was added into into the samples. pH was measured and adjusted before putting the samples for another 24 hrs rotation at 40 rpm. After a total of 24+24 hrs ripening, the samples were centrifuged in a Hettich Universal 1200 centrifuge for 20 minutes at 2500 rpm. A pipette was used to carefully extract the brine (supernatant) from the glass, leaving the mineral behind, and then transferred into a clean glass. pH was measured for all

samples, at ambient temperature. 25 μl of supernatant was pipetted with a manual pipette and then diluted 200 times with DI water pH $\sim$ 3. Reference samples were made from 25 μl brine-reference solution and diluting it 200 times with DI water pH $\sim$ 3. Preparation data is presented in table A6 - A13. All pH measurements were conducted at ambient temperature.

4.3.9.3 Static adsorption test

The samples were put into Thermo Scientific Genesys 10S UV-VIS spectrophotometer measuring absorbance using peak absorbance wavelength (312.5 μm). Reference LS and LS-supernatant samples were put into the machine, reference LS as blank. The spectrophotometer was zeroed according to reference and then absorbance was measured for the LS-supernatant samples. This was done similar for all HS samples. Final pH (real pH) was measured for all samples. Data was transferred into excel sheet, table A6 - A13. Equation 26 and equation 27 were used to calculate adsorption for the measured absorbance, calculations are presented in appendix A.6.2. Adsorption vs real pH was plotted for the feldspar minerals, figure 29 and figure 30.

4.3.10 Static pH screening test

To evaluate representability of the prepared mineral sample and study the influence of feldspars regarding pH and salinity, a pH screening test was conducted for the anorthite feldspar and compared to previous test results done at the University of Stavanger. Brines with different salinities were prepared according to the composition specified in table 8.

The anorthite sample that was used came from the same batch that was prepared for the adsorption tests and had been milled 7 minutes and then settled to remove the smallest particles. 10 wt% of anorthite was mixed with 90 wt% of NaCl-brine at different salinities. The pH of the mineral-NaCl brine solution was adjusted to an initial pH $\sim$ 5 using HCl and NaOH. The samples were rotated for 24 hrs. After anorthite had been in contact with the NaCl-brines for 24 hrs, they were centrifuged for 20 minutes, excreting the brine from the mineral. A pipette was used to carefully extract the brine from the glass, leaving the mineral behind, and then transferred into a clean glass. This was done for each sample, a total of 5 samples. Final pH was measured. A plot of pH vs salinity was made to present the results, figure 31. Measured pH and brine-mineral data are presented in table 10. All pH measurements were done at ambient temperature.

Table 10: pH screening data and measured pH at ambient temperature

Salinity (ppm)	Brine(g)	Anorthite (g)	Brine + An adjusted pH	Brine + An pH after 24 hrs	ΔpH after 24 hrs
0	9.0000	0.9920	4.97	9.51	4.57
5000	9.0004	0.9935	4.93	9.18	4.25
30000	9.0000	0.9945	4.89	8.95	4.06
50000	9.0003	0.9863	4.94	8.89	3.95
100000	9.0004	0.9922	5.11	8.85	3.74

4.3.11 Ion composition analysis

After conducting a pH screening test for anorthite Ion Chromatography (IC) was used to analyse the ions present in the brine that had been in contact with the feldspar. The samples, which had

already been excreted by a centrifuge as described in pH screening procedure, were diluted 500 times by Gilson GX-271 Liquid Handler and filtrated through a $0.2\mu m$ syringe filter to remove any particles. Diluted and filtrated samples were transferred to 2 ml vials. Low salinity water and high salinity water with known ionic composition were used for reference and calibration. Dionex ICS-5000 + DP was used to determine the ion composition in the brines. All prepared samples and references were put into the IC machine and the pattern for injection was specified according to the rack positions of the sample vials.

After the IC machine has finished analysing the samples, Chromeleon 7 was used to identify the peaks. Cations and anions show up as peaks based on the time they spent going through the column and their conductivity. The area below the curves are given in $\mu S \cdot min$. A table of analysed data was copied into excel for calculations, table A14. The area below the curves can be converted into ion concentration by using the fact that sample and reference are proportional given by the following relation, equation 28.

$$C_{sample} = \frac{C_{ref} \cdot A_{sample} \cdot D_{sample}}{A_{ref} \cdot D_{ref}} \tag{28}$$

where

C_{sample} is the concentration of sample in $mmole/l$

C_{ref} is the concentration of reference fluid in $mmole/l$

A_{sample} is the area of sample in $\mu S \cdot min$

A_{ref} is the area of reference fluid in $\mu S \cdot min$

D_{sample} is the dilution rate of sample

D_{ref} is the dilution rate of reference

5 Results

The objective of this thesis was to optimize mineral samples to perform reliable static adsorption and pH screening studies to understand feldspars influence on initial wetting and wettability alterations. In accordance with the objective this section display the results from optimal mineral preparation, static adsorption of quinoline onto feldspar minerals and static pH screening test.

5.1 Optimal Mineral Preparation

New milling equipment has been used to prepare the feldspar minerals. Different milling times have been tested, and the resulting samples have been analysed by BET and SEM to find the most optimal and homogeneous particle size distribution. Very small particles have been removed by sedimentation.

5.1.1 BET surface area

Figure 19 shows how the BET surface area of the particles increased as a function of milling time. By increasing the milling time and thereby reducing the average particle size, the BET surface area is increasing accordingly. Both minerals surface area increases almost linear, following a clear trend. This stable increase in both feldspars, and the resulting trend, indicates proper mineral preparation. Microcline has a higher slope compared to anorthite, suggesting microcline being more brittle and easier broken.

At 7 minutes milling time, two different BET surface area values are measured, one for settled and one for unsettled mineral sample. The settled minerals were expected to have a bit lower surface area than the unsettled because the smallest particles were settled out. This is true for anorthite while for microcline it is not. This unexpected result could be due to contamination in sample glass, human error, uncertainties in measurements or failure in the settling process. Clusters of small particles could affect the success of a settling procedure. Several clusters of small particles were observed in the microcline sample in the analysis of SEM images as will be shown later in figure 27. A large amount of very small particles contribute with increased surface area. These large quantity of small particles are affecting the BET surface area values resulting in a higher surface area.

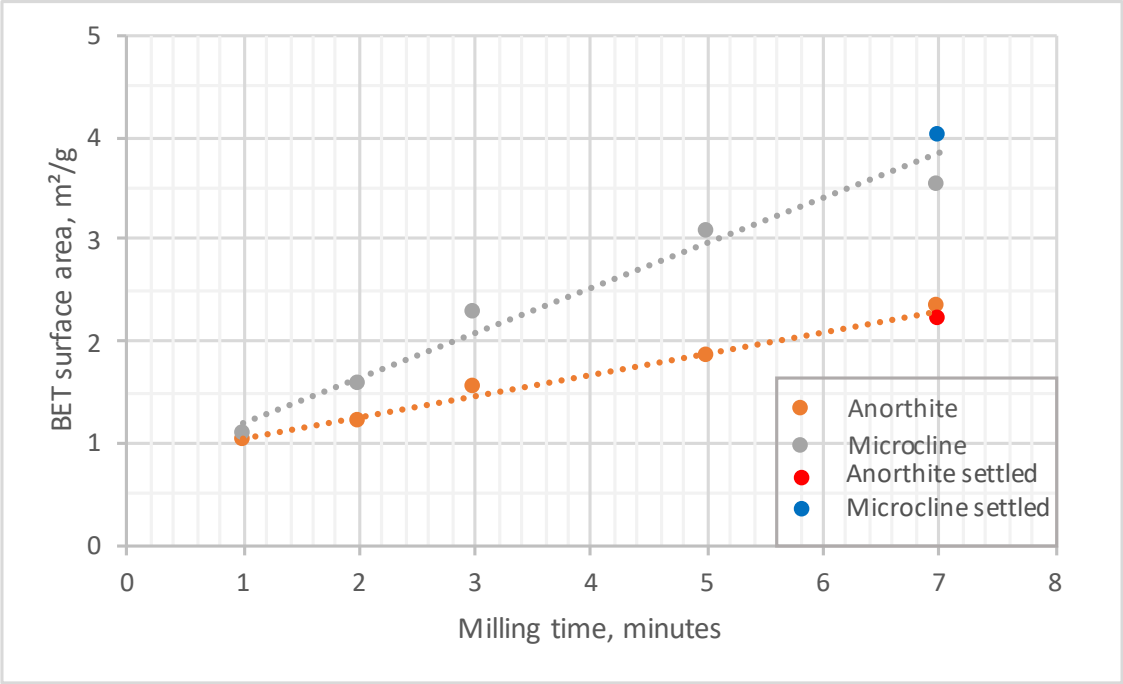

Figure 19: BET surface area vs milling time

5.1.2 SEM analysis

To analyse how the mineral samples were affected by different milling times the samples were inspected using a SEM. Unmilled samples that were prepared using the sample preparation kit were inspected as well. To obtain a optimal mineral sample preparation, different milling times were tested and the resulting particle size distribution (PSD) was determined from SEM pictures. Large and small particles were measured in several SEM images using the SEM software, to analyse how the PSD range were changing with milling time. It is important to point out that the PSD range is not representative for the distribution of the sample, as it is based on the smallest and largest particles as described in the procedure section. The PSD range is mainly illustrating the range from smallest to largest particle size, which was helpful in analysing how the milling time affected the samples. For the samples that were going to be used in further analysing studies a more representative PSD was made, as described in the procedure section. The microcline samples behaved almost identical to anorthite, therefore only the analysis results from the final milling time have been presented in this section, the rest (SEM images and PSD) are presented in appendix A.7.8 - A.7.12. It is important to notice the scale in the SEM images, as this is varying for each picture.

5.1.2.1 Anorthite, unmilled

Figure 20 shows how pre milling preparation affected the mineral sample. As can be seen in the SEM image, the sample consists of very large particles and very small particles. The smaller particles are reactive towards the larger particles, sticking onto them. Larger particles are covered with dust particles. This particular sample is not likely to produce stable and repeatable results due to high heterogeneity and large span of particle sizes. Inspection of particle sizes also revealed particles larger than 500 microns, thus the sieve was not capable of holding back all particles $\leq 0.5mm$.

This is related to the shape of the particles, very few of them are symmetric and regularly shaped. Many of them are rectangular having one length longer than another. Depending on orientation of the particle when it goes though the sieve, a larger particle can escape the mesh of a smaller size if it is oriented in such a way that the smallest side can pass the mesh size. Also smaller particles can be prevented from going through a larger mesh size if they are packed in clusters. Sieving is therefore not the most accurate procedure when sorting particles and considering PSD.

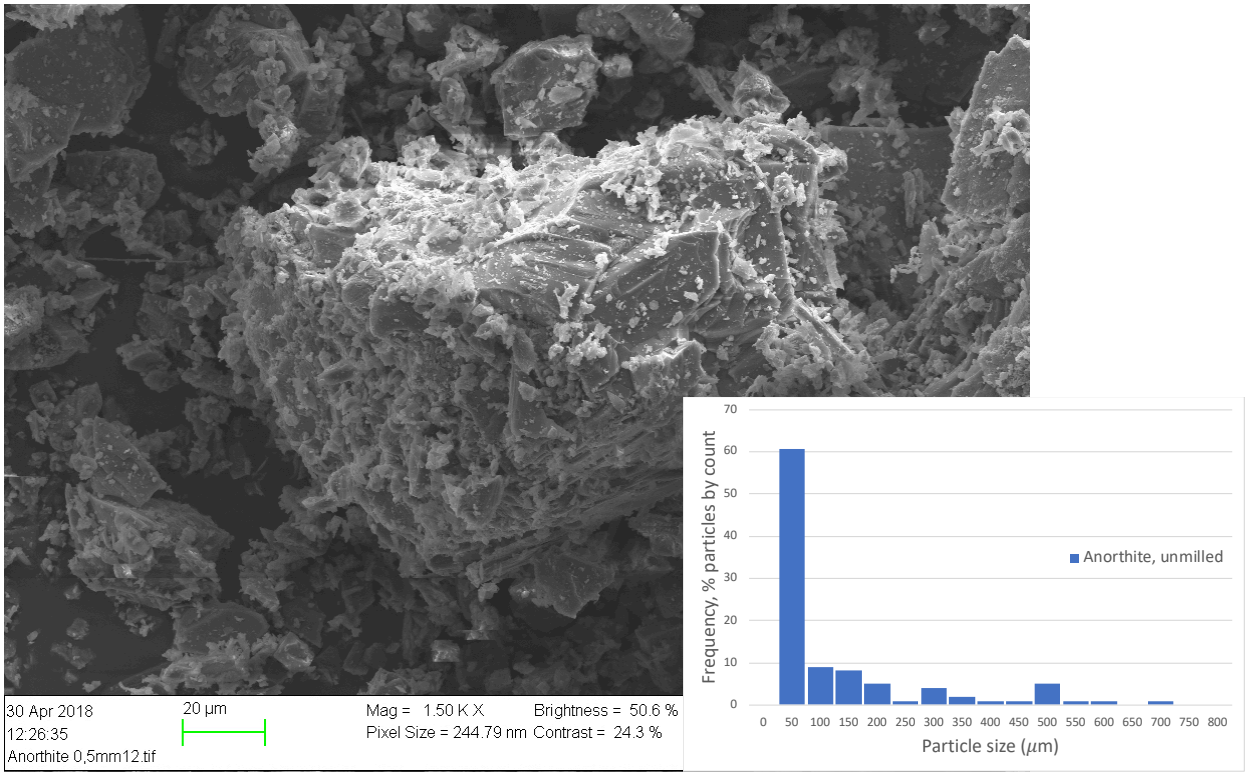

Figure 20: SEM image and PSD of an unmilled anorthite sample which has been crushed and sieved through 0.5 mm mesh using the milling preparation set.

5.1.2.2 Anorthite milled 1 minute

After milling the particles 1 minute using the XRD mill, the particle sizes were reduced significantly compared to the unmilled sample, figure 21. The sample consist of large particles and very small particles. Maximum measured particle size is $175\mu m$. Small particles are sticking onto surfaces of the larger particles. The shapes are non symmetric, almost rectangular for many of the larger ones. As can be seen in PSD to the right the sample has a wide range of particle sizes after just 1 minute milling. Particle sizes varies from $< 5\mu m$ to $180\mu m$. The PSD is skewed to the left, having a large amount of small particles compared to large ones. Samples milled 1 minute are too heterogeneous with too large PSD span to provide representative sample for stable analysis.

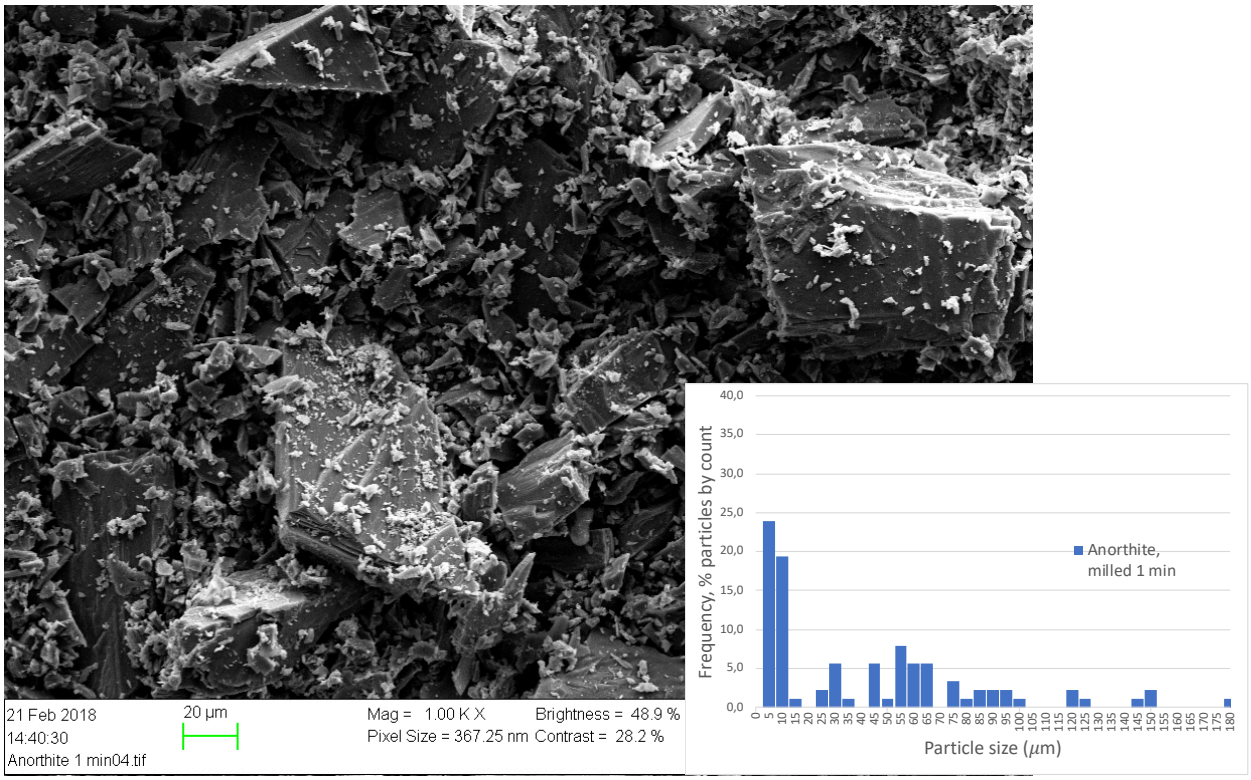

Figure 21: SEM image and PSD of anorthite sample, milled 1 minute

5.1.2.3 Anorthite milled 2 minutes

Inspection of SEM images after 2 minutes milling, figure 22, show large difference in both size and shape. The largest particle size has decreased compared to 1 minute milling sample, quantified to be $154\mu m$. The PSD is skewed to the left, having a much larger amount of small particles compared to large ones. The sample is too heterogeneous with too large PSD range and a longer milling time was considered.

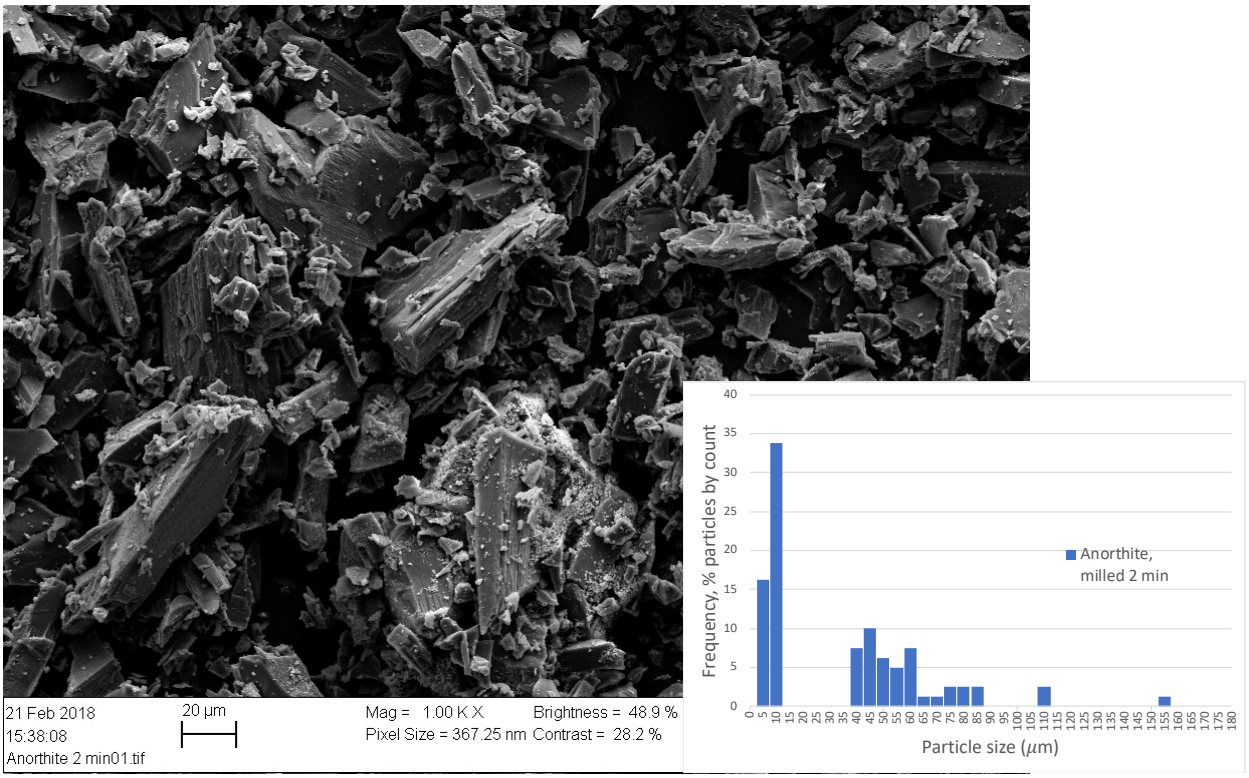

Figure 22: SEM image and PSD of anorthite sample, milled 2 minutes

5.1.2.4 Anorthite milled 3 minutes

Analysis of SEM images for the samples milled 3 minutes, figure 23, show improvement compared to shorter milling times, but still samples had too large span of particle sizes resulting in heterogeneous sample. Compared to the previous results, the distribution is starting to gather and becoming less spread which is what is the goal for the mineral preparation. Still there are too high amount of small particles. Particles are different both in shape and size. As the milling time is increasing, particles become more homogeneous due to reduction in the largest particle size. Largest particle size was measured to be $64\mu m$. Not a lot of dust are identified, suggesting gentle milling.

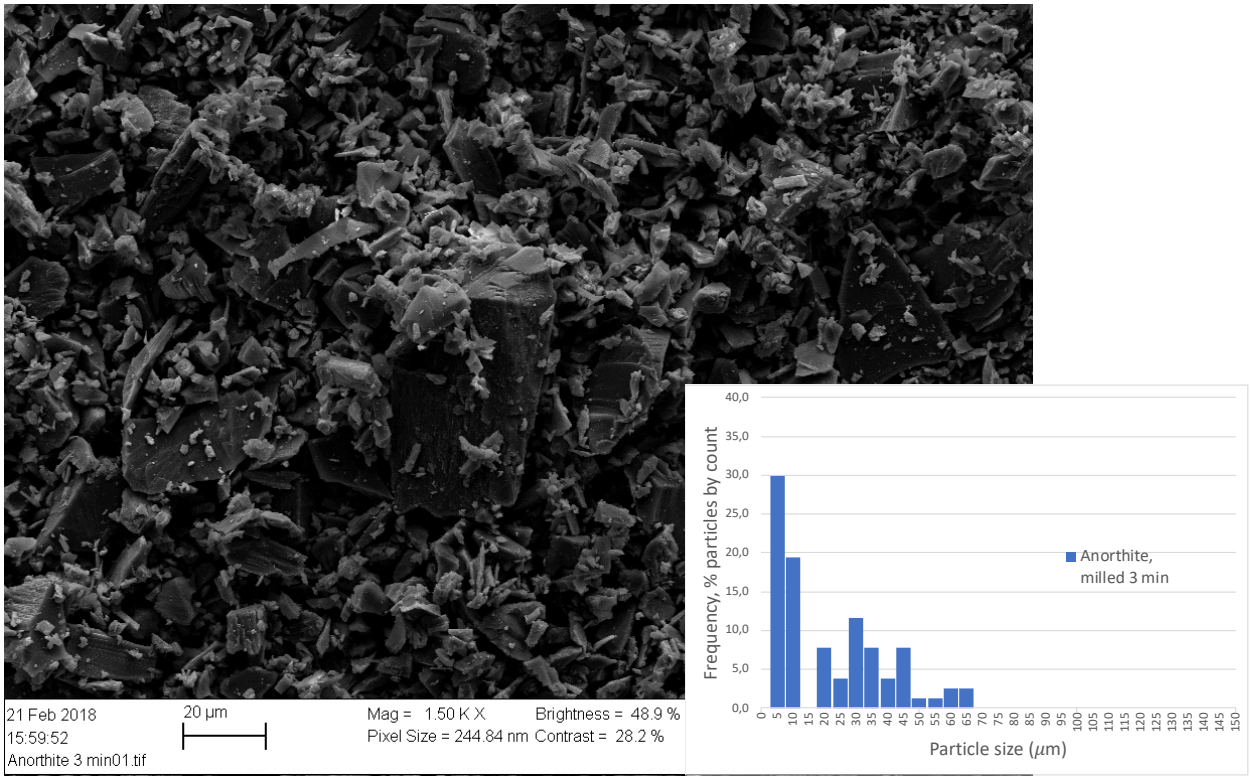

Figure 23: SEM image and PSD of anorthite sample, milled 3 minutes

5.1.2.5 Anorthite milled 5 minutes

After milling the sample 5 minutes, the largest particles have decreased in size, figure 24. Largest particle was measured to be $50\mu m$. The scale should be noticed, as it is smaller than previous SEM images for shorter milling times. Shapes are non-symmetric and irregular. A less heterogeneous PSD is observed with particles starting to gather in range. Difference between smallest and largest size is still too large. The small particles are dominating and shifting the distribution to the left.

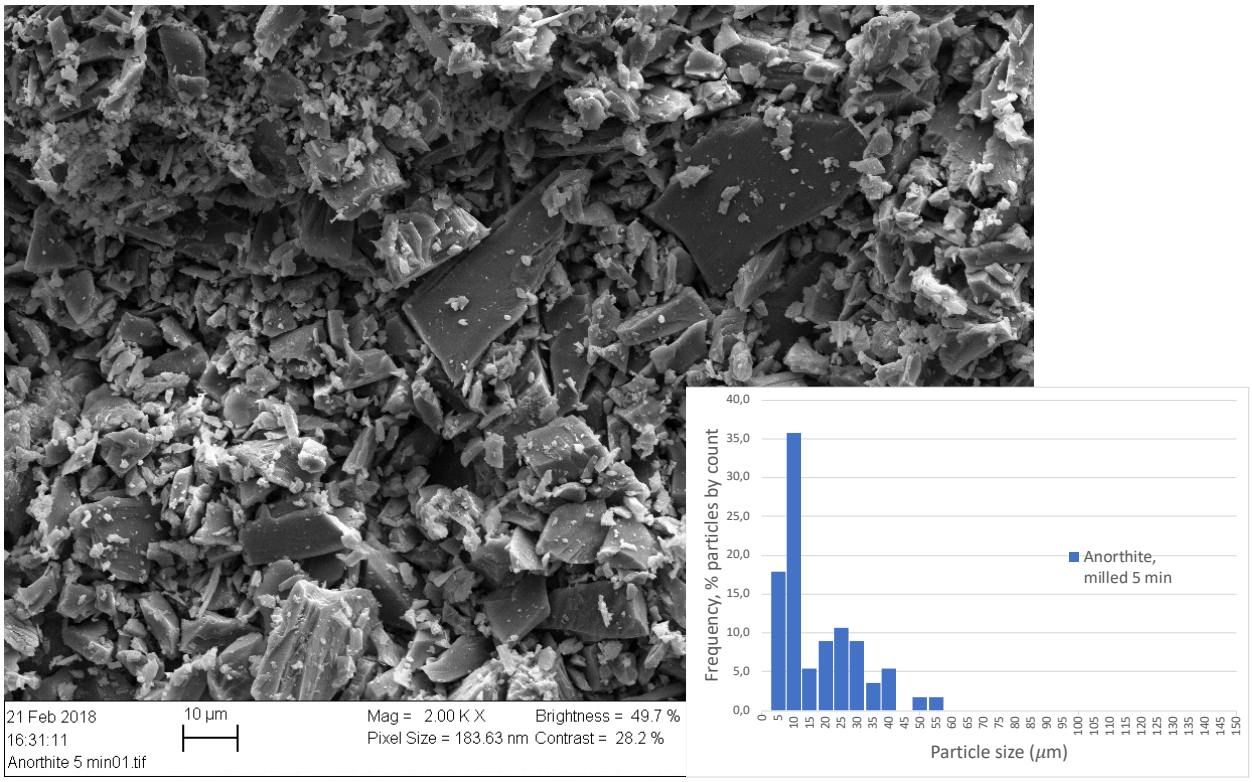

Figure 24: SEM image and PSD of anorthite sample, milled 5 minutes

5.1.2.6 Anorthite milled 7 minutes

After milling 7 minutes, the largest particle was approximately 30 microns, figure 25, and it was decided to not increase the milling time further. The sample is still not homogeneous, but continued milling would make the particles very small and very reactive. Several clusters of small particles can be identified, figure 25.

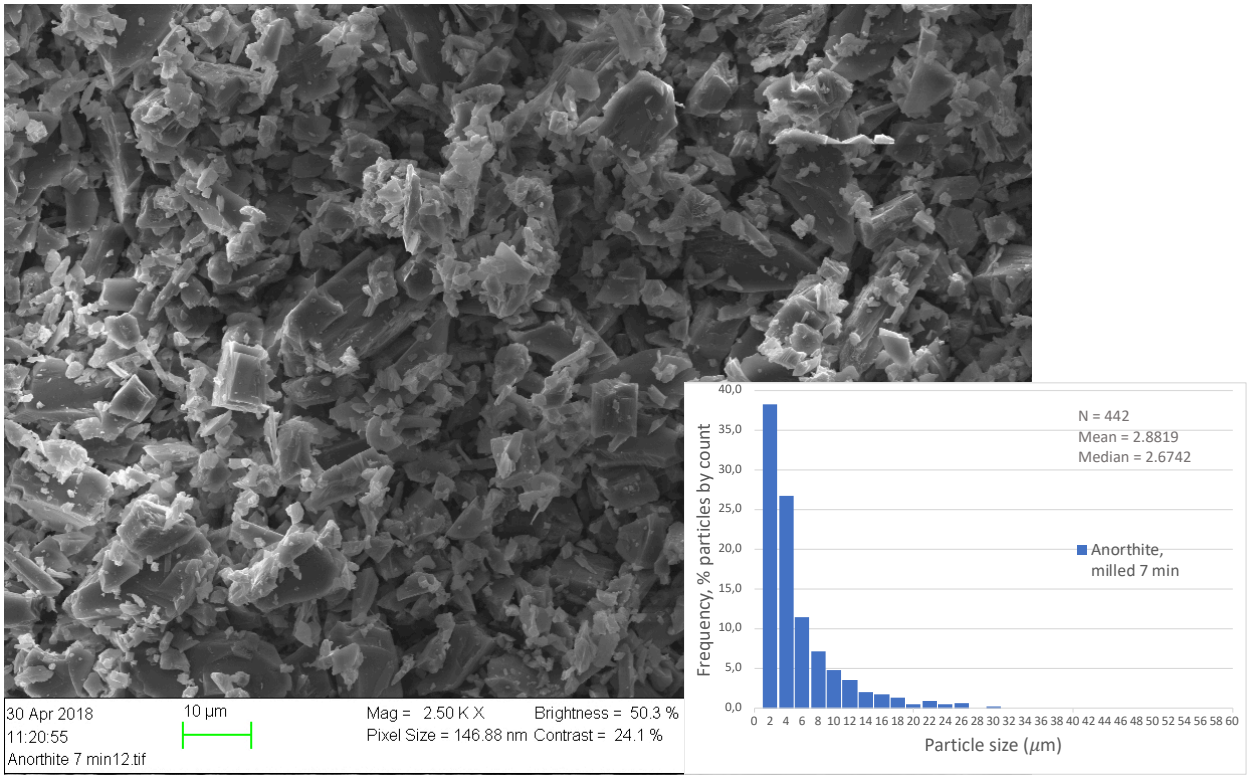

Figure 25: SEM image and PSD of anorthite sample, milled 7 minutes

The particle size range is in the fraction of clay and silt, figure 7. At this range, the chemical properties of the material will depend on shape and size, and it is therefore vital to have shape and sizes in as narrow range as possible. SEM analysis of the milled particles identified too many small particles present, which will be more reactive than larger ones. To remove these, a sedimentation procedure was done. Abdullah (2016) used sedimentation procedure to separate the smallest particles from the larger ones, and managed to improve her results. It was decided to perform the same procedure for the milled particles. After analysing all SEM and BET for the milled samples, a final milling time of 7 minutes gave the best distribution of particles.

5.1.2.7 Anorthite milled 7 minutes and settled

In figure 26 the sample has been settled after milling. Several small particles can be identified together with larger ones. Ideally, particles in the clay fraction ($< 2\mu m$) should have been separated from the samples, but quite large quantities are still present. Compared to the unsettled sample the amount of particles $< 2\mu m$ have decreased with settling, suggesting that the settling had some effect, yet not as much as hoped for. Estimation of particle sizes that are expected to be removed from the settling procedure is done by Stokes law, equation 21, calculations are presented in appendix A.6.1. According to calculations, settling procedure should remove particles $< 3.8\mu m$. Stokes law assumes spherical particles, the SEM analysis reveal very few spherical particles, at least that can be seen with the naked eye. Still, as the particles are milled to very small sizes, they become more and more even in shape and can be approximated as spherical particles. Several factors could impact the result. Clusters of particles and the very high reactivity of smaller particles sticking onto larger ones could have impacted the settling process. The sample is still heterogeneous to some extent, but considered within an acceptable PSD range.

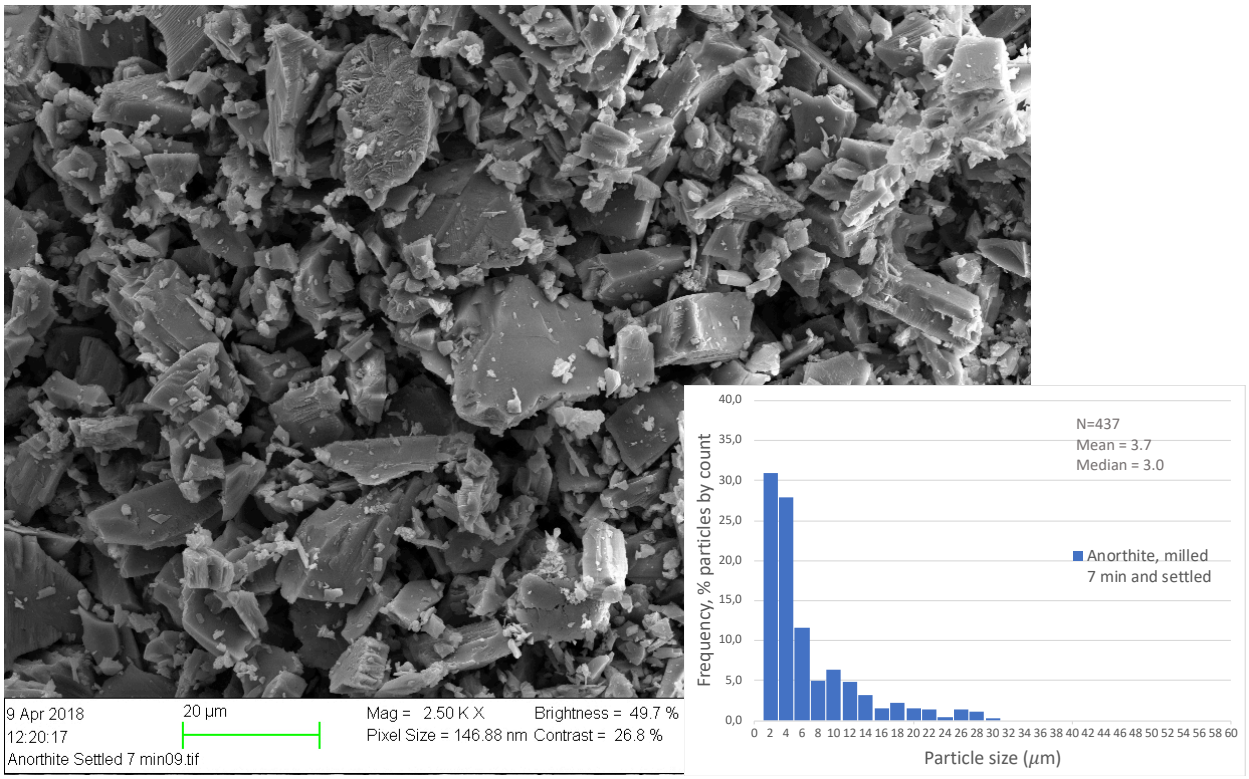

Figure 26: SEM image and PSD of anorthite sample, milled 7 minutes and settled to remove small particles

5.1.2.8 Microcline milled 7 minutes

Figure 27 displays the PSD for microcline milled 7 minutes. The largest measured particle is $\leq 34\mu m$, and PSD is nicely gathered in a small range. The small particles are dominating and the distribution is skewed to the left. A total of 598 particles were measured to determine the PSD of the sample. Median particle size is 3.2 μm meaning that 50 % of the particles are below this value and 50 % above.

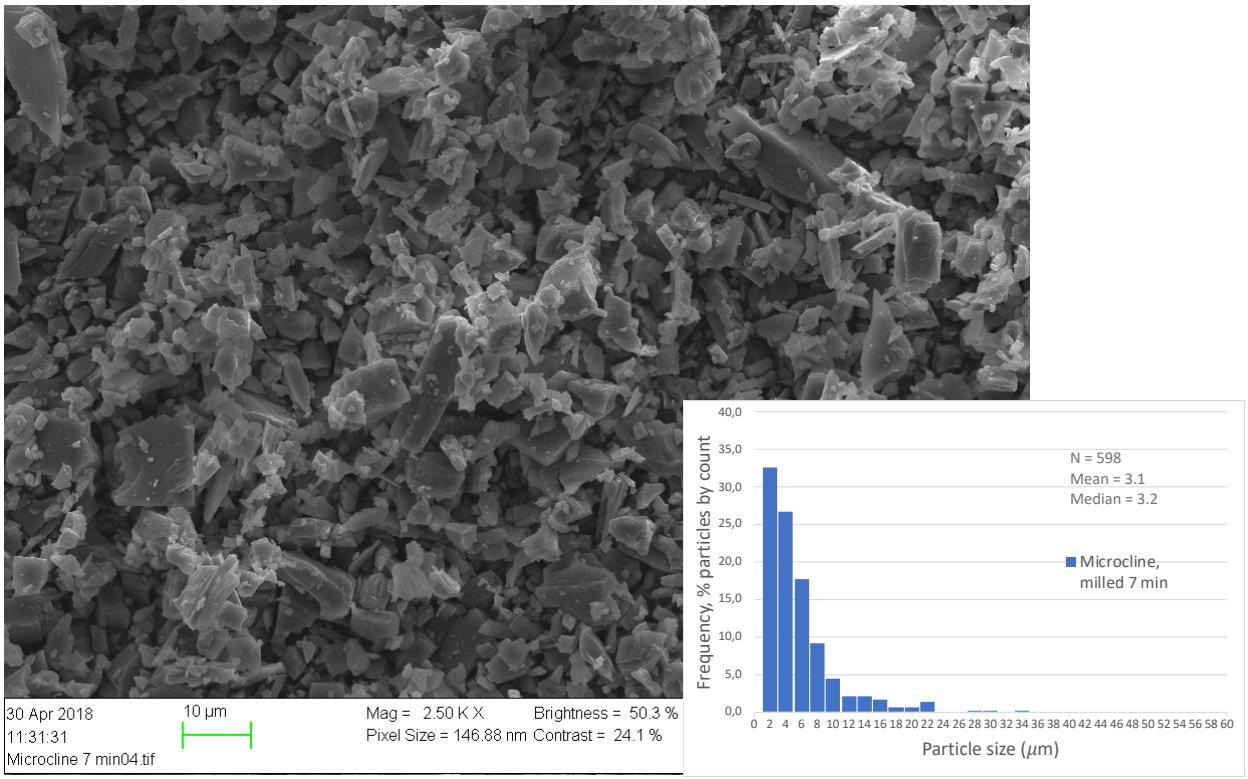

Figure 27: SEM image and PSD of microcline sample, milled 7 minutes

5.1.2.9 Microcline milled 7 minutes and settled

Figure 28 displays the SEM image and the PSD for microcline milled 7 minutes and then settled. The PSD has been determined from SEM images as described in procedures. A total of 425 particles were measured, giving a median of $2.8\mu m$. The largest particle size is $\leq 34\mu m$, and PSD is nicely gathered in a small range. A sedimentation procedure was performed for this sample, and the amount of particles $\leq 2\mu m$ was expected to go down compared to the unsettled sample that was milled 7 minutes, but it is actually higher. This high amount of small particles present was also observed in the BET analysis for microcline. The settled sample had a higher surface area than the unsettled one, which should have been opposite. Clusters of small particles could impact the success of a sedimentation procedure, several clusters were identified in the SEM analysis, figure 27. There are also several uncertainties in the result. The PSD is determined from random SEM images, that only represent small sections of the mineral sample. Also, the mineral samples itself can impact the results. When working with dry powder at this particle size range, there will always be some differences within each sample.

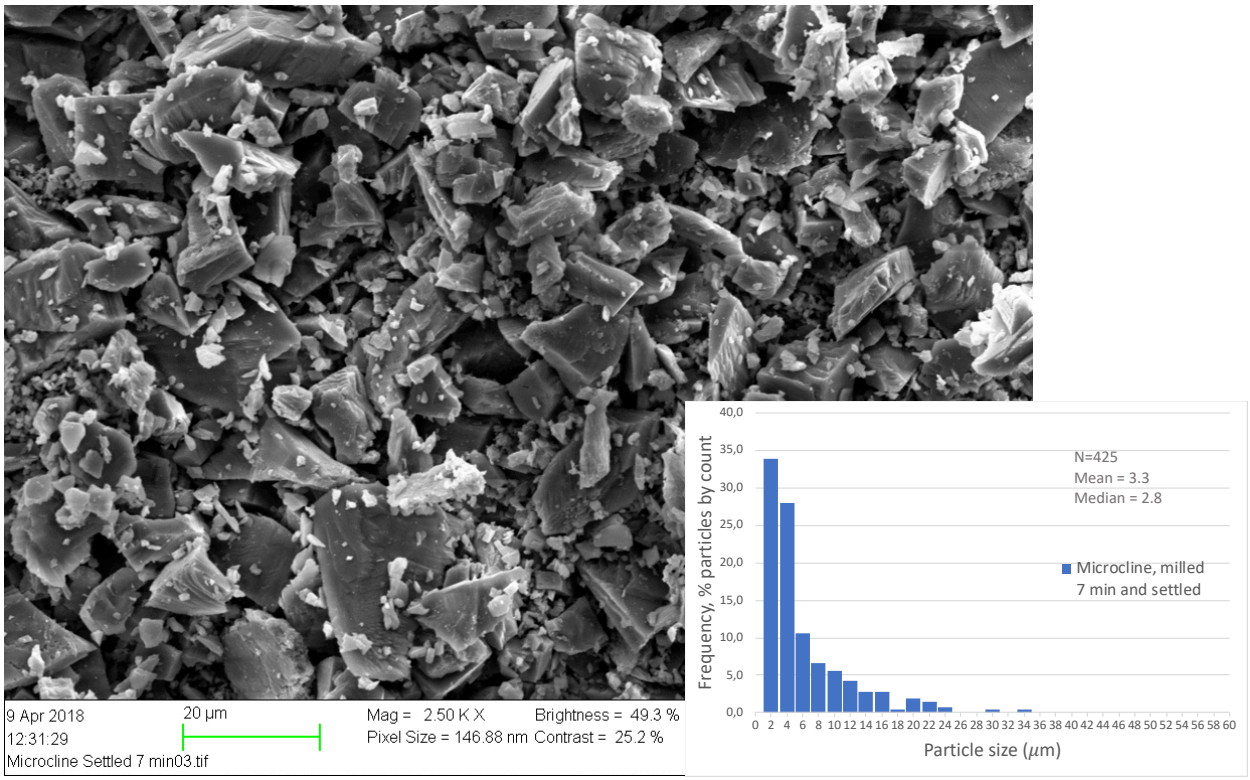

Figure 28: SEM image and PSD of microcline sample, milled 7 minutes and settled

5.2 Influence of feldspar minerals reactivity on solid / liquid interface in reservoirs

After making optimized mineral samples with PSD and BET surface area within acceptable range, their reproducibility was analysed from static adsorption tests and static pH screening tests.

5.2.1 Adsorption of Polar Basic Organic Components onto Feldspars

Static adsorption of quinoline onto feldspar minerals were studied using both HS and LS brines. Three parallel samples have been made for each test, one with low pH, one with intermediate pH and one neutral pH. Brines and mineral sample have been equilibrated 24 hrs before adding quinoline. After adding quinoline, pH has been adjusted to pH $\sim$ 3, pH $\sim$ 5 and pH $\sim$ 7, before letting the samples equilibrate 24 hrs. After equilibration, real pH was measured at ambient temperature. Measured absorbance was used to calculate adsorption. The calculated adsorption values have been plotted against the measured real pH of the solution after being equilibrated 24+24 hrs, figure 29 and figure 30. Measured values and calculations are presented in the appendix, table A6 - A13.

Figure 29 shows adsorption of quinoline onto anorthite at different pH for LS and HS brines. Generally low adsorption are observed for anorthite, all samples have adsorption below $2.5 mg\ base/g\ anorthite$ at any of the tested pH. The results are not very consistent. Variations are most likely caused by uncertainties in the experiment. The adsorption tests consisted of several steps as described in procedures, each adding additional uncertainty to the results. Feldspars are highly reactive in the presence of water and will exchange cations with the water phase, their reactivity depends on both salinity and pH. Protonation of quinoline is dependent on pH, and will

vary accordingly. No trend can be identified within the tested pH range, and no clear dependence on pH is observed. All tests show very little adsorption in the first sample at low pH. No repeatability is observed in the tests.

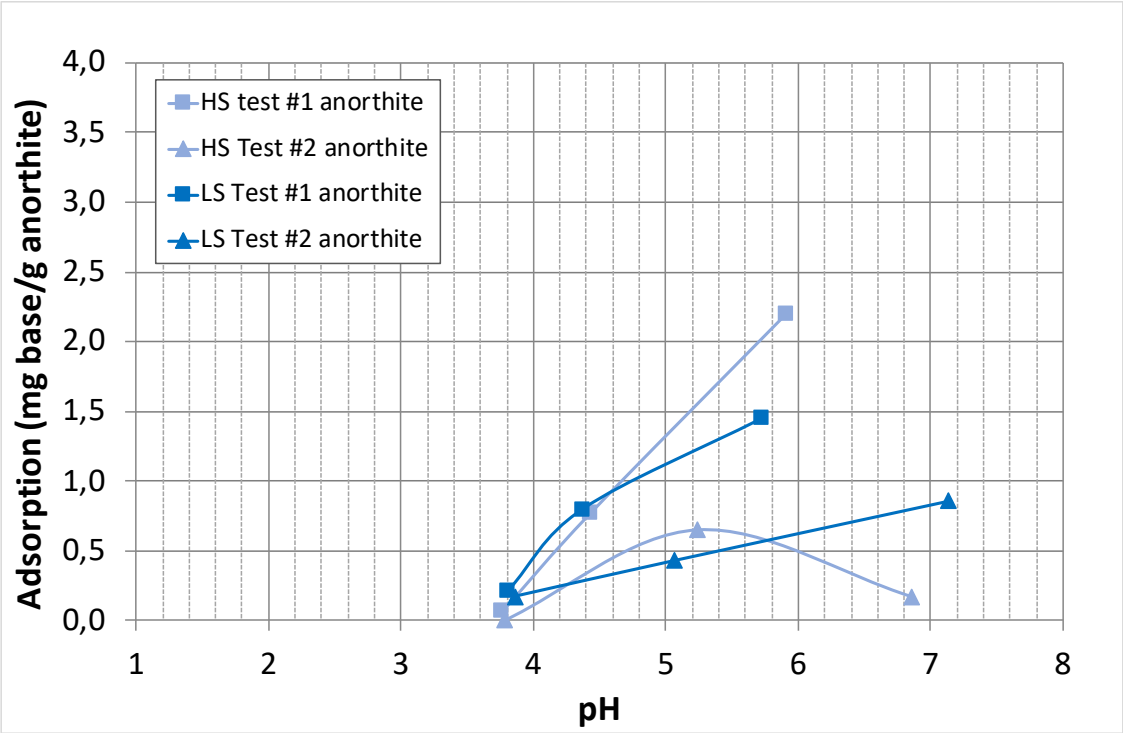

Figure 29: Adsorption vs real pH, ambient temperature, LSQ and HSQ with anorthite

Results from the static adsorption of quinoline onto microcline are shown in figure 30. Microcline behaves very similar as anorthite regarding adsorption, figure 29, large variations and no trends can be identified. None of the samples show any dependence on pH. Most adsorption values are within a ~ 2.0 margin, the very high adsorption above this range is probably not representative. Variations are most likely due to uncertainties caused by the many steps in the adsorption test procedure and the several factors affected by the difference in reactivity of the brine, feldspar and quinoline. The results are very inconsistent. Test #1 have larger adsorption values compared to the repeated test #2. All tests show very little adsorption for the first sample, and then adsorption increase as the pH increases.

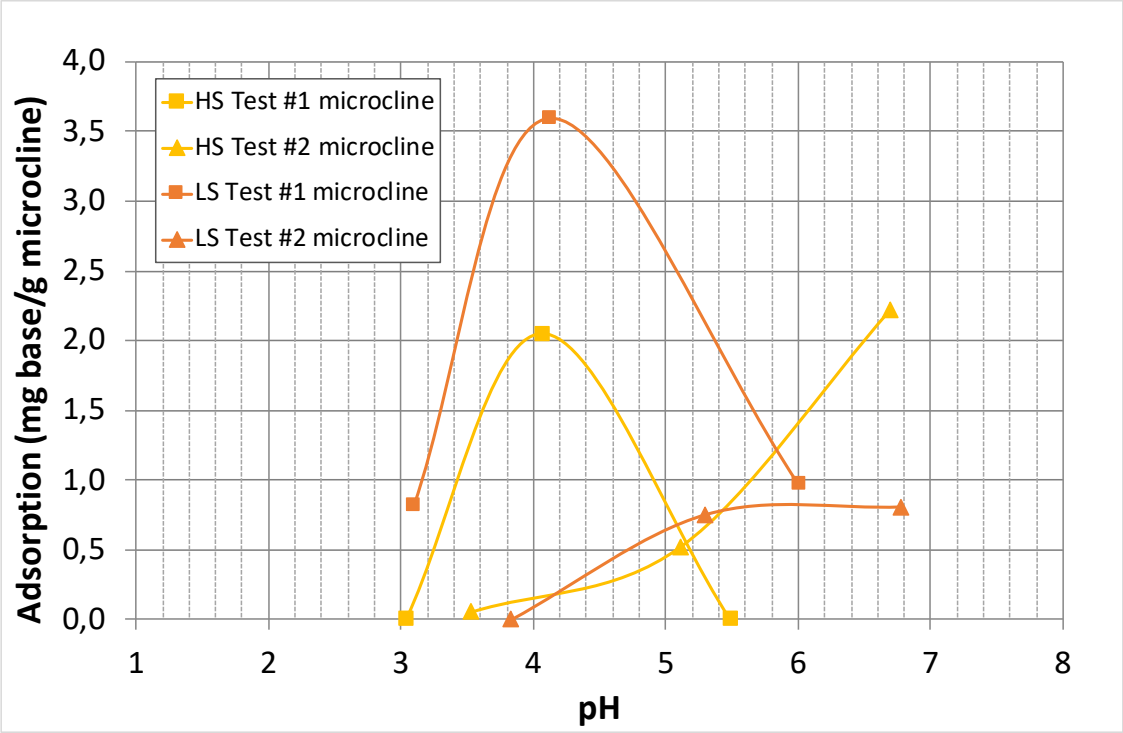

Figure 30: Adsorption vs real pH, ambient temperature, LSQ and HSQ with microcline

5.2.2 pH Screening Results Using New Preparation Method

10 wt% of anorthite was mixed with 90 wt% of brine, then pH of the brine/minral sample was adjusted to an initial pH $\sim$ 5 before equilibirated at ambient temperature for 24 hrs. All pH measurements are conducted at ambient temperature.

Results from the pH screening test using optimized mineral samples are presented in figure 31. A pH increase, from the initial pH $\sim$ 5, is observed for all salinities. The largest pH response is observed with DI water, with an increase of 4.5 pH units. A decrease in pH response is observed at 1000 ppm salinity. Then as salinity is increasing, the increase in pH is decreasing gradually. At 100 000 ppm the pH in the sample has increased approximately 3.8 pH units. Measured pH data is presented in table 10.

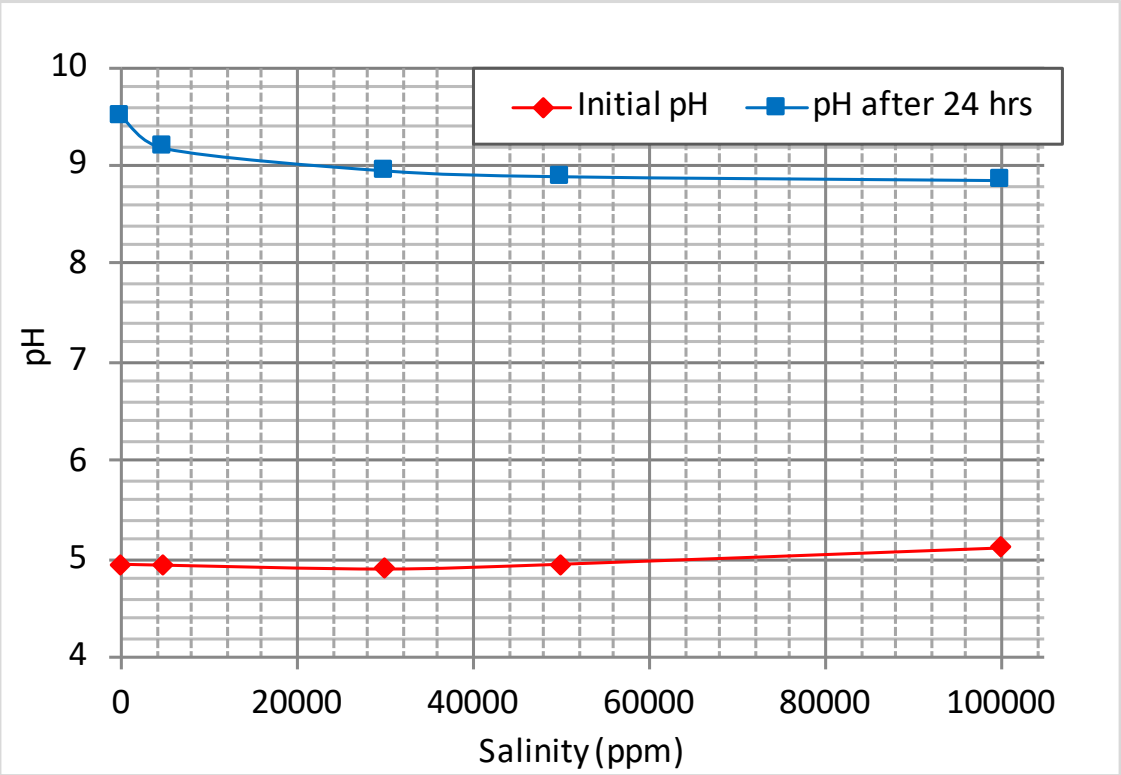

Figure 31: pH screening test results for anorthite, ambient temperature. Initial pH is the adjusted pH to approximately pH 5. pH after 24 hrs is the measured pH after equilibrating the mineral+brine with pH 5 for 24 hrs

5.2.3 Ion Composition Analysis

An IC analysis was performed on the brine that has been equilibrated with anorthite for 24 hrs. An initial inspection of the raw data, table A14 was performed to verify if the results were trustworthy. E.g. verifying high sodium concentrations for the HS calibration brine and low sodium concentrations for the LS calibration brine. To perform an IC analysis, the salinity brines had to be diluted. It was not possible to see any trace elements in the diluted samples because the concentration was extremely low. It was possible to identify some trace elements in the DI sample because this was not diluted. Results from the DI IC analysis are presented below.

From the IC of DI water analysis, it was possible to see traces of ions in the solution, figure 32. Traces of both Na^+, K^+ and Ca^2+ were detected in the sample, suggesting that the anorthite sample was not pure. The traces of ions in the solution confirm that there has been an ion exchange in the brine, between the mineral and the liquid.

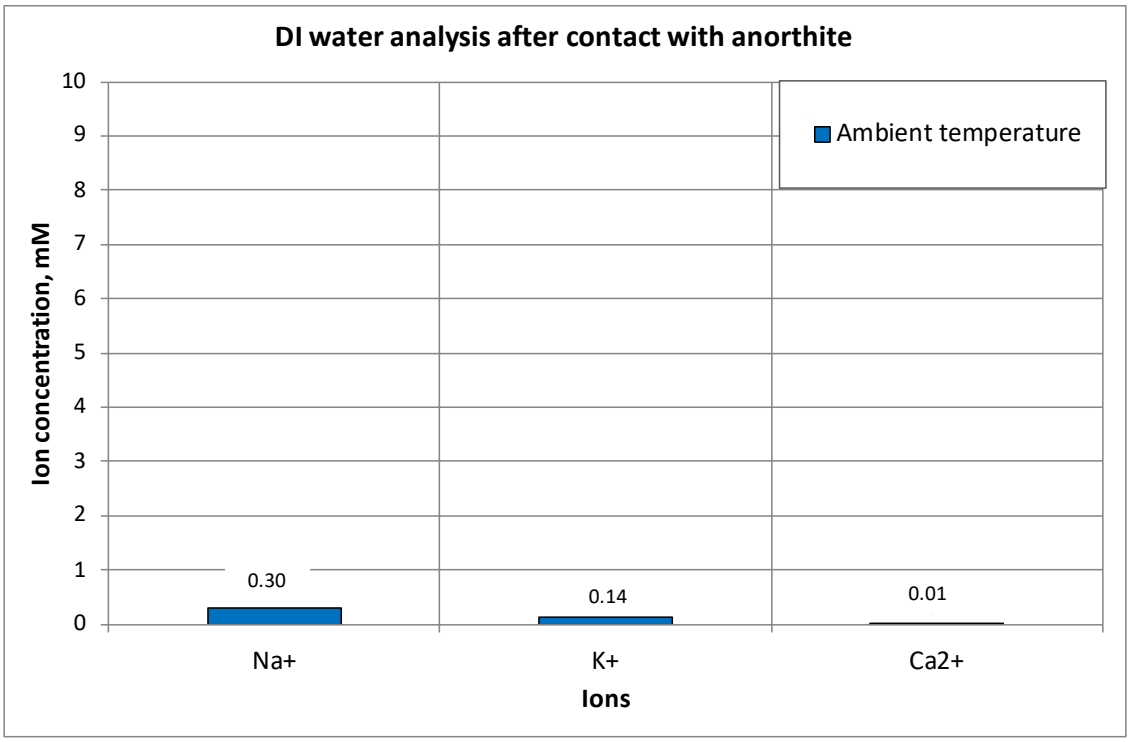

Figure 32: IC analysis of DI water equilibrated 24 hrs with anorthite

6 Discussion

The experimental results are discussed and compared with experiments performed by other students at the University of Stavanger and in relation to published articles for low salinity EOR processes where changes in pH is the promoted mechanism behind the wettability change in the rock. Other mineral preparation procedures are also discussed.

6.1 Optimal mineral preparation

Previously there has been performed several attempts at the University of Stavanger to identify the behaviour of feldspar minerals regarding initial wetting and influence on wettability aleterations in a Smart water EOR process. Andersen (2015) analysed the influence of feldspar minerals on pH by doing static pH screening tests. Frafjord (2015) performed static adsorption tests on clays to determine how they reacted and managed to get repeatable and stable results. Then Abdullah (2016) performed static adsorption tests on feldspars, which unfortunately resulted in unstable and non conclusive results. Harestad (2017), Tat (2017) and Algazban (2017) tried to repeat the results obtained by Abdullah (2016) by using the same milling equipment combined with a sedimentation procedure and ripening process and managed to improve the results.

For all the previous tests rock samples were milled using a Retch Planetary Ball Mill PM 100. This resulted in heterogeneous particle size distribution with a lot of dusty particles. Depending on size of mineral surfaces, the reactivity is different. Small particles react stronger than large particles, and a heterogeneous particle size distribution will give unreliable and unstable results. Main motivation for this thesis has been to optimize the mineral samples using new milling equipment and then redo some of the adsorption and pH tests done by Abdullah (2016), Harestad (2017), Tat (2017) and Andersen (2015) to compare and verify results. When the samples were prepared using the Retch Planetary Ball Mill PM 100 the procedure will be referred to old preparation procedure. While preparation of minerals using the new XRD mill will be referred to as new preparation procedure.

6.1.1 Comparison milling equipment

In previous experiments performed at the University of Stavanger (Andersen, 2015; Abdullah, 2016), mineral preparation was performed using Retch Planetary Ball Mill PM 100. This ball mill has extremely high centrifugal forces creating very high pulverization energy, which result in extremely fine particles (RETSCH GmbH, 2018). For many purposes this is a effective and good milling technique, but it turned out to be a unwise choice for the feldspar analysis. Problems arose due to uneven particles with high level of heterogeneity. Some particles were too big and some too small which gave unpredictable and unstable results. In the feldspar adsorption analysis, PSD has shown to be very important (Abdullah, 2016). If the PSD is too heterogeneous and the particles are too small, as the values we are looking for are very sensitive, it is difficult to observe any trends in the results. It is therefore vital to control the milling of the particles, ensuring homogeneous PSD and preserve the crystal lattice of the minerals. The main goal in this thesis has therefore been to optimize the mineral preparation procedure using a new ball mill; The Retch XRD Mill McCrone. This mill has a very specific application area and is primarily used for preparation of samples of materials that are going to be analysed by XRD. A key point is the preservation of the crystal lattice structure. Other ball mills have an aggressive modus operandi which will destroy the crystal lattice. Irregularities in the crystal lattice provide a great number of unsatisfied bonds at the edges and as a result possibly increase the CEC (Carroll, 1959). This could greatly influence the analysis

results.

The McMCrone Mill however, employ very gentle modus operandi which will preserve the crystal lattice and will not induce any additional CEC to the sample (Retsch, 2018). By using the XRD mill and other preparation techniques, the main goal has been to find a procedure where a balance between particle sizes, homogeneity, and surface area are maintained. This ensures optimized samples for representative and stable analysis of the influence of feldspar minerals regarding adsorption of polar organic components and pH changes in a system.

6.1.1.1 Comparing SEM images for old and new prepartion procedure

Andersen (2015) used Retch Planetary Ball Mill PM 100 to mill the feldspar minerals 7 minutes. He analysed the samples using a SEM, figure 33 and figure 34. The samples looks crushed and destroyed compared to the particles that were milled 7 minutes using the XRD mill, figure 25 and figure 27. Particles that are crushed and destroyed will have more broken bonds and be more reactive than particles that are more preserved. The largest measured particle in the old preparation procedure is below $18\mu m$, while the largest particle identified using new preparation procedure is $30\mu m$. A large amount of small, dusty particles are identified in the SEM picture. The samples that have been milled with the XRD mill looks more preserved, with less dusty particles and a more homogeneous distribution. All of which is a result of the less aggressive modus operandi in the XRD mill compared to the Planetary mill.

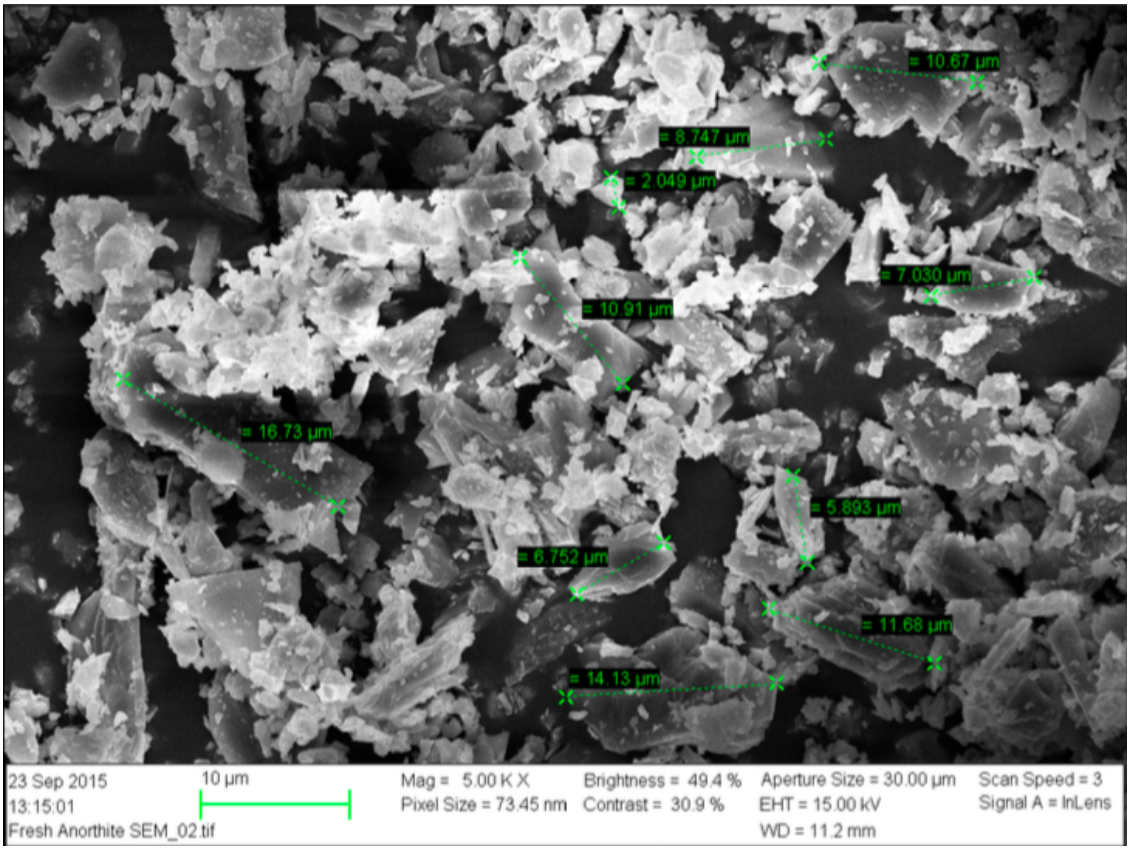

Figure 33: SEM image of anorthite after 7 minutes milling in Planetary ball mill (Andersen, 2015)

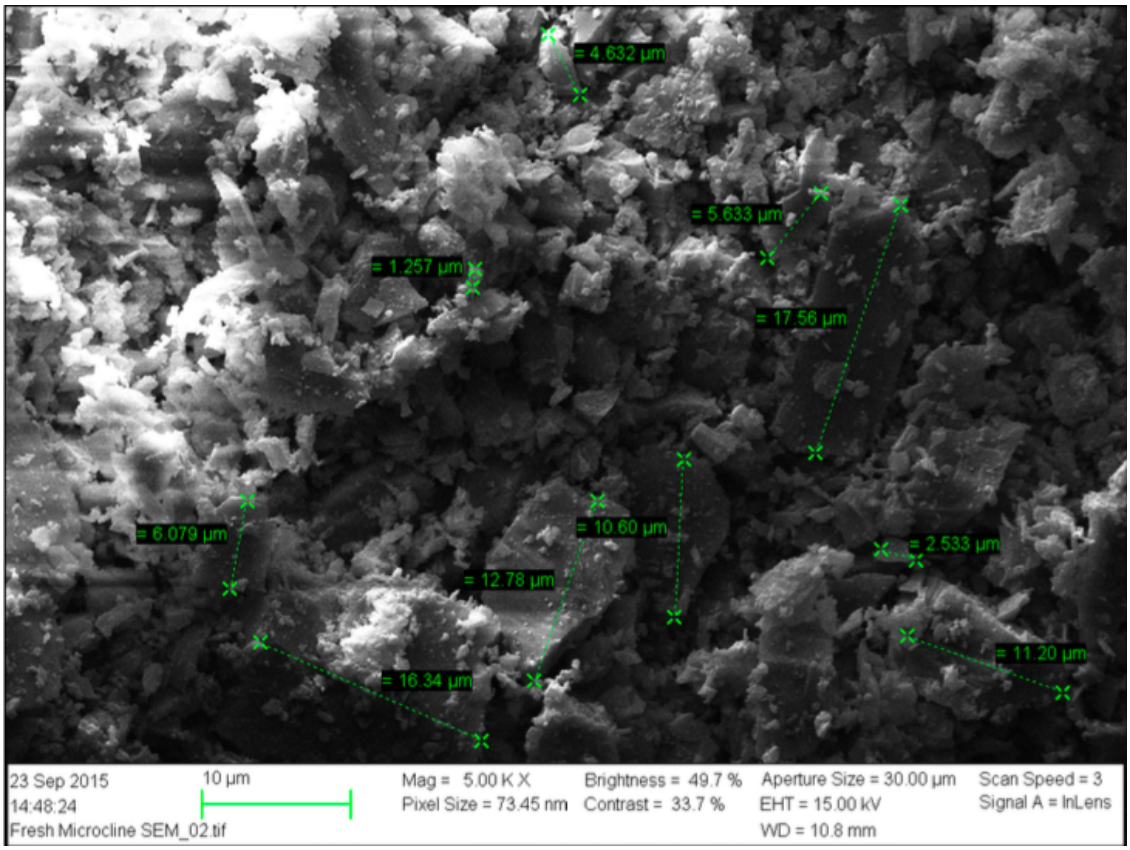

Figure 34: SEM image of microcline after 7 minutes milling in Planetary ball mill (Andersen, 2015)

6.1.2 Effect of milling time

Increasing milling time affected the particle sizes and consequently the BET surface area and PSD.

6.1.2.1 BET surface area

The BET surface area of the samples that were prepared using the XRD ball mill show a stable increase with milling time, figure 19. The stable increase suggest controlled milling of the particles which could make it possible to predict BET surface area from milling time.

A similar BET surface area measurement was performed by Andersen (2015) and Abdullah (2016). Comparing the specific surface areas for anorthite and microcline with their results, the areas of the optimized preparation samples are a bit lower, table 11. All mineral samples have been milled for 7 minutes, however samples milled using the Planetary mill provide a higher BET surface area. A very large amount of dusty, small particles were observed in the SEM images for the samples prepared with the planetary ball mill, figure 33 and figure 34. These small particles combined with a maximum particle sizes $< 18\mu m$ within the particle range are providing a higher surface area of the samples. Samples with large BET surface area are more reactive with higher CEC, which will affect analysis results.

Table 11: Comparison BET surface area from different preparation procedures

Mineral	Milling equipment	Milling fluid	Milling time ($minutes$)	BET surface area (m^2/g)
Anorthite	XRD ball mill	DI water	7	2.35
Anorthite	XRD ball mill	DI water	7*	2.23
Microcline	XRD ball mill	DI water	7	3.54
Microcline	XRD ball mill	DI water	7*	4.03
Microcline (Andersen, 2015)	Planetary ball mill	Methanol	7	4.66
Anorthite (Andersen, 2015)	Planetary ball mill	Methanol	7	3.26
Anorthite (Abdullah, 2016)	Planetary ball mill	DI water	7*	3.14

* the sample has been settled after milling

6.1.2.2 Particle Size Distribution

Figure 35 show how the maximum particle size decreases with increasing milling time. Both feldspars show a stable decline in size, microcline particles decreasing more rapid than anorthite. As the milling time increases, the particle sizes are getting smaller and smaller, as a result the particles will get more reactive. The particle size influences properties of the mineral, like surface area, shape and its reactivity in chemical reactions. The distribution of particles are often classified in terms of fractions, sand ($20\mu m - 2mm$), silt ($2 - 20\mu m$) and clay fraction ($< 2\mu m$), each having very different reactivity (TerraGIS, 2007).

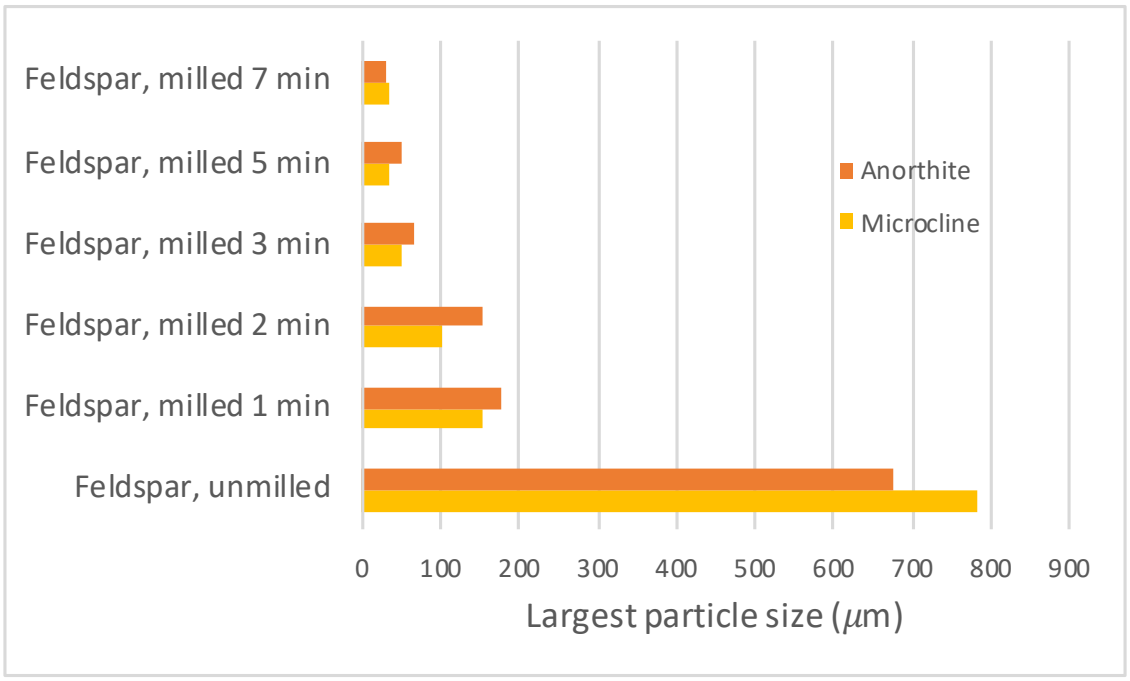

Figure 35: Maximum particle size of anorthite and microcline at different milling times. Particle sizes were obtained by identifying the largest particles from SEM pictures and measure them individually. On the y-axis the milling time for the mineral is increasing upwards.

The PSD for the feldspars are shown in the results section, figure 20 - 28. Before milling, the sample contained particles both from the clay fraction, silt fraction and sand fraction, each fraction having very different reactivity. The unmilled samples were very heterogeneous with a large PSD range. As the milling time is increased, the largest particle size is decreasing, the PSD range is narrowed. After 7 minutes milling time the largest particle is within the silt fraction. Continued milling would narrow the PSD range more, but as a consequence of this the amount of very small particles are also increasing. Increasing amount of small particles results in a higher surface area and higher reactivity. Therefore a 7 minutes milling time was considered a good choice for the optimal mineral preparation.

6.1.3 Effect of sedimentation process

After 7 minutes milling, the PSD of the feldspars show a left skewed distribution due to the large amount of particles $\leq 4\mu m$, figure 25 and figure 27. The PSD range contain both clay and silt fraction. At these fractions the chemical properties of the material will depend on shape and size, and it is therefore vital to have shape and sizes in as narrow range as possible. SEM analysis identified too many small particles present, which will be more reactive than larger ones. These small particles could affect analysis results due to difference in reactivity and surface area. It was attempted to remove the clay fraction ($< 2\mu m$) from the PSD range of the sample using a sedimentation procedure. In previous experiments (Abdullah, 2016), settling of the minerals had successfully removed the smallest particles, and this procedure was therefore chosen as a part of the preparation. In this way a more homogeneous PSD can be achieved, where more precise and repeatable results are expected.

After the sedimentation procedure, the amount of small particles had decreased but still the amount of small particles were high, figure 26 and figure 28. Calculated particle size that should

have been separated was $\sim 3.8\ \mu m$. SEM analysis identified several particles below this size, some even below $1\mu m$. Particles in the clay fraction are highly reactive, sticking onto larger particles and clustering. This have probably impacted the settling process.

The PSD of the samples after 7 minutes milling and settling are within an acceptable range, and the samples are expected to give representative results, figure 26 and figure 28.

6.1.4 Comparison with other preparation and analysis techniques

In previous adsorption experiments, a sedimentation process was performed on the samples to remove dust and small particles (Abdullah, 2016). Abdullah (2016) performed the settling initially with methanol to avoid loosing reactivity on the minerals. She also did a settling procedure using DI water. Feldspars in contact with water will exchange ions and thus loose reactivity which could underestimate results. However, feldspars settled with DI water and feldspars settled in methanol did not show large differences in reactivity. The milled minerals are highly reactive, so reactive that the adsorption tests did not show any negative impact from settling with DI water. Also, Methanol is poisonous and needs extreme care when handled. DI water is easier to work with and a safer choice when preparing the mineral samples, therefore it was chosen as milling and settling brine for all mineral preparation.

Mani et al. (2011) used ultrasonication combined with ball milling to produce nano-sized clay particles. By doing this they managed to improve the PSD of the clay-particles, and got a narrowed particle size distribution. One of their goals was to increase the specific surface area of the clay by reducing the clay particles and thereby increase the chemical activity of the inorganic materials. In ball milling, particles are reduced in size and get highly reactive. The problem of agglomeration arises when powder is in dry form. Dry particles usually consists of aggregates and agglomerates that can be dispersed using different chemicals, like xylene, to produce individual particles. In a ultrasonication process, particle assembly is disaggregated and deagglomerated due to cavitation phenomenon. As some of the very small particles were not removed by the sedimentation procedure, an ultrasonication process prior to settling of the particles could have improved the sedimentation process.

Mani et al. (2011) used laser diffraction for PSD ananlysis on nano-sized clay particles before and after an ultrasonication process. The PSD showed large changes after the ultrasonication process, suggesting that agglomerates of particles were present and affected the PSD results. By inspecting the particles using a SEM, the problem with agglomorates affecting the PSD measurements are removed. It was possible to identify clusters of small particles, which could have been detected as larger particle in a laser diffraction procedure.

A sedimentation procedure was performed on the milled sample, however this only partly succeeded in removing very small particles from the samples. Another method for controlling PSD of a sample is wet sieving. Wolfe et al. (2007) used wet sieving to produce a certain PSD range of a mineral sample. Combining a Büchner funnel with vacuum, and using filters to trap particles below a certain micron size, they managed to control the PSD of the samples according to a pre-specified range. Appropriate mesh sizes made it possible to produce a very specific PSD range. Prior to the wet sieving, they dispersed agglomerated particles by an ultrasonication process, making sure that small particles were not clustering and thus prevented from being sieved through mesh sizes larger than the particle. Wet sieving could be an approach for controlling the PSD of the feldspar minerals as well. A large drawback is the uncertainties caused by irregular shapes and sizes of the particles.

In the pre milling preparation samples were initially sieved through a 0.5 mm mesh. Analysis of the SEM images identified particles at almost 800 microns in size, which clearly shows how

uncertain the sieving technique is when analysing particle sizes.

6.2 Influence of feldspar minerals on solid / liquid interface in reservoirs

Smart Water EOR method has been discussed in the theoretical part of this thesis. The Smart Water EOR group at the University of Stavanger consists of several researchers that are developing methods for confirming the chemical mechanisms of wettability alteration in reservoirs, as first stated by Austad et al. (2010). The mineralogy in sandstones are very important in regarding the establishment of initial wetting and wettability alterations (Austad et al., 2010; Piñerez Torrijos, 2017; Mamonov et al., 2017; Aksulu et al., 2012; Piñerez Torrijos et al., 2017; Strand et al., 2014; Aghaeifar et al., 2015; RezaeiDoust et al., 2011; Reinholdtsen et al., 2011). It was noticed that from a chemical point of view wettability can be established by adsorption of various polar components from crude oil onto mineral surfaces. It was also noticed that this process is pH dependent. The feldspar minerals can affect the pH, it can buffer the pH and control the pH in the reservoir, which has been confirmed by many tests (Strand et al., 2016; Mamonov et al., 2017; Reinholdtsen et al., 2011; Aksulu et al., 2012; Piñerez Torrijos et al., 2017; Strand et al., 2014). Feldspar minerals can control pH of a system, and to confirm the contribution of feldspars it was decided to perform different types of studies. First type, a static adsorption study to see if the polar components can actually be adsorbed onto feldspar minerals and how important is that in terms of sandstone reservoirs and wettability. The second is to study the actual contribution of feldspar onto pH buffering / pH changes from static pH screening tests accompanied by IC analysis.

6.2.1 Adsorption of polar organic basic components onto feldspar minerals

It has been verified by several experiments that clay minerals are capable of adsorbing polar organic components onto the mineral surface and thus control initial wetting. Feldspars have a net negative charge and CEC thus could potentially contribute in adsorbing polar organic basic components. To verify if feldspars are adsorbing polar organic basic components static adsorption tests were performed. Initial static adsorption studies were tested on clay minerals (Frafjord, 2015). She managed to get stable, reliable and repeatable results.

Using the old mineral preparation procedure it was performed some studies on feldspars previous years by other students, (Abdullah, 2016; Harestad, 2017; Algazban, 2017; Tat, 2017). Due to heterogeneous mineral samples the results were non conclusive, figure 1. In this thesis the minerals have been prepared using different milling equipment which applies a very gentle milling technique compared to the milling equipment that was used previously. The milling time has been controlled to have a balance between BET surface area and homogeneous PSD. One key point is the preservation of the crystal lattice.

In the results from the adsorption tests using the new mineral preparation some adsorption could be observed, figure 29 and figure 30. This adsorption was a bit higher compared to previous tests figure 2 and figure 3, however the adsorption is still low.

No trend could be identified in the results, but all tests showed minimum adsorption in the first sample at low pH followed by an increase in adsorption for sample 2 at higher pH. No conclusions can be made from this, yet there could be some interactions at this low pH, preventing the base from adsorbing. Clays have maximum adsorption at pH around 5, where the polar organic components are highly protonated. Maybe the adsorption onto feldspars also is affected by pH. The solubility of feldspars is dependent on pH both at acidic and basic conditions (Gülgönül et al., 2012). According to Blum (1994) the experimental dissolution rate has shown to increase with increasing proton activity at pH < 6. This could explain why there are less adsorption observed at this very low pH.

At low pH, there are more free protons in solution that are highly reactive towards the feldspar minerals which will compete and prevent adsorption of polar organic components. The observed increase in adsorption onto feldspars with increase in pH could be caused by less free protons in solution. The polar organic components would have higher chances of adsorbing onto the mineral surface when there are less reactivity at the surface. However, due to the unstable results these are only speculations and can therefore not be concluded.

Some variations were observed in the adsorption results, figure 29 and figure 30. Feldspars are chemically unstable at ambient temperatures in the presence of water (Grotzinger and Jordan, 2010) and will react immediately with the water phase through cation exchange. Their reactivity is also dependent on pH (Gülgönül et al., 2012). This generate additional uncertainty in the adsorption results. The addition of the polar organic components increases the uncertainty even more. Quinoline are more or less protonated depending on pH, and will adsorb and desorb accordingly. Feldspars have shown to influence the pH of a system, which will impact the chemical reactions during the adsorption of the polar components making it hard to monitor and get stable results. This mixture in pH by mineral and liquid interactions is quite complicated and hard to quantify and will generate extra uncertainty in the results.

6.2.2 Comparison adsorption of polar organic basic components onto feldspars and kaolinite

The static adsorption tests showed that the feldspars managed to adsorb some quinoline, but compared with kaolinite (Frafjord, 2015) the adsorption is generally low, figure 36. Kaolinite adsorption show dependence on pH while it is hard to identify any pH dependence in the feldspar adsorption. A clear trend is observed in the kaolinite adsorption, this trend was similar for other clays as well (Frafjord, 2015). The adsorption is highest at pH around 5, which is very close to the pK_a value for quionline. At pH values below and above the vertex, adsorption onto kaolinite decreases. Low pH has high concentration of H^+ and quinoline is protonated by the high H^+ activity. The protonated quinoline is attracted to clay surface. Excessive presence of higher affinity H^+ takes priority to the clay surface and a decrease in adsorption is observed. At high pH the adsorption decreases. This is caused by the high $[OH^-]$ which reacts with the quinoline proton and neutralizes it. This neutrally charged organic compound will not be able to adsorb to the kaolinite surface, resulting in a more water-wet system.

No trend can be identified in the feldspar adsorption, the values varies from test to test but generally the adsorption onto the feldspars are below 2, the higher adsorption values are probably erroneous. The variations are caused by uncertainties in the experimental procedure. Also, as mentioned previously, feldspars are highly unstable in the presence of water. Kaolinite show a much more stable behaviour in contact with water at ambient temperature due to its 1:1 structure, which generates more repeatable results. Also the clays have a homogeneous PSD within a very narrow range.

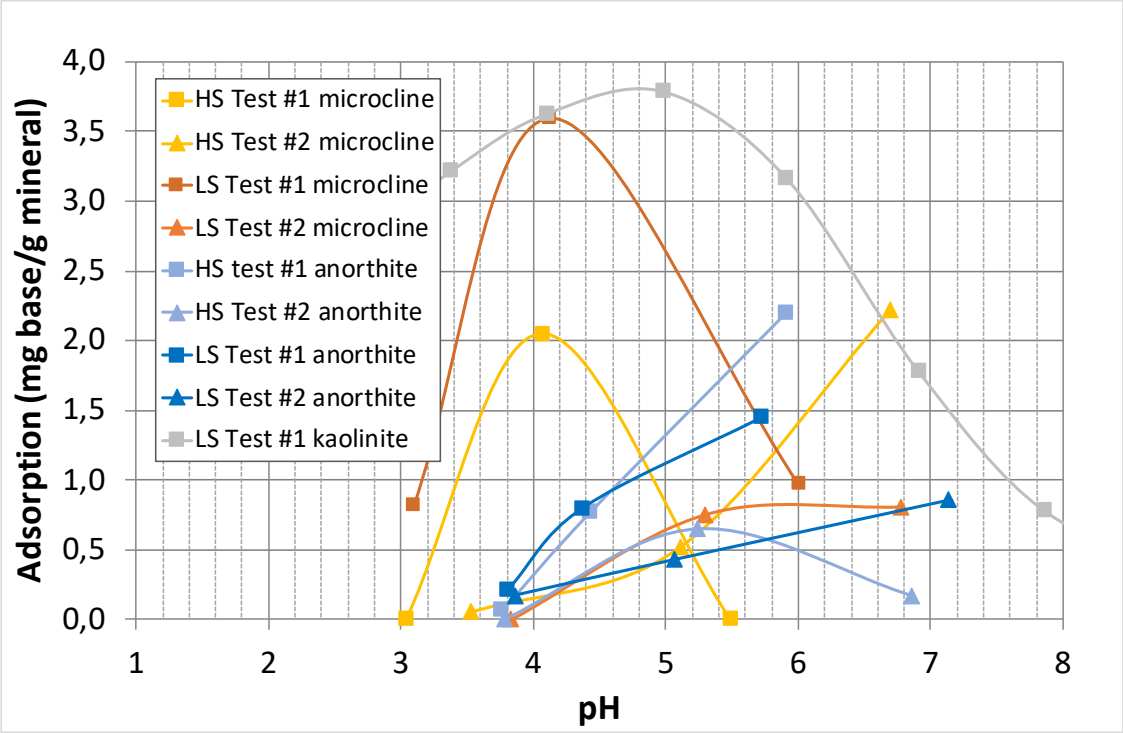

Figure 36: Adsorption of polar basic organic components onto feldspars and kaolinite. Kaolinite results from Frafjord (2015)

The feldspar minerals used in the static adsorption tests have been milled into a particle size below 34 μm. Typical sandstone reservoirs have feldspars comprised of particles with larger sizes which are less reactive and have lower CEC. As pointed out by Carroll (1959) the CEC of minerals increases as the particles size decreases. A silt fraction of a mineral will have lower CEC compared to a clay fraction. Adsorption onto these larger particles will be less than for smaller particles, thus generally based on the observed results, feldspars are not expected to contribute much in adsorbing polar organic components, but they can not be completely excluded.

Surface area is an important factor in adsorption studies. The exchange capacity increases as the grain size decreases because there is a larger surface area and more broken bonds (Carroll, 1959). Clay minerals are very important in adsorbing polar organic components onto a surface and thereby impact initial wetting in a reservoir, mostly due to their very large surface area, permanent negative charge and high CEC. Feldspars have many of the same properties, but the surface area is lower. The mineral samples that were used in the adsorption studies were milled to a silt fraction range with increased BET surface area to a comparable range as clay minerals. Yet, even with comparable BET surface area, the feldspar mineral did not manage to adsorb as much quinoline as the clay mineral. In a real sandstone reservoir the surface area of feldspars are much smaller than the measured BET surface area of the milled samples. Thus, in a real reservoir setting the difference between the adsorption will be even more significant than can be observed at the lab.

6.2.3 How feldspars are affecting pH at different salinities

A pH study, that have been conducted previously byAndersen (2015), was done using new and optimized mineral samples. Andersen (2015) was using the old preparation procedure to study different feldspars influence on pH at different salinities. He concluded that the change in pH was

highest at low salinities and then pH increment decreased at higher salinities and temperatures. To confirm the results obtained by Andersen (2015), and also the test the reproducibility of the optimized mineral samples, the same pH study was performed using mineral samples prepared with new preparation procedure. Previous pH studies was performed at different temperatures on both albite, microcline and anorthite. In this thesis only anorthite has been tested, at ambient temperature.

Figure 31 show how anorthite is influencing pH and how the reaction is dependent on salinity. The results from the new preparation procedure are a bit lower, which was expected, but they are following the same trend as the previous results, figure 37. The chemical mechanism behind the observed increase in pH is caused by cation exchange between the mineral surface and protons in the brine, equation 29

$$CaAl_2Si_2O_8 + H_2O \rightleftharpoons HAl_2Si_2O_8 + Ca^{2+} + OH^- \tag{29}$$

Increase in pH is highest in DI water and then as salinity increase the pH increment decrease, figure 31. When there are no Na^+ in the brine, an exchange of Ca^{2+} ions by H^+ ions happens. This cation exchange releases hydroxide ions into the solution and an increase in pH is observed. Dissolved cations in solution affect the kinetics of feldspars very significantly. The dissolution rate of feldspar decreases when dissolved alkali ions such as Na^+ and $K+$ are added to solution due to the competition of ions with protons on the surface (Gülgönül et al., 2012). In the NaCl brines there are Na^+ present that will compete in the ion exchange, thus less protons will participate and we observe a decrease in pH increment. Higher salinity results in lower increase in pH, which was observed in the experiments, the results are in line with theory.

In previous pH study the results from anorthite did not behave fully in accordance with theory at ambient temperature, figure 37. A high increase in pH was observed with DI brine, but as salinity in the brine increases the pH increment is not decreasing accordingly. The large amount of crushed very small particles caused by extremely high centrifugal forces in the planetary ball mill that were present in the anorthite samples, figure 33, could have significant impact on the analysis results. This could explain why it previously was observed only a minor change in pH for the different salinities at ambient temperature. Results from present pH screening study, figure 31, show a steady decrease in pH increment as the salinity is increased, which is more in line with what we expect will happen. The results obtained by the optimized samples behave more in accordance with theory and are probably more representative than results obtained using samples from the old preparation procedure.

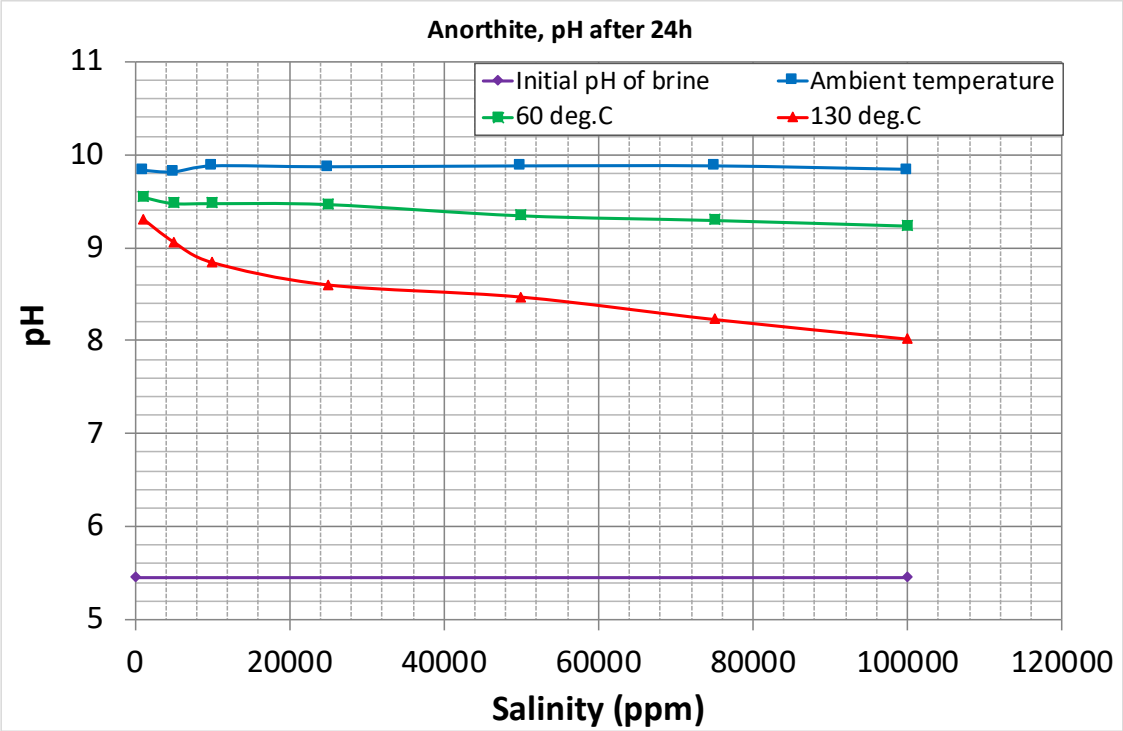

Figure 37: Results from the static pH screening test for anorthite at different temperatures (Andersen, 2015)

Comparing the pH screening result from anorthite with the results from other feldspars (Andersen, 2015), figure 38, anorthite gives the largest ΔpH, then albite and microcline. This order can be explained by the relative stability of the different feldspars, figure 5, where microcline is the most stable feldspar. Stability of feldspar minerals:

$$Microcline > Albite > Anorthite$$

Anorthite is the least stable feldspar, and are not very abundant in sandstone reservoirs. Microcline however are more stable and therefore more frequently found in sandstones. All feldspars are following the same trend, highest ΔpH at low salinity then increment in pH decreases as the salinity increases. Because of the higher stability, microcline will exchange less cations with protons compared to anorthite. Less hydroxides will be released into the solution, resulting in a lower pH increment.

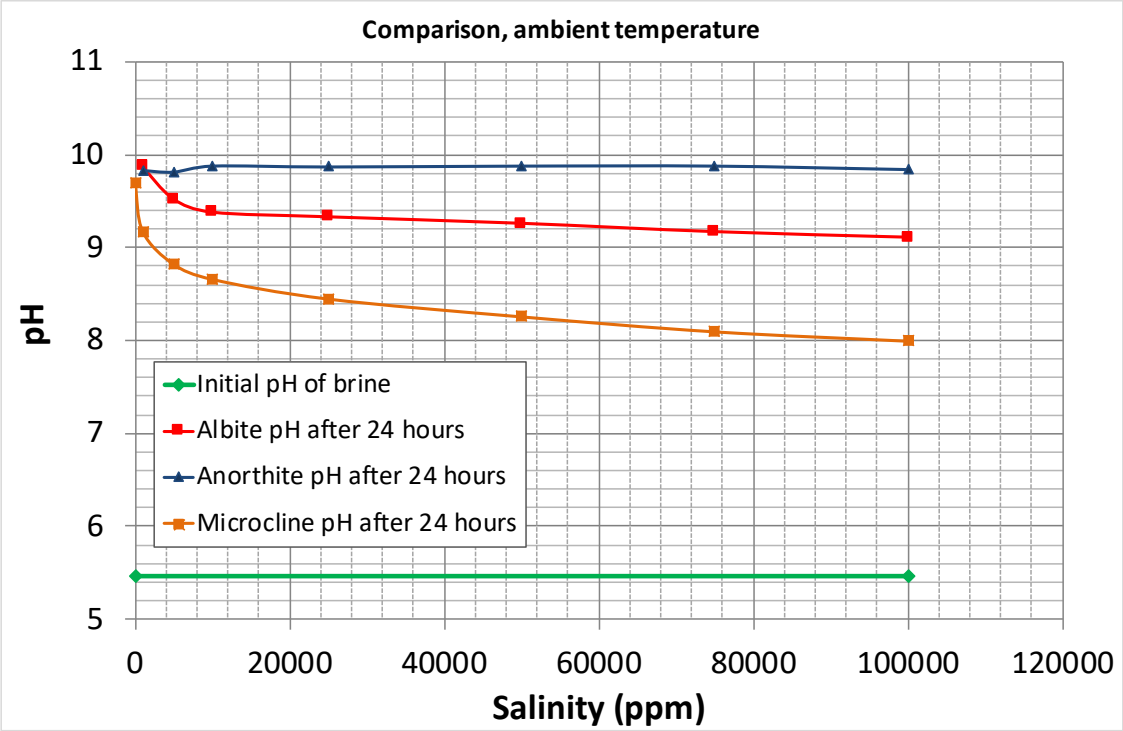

Figure 38: feldspar pH test results at ambient temperature, (Andersen, 2015)

An IC analysis was done on the brine that had been in contact with anorthite, to evaluate the chemical composition of the brine and to confirm results obtained by Andersen (2015), figure 39.

From the IC of DI water analysis performed in the present study, it was possible to see traces of ions in the solution, figure 32. In the DI test, only very little ions were detected in the solution, and in the LS and HS tests no Ca^{2+} ions were detected. This is because of the dilution of the salinity brines, which was necessary to do prior to IC analysis of the brines. The pH screening, figure 31, shows a steady decrease in pH as the salinity is increases, suggesting less hydroxides released into the brine. Less cations are exchanged and there will be less Ca^{2+} ions released into the solution. A decrease in pH from 9 - 8 is a concentration of $10^{-9}M - 10^{-8}M$, which is a very little amount of ions. When the solutions are diluted 500 times, it will not be possible to see any of this tiny concentrations, and therefore the IC results are in line with what is expected.

The DI test on the other hand was not diluted, and the trace ions present in this solution verify that there is ion exchange between the mineral surface and the brine.

The results from the optimized samples behave in accordance with the results obtained in previous tests. From the DI test at ambient temperature, it was possible to see traces of Na^{+}, K^{+}, and Ca^{2+} ions in the solution, showing that the anorthite sample is not 100 % pure. Both studies confirm that there is an ion exchange between the mineral and the brine which will give an increase in pH as the protons are exchanged from the DI water.

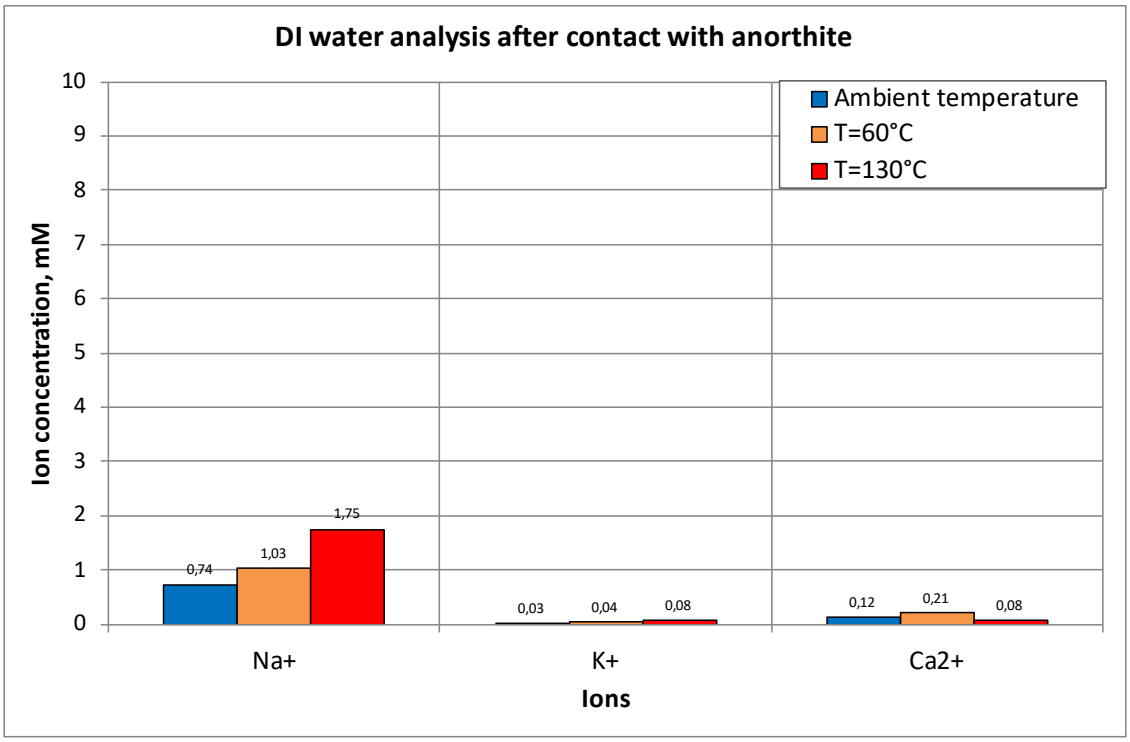

Figure 39: Plot of IC results for anorthite (Andersen, 2015)

6.2.4 Effect of feldspars on initial wetting and wettability alteration processes in Smart Water EOR

Clays are chemically unique because of their very large surface area, high CEC and permanent negative charge. This make them great adsorbants for polar organic components, and clays are therefore considered the main wetting mineral i sandstone reservoirs (Austad et al., 2010). Feldspar minerals have permanent negative sites that needs to be charge-balanced by cations, and could potentially adsorb polar organic components and thus influence initial wetting. Experimental studies have revealed that feldspars could adsorb some polar organic components, but compared to clays the adsorption is low (Mamonov et al., 2017; Abdullah, 2016; Harestad, 2017; Tat, 2017; Algazban, 2017). This was also verified by the adsorption tests done using new optimized mineral samples. Both microcline and anorthite managed to adsorb some polar organic components, but the adsorption was low compared to adsorption onto clays. Mostly it is related to the surface area, the feldspars do not have as large surface area as clays. Also it depends on CEC, because CEC is lower for feldspars than clay minerals. In general feldspar minerals can not be excluded completely regarding adsorption of polar organic components, but in comparison with clay they have much lower contribution due to lower surface area and CEC (Mamonov et al., 2017).

A reservoir system consisting of FW, oil/gas and rock is initially in a state of chemical equilibrium. Studies have revealed that pH affects the reactivity of polar organic components towards mineral surfaces and thereby affects initial wetting (Mamonov et al., 2017; Austad et al., 2010; Frafjord, 2015; Aksulu et al., 2012). At acidic conditions organic components can be adsorbed to a surface, creating mixed wet or neutral wet conditions. To achieve any effect of a Smart Water flood, mixed wet to slightly water wet initial conditions are needed (Strand et al., 2016). The adsorption of the organic components onto clay minerals are dependent on pH, temperature, ion composition and salinity of the FW (Aghaeifar et al., 2015).

Minerals are considered the main factor in controlling pH in a reservoir. Feldspar are highly unstable in aqueous solutions participating in cation exchange with protons resulting in increased pH. The IC analysis results only revealed traces of ions in the solution, still the pH was increased more than 4 pH units in the static pH screening tests. Only minor amount of cation exchanges are needed to influence pH. A pH gradient of 3-4 pH units will give a significant change in the H^+ concentration, i.e from 10^{-5} to 10^{-9} M. However, the mass linked to this pH change is not very significant and therefore a pH change will have relatively small effect on the properties of the minerals, but could impact the reactivity of the polar organic components quite a lot (Piñerez Torrijos et al., 2017).

The presence of feldspars must be taken into account when the low salinity EOR potential for a reservoir is under consideration. The static pH screening tests and IC analysis performed using optimized mineral sample confirms that anorthite is capable of increasing the pH, and that cation exchange is the mechanism behind this.

The salinity of the reservoir is also an important factor regarding the pH contribution from the feldspars. The static pH screening results confirmed that the salinity of a system affects the chemical reactions in the system. A decreased pH increment was observed with higher salinities, thus influencing the initial pH of FW in a reservoir.

Studies have shown that feldspars are important both regarding initial wetting and wettability alteration but this is mainly due to their influence on pH (Austad et al., 2010; Strand et al., 2016, 2014; Piñerez Torrijos et al., 2017; Mamonov et al., 2017; Reinholdtsen et al., 2011; Aghaeifar et al., 2015). The presence of feldspar in reservoir rock could create alkaline conditions in a moderate saline FW, where polar organic components can not adsorb onto the clay surface, thus making the reservoir too water wet to observe any LS EOR effect. While in a high salinity FW the feldspar would be less reactive, resulting in acidic conditions promoting mixed wet conditions where significant LS EOR effects could be obtained. At these mixed wet conditions the feldspars could also contribute with increase in pH when a LS brine is injected, thus contribute positively in a wettability alteration. (Reinholdtsen et al., 2011; Strand et al., 2014).

6.3 Uncertainties

With all experimental work, there are uncertainties that should be evaluated. All instruments and equipment used in this thesis have a certain error which is listed by the manufacturer. Calibration and maintenance are important to maintain this listed error. Operation of these apparatus should be conducted by trained people to minimize measuring errors. Variation in temperature, storage and contaminations could also affect results and thus provide uncertainty. Chemicals have uncertainties in terms of content, concentration and composition. Minerals have uncertainties regarding composition, reactivity, PSD and shape. Also there are human errors related to execution of the experiments. All of which contribute to uncertainty in the obtained results. Validation of results can be achieved by evaluating the repeatability of the results, by comparison with previous results or by identifying trends.

The feldspar minerals in particular are difficult to analyse, due to their very unstable behaviour in contact with the water phase. Depending on pH and salinity of the brine, feldspars are behaving differently. This adds large uncertainties and variations into the results. Addition of extra phases like organic bases will increase the uncertainty, where repeatability is hard to achieve. Organic bases are more or less protonated depending on pH, and as feldspars have proven to influence pH in a system, the behaviour is difficult to monitor. To minimize these variations, it is vital to control factors that can affect the analysis results, like PSD, BET surface area and preservation of the crystal lattice . If this is not managed, results will be highly variable, with little to no stability and

repeatability. In worst case this could potentially result in wrongful conclusions in further analysis studies.

7 Conclusion

The objective of this thesis has been to optimize mineral samples to perform reliable static adsorption and pH screening studies to understand feldspars influence on initial wetting and wettability alterations. In accordance with the objective the results have been analysed and discussed and some conclusions can be made.

The results from the adsorption studies are in line with previous findings. Both anorthite and microcline are capable of adsorbing some polar components onto the surface, yet it was not possible to quantify their adsorption behaviour or dependence on pH and salinity in detail due to varying results that did not show any trends. The only conclusion that can be made is that there is some adsorption and that the adsorption is generally low. Further work is needed to optimize mineral samples, as they are an important part in continued analysis in understanding feldspars contribution both regarding initial wetting and in a Smart Water flooding for EOR.

The new milling device, Retsch XRD mill McCrone was able to provide a controlled milling of the feldspar samples, resulting in better preservation of the minerals, creating less dusty particles and a more homogeneous sample compared to ball mills used in previous adsorption studies. The samples were expected to give reliable and representative results. It turned out to be very hard to end up with stable results when working with feldspar. The optimal mineral samples did not manage to provide reliable and repeatable results in adsorption studies, but showed stable values in pH screening tests.

Mineral preparation and PSD can have significant affect on analysis results, especially in the adsorption studies. The addition of polar organic components increased the uncertainty in the tests, resulting in large variations that are hard to conclude from. However, all tests, both previous and the tests performed in this thesis, have shown that the feldspars are capable of adsorbing polar organic bases but the adsorption is generally low compared to clays.

In the pH screening tests the results were very consistent and behaving in accordance with results obtained by previous students. A trend could be observed and the results were in line with theory. In the pH screening test only two phases are acting which is decreasing the uncertainty significantly, resulting in stable and reliable results of which conclusions can be drawn.

- Feldspar minerals should be prepared using milling equipment that effectively preserves the crystal lattice. A 7 minute milling time combined with sedimentation process produced proper balance between PSD, BET surface area and homogeneity.
- The PSD of the mineral sample is important and can influence analysis results
- The optimal mineral samples did not manage to produce representative and reliable adsorption results. Improvement in the preparation procedure is needed.
- The optimized anorthite sample provided trustworthy static pH screening results.

Based on the results that was obtained using optimized mineral samples some general conclusions can be made:

- Feldspars are highly reactive in presence of water which makes it is hard to produce reliable and repeatable results in feldspar studies.
- Feldspars are capable of adsorbing polar organic components, the adsorption is generally low compared to clay minerals.
- Cation exchange take place between feldspar and water phase.

- Feldspars can influence initial wetting and wettability alteration through cation exchanges resulting in pH changes.
- Feldspars influence on pH gradient decreases with increasing salinity. Feldspar contribution depends on salinity of FW and brine.
- Feldspars could affect the initial wetting and influence the wettability alteration in a reservoir due to its influence on pH.

8 Future work

Even though the new milling equipment managed to produce more homogeneous samples with controlled BET surface area and PSD, it still did not manage to produce representative adsorption results and should be improved:

- Analysis of SEM images and the consequent PSD revealed some small particles (clay fraction) still present in the settled samples. The sedimentation process managed to remove most of the particles below 1 μm but it did not succeed in separating all of them. This was probable due to the highly reactive small particles sticking onto larger particles, or clustering. A ultrasonication procedure similar to the one described by (Mani et al., 2011) could be done on the milled samples prior to a sedimentation procedure. Then agglomeration of small particles would be dispersed and easier removed in a settling process.
- To better control the PSD range a wet sieving process should be considered. In this way particles below a certain micron size can be trapped by a filter, and sieves with mesh sizes according to a pre defined PSD range could be used to produce a specific PSD range. This range should be as narrow as possible, preferrably within the silt fraction. Particles above a certain size would be effectively removed, without needing to increase milling time.

After making optimized mineral samples with a very narrow PSD within the silt fraction, the adsorption studies should be repeated. To quantify the variations from sample to sample several identical samples should be made and then analysed. For example 10 repeated tests with identical conditions (composition, pH, salinity and temperature).

All tests should be repeated at high temperature

References

Abdullah, N. (2016). Reservoir wetting in sandstone reservoirs, adsorption of polar basic oil components onto quartz and feldspar minerals. Master's thesis, University of Stavanger.

Aghaeifar, Z., Strand, S., Austad, T., Puntervold, T., Aksulu, H., Navratil, K., Storas, S., and Hamso, D. (2015). Influence of formation water salinity - composition on the low - salinity enhanced oil recovery effect in high-temperature sandstone reservoirs. *Energy & Fuels*, 29(8):4747 – 4754. https://pubs-acs-org./doi/abs/10.1021/acs.energyfuels.5b01621.

Aksulu, H., Håmsø, D., Strand, S., Puntervold, T., and Austad, T. (2012). Evaluation of low-salinity enhanced oil recovery effects in sandstone: Effects of the temperature and ph gradient. *Energy & Fuels*, 26(6):3497–3503. https://doi.org/10.1021/ef300162n.

Algazban, S. (2017). Smart water injection into sandstone reservoirs for enhancing oil recovery influence of albite on sandstone wetting. Bachelor thesis, University of Stavanger.

Andersen, Y. (2015). Smart water in sandstone reservoirs - Contribution of feldspar minerals to pH. Bachelor thesis, University of Stavanger.

Anderson, W. (1986). Wettability literature survey- part 2: Wettability measurement. *Journal of Petroleum Technology*, 38(11):1246–1262. https://doi.org/10.2118/13933-PA.

Austad, T. (2013). Chapter 13 - water-based EOR in carbonates and sandstones: New chemical understanding of the EOR potential using smart water. In Sheng, J. J., editor, *Enhanced Oil Recovery Field Case Studies*, pages 301 – 335. Gulf Professional Publishing. https://doi.org/10.1016/B978-0-12-386545-8.00013-0.

Austad, T., RezaeiDoust, A., and Puntervold, T. (2010). Chemical mechanism of low salinity water flooding in sandstone reservoirs. Paper SPE 129767 prepared for presentation at the 2010 SPE Improved Oil Recovery Symposium, Tulsa, Oklahoma, 24-28 April. http://dx.doi.org/10.2523/129767-ms.

Baviére, M. (1991). *Basic concepts in enhanced oil recovery processes*, volume 33 of *Critical reports on applied chemistry*. Published for SCI by Elsevier Applied Science, London.

Bjørlykke, K. (1989). *Sedimentology and petroleum geology*. Springer, Berlin.

Blum, A. E. (1994). Feldspars in weathering. In Parsons, I., editor, *Feldspars and their reactions*, pages 595 – 624. Springer-Science+Business Media, B.V. https://doi.org/10.1007/978-94-011-1106-5.

Carroll, D. (1959). Ion exchange in clays and other minerals. *Bulletin of the Geological Society of America*, 70(6):749–779.

Fanali, S., Haddad, P., Lloyd, D. K., Poole, C., and Schoenmakers, P. (2013). *Liquid chromatography : fundamentals and instrumentation*. Handbooks in Separation Science Ser. Elsevier. https://ebookcentral-proquest-com.ezproxy.uis.no.

Frafjord, G. (2015). Wettability and low salinity EOR effects in sandstone reservoir. adsorption of polar compound onto kaolinite clay. Bachelor thesis, University of Stavanger.

Gilson (2015). Gx-271 aspec, solid phase extraction brochure. online product brochure. http://www.gilson.com.

Goodhew, P. J., Humphreys, J., and Beanland, R. (2000). Electron microscopy and analysis. https://ebookcentral-proquest-com.ezproxy.uis.no/lib/uisbib/detail.action?docID=168520.

Green, D. W. (1998). Enhanced oil recovery. https://ebookcentral-proquest-com.ezproxy.uis.no/lib/uisbib/detail.action?docID=3405015.

Greenwood, N. N. (1984). *Chemistry of the elements*. Pergamon Press, Oxford.

Grotzinger, J. and Jordan, T. (2010). *Understanding earth*. W. H. Freeman and Company, New York, sixth edition.

Gülgönül, I., Karagüzel, C., Çinar, M., and Çelik, M. S. (2012). Interaction of sodium ions with feldspar surfaces and its effect on the selective separation of na- and k-feldspars. *Mineral Processing and Extractive Metallurgy Review*, 33(4):233–245. https://doi.org/10.1080/08827508.2011.562952.

Harestad, A. (2017). Smart water injection into sandstone reservoirs for enhancing oil recovery influence of microcline on sandstone wetting. Bachelor thesis, University of Stavanger.

Holleman, A. (2001). *Inorganic chemistry*. Academic Press, 1st english ed. by nils wiberg edition.

HORIBA Instruments Inc (2012). A guidebook to particle size analysis. online resource. Retrived 28. April 2018. https://www.horiba.com/fileadmin/uploads/Scientific/Documents/PSA/PSA_Guidebook.pdf.

Lager, A., Webb, K., and Black, C. (2007). Impact of brine chemistry on oil recovery. IOR 2007-14th European Symposium on Improved Oil Recovery.

Lager, A., Webb, K., Black, C., Singleton, M., and Sorbie, K. (2008a). Low salinity oil recovery - an experimental investigation. *Petrophysics*, 49(1):28–35.

Lager, A., Webb, K. J., Collins, I. R., and Richmond, D. M. (2008b). Losal enhanced oil recovery: Evidence of enhanced oil recovery at the reservoir scale. SPE Symposium on Improved Oil Recovery, 20-23 April, Tulsa, Oklahoma, USA. https://doi.org/10.2118/113976-MS.

Lajunen, L. H. J. and Peramaki, P. (2004). *Spectrochemical Analysis by Atomic Absorption and Emission*. Royal Society of Chemistry, 2nd edition. https://ebookcentral-proquest-com.ezproxy.uis.no/lib/uisbib/detail.action?docID=1186095.

Ligthelm, D. J., Gronsveld, J., , Hofman, J., Brussee, N., Marcelis, F., and van der Linde, H. (2009). Novel waterflooding strategy by manipulation of injection brine composition. Paper SPE 119835 presented at the 2009 SPE EUROPEC/EAGE Annual conference and exhibition. Amsterdam, The Netherlands. https://doi.org/10.2118/119835-MS.

LLC, C. (2018). Microsphere settling velocity calculation. Online resource. http://www.cospheric.com/microsphere-settling-time-calculation.aspx.

Mamonov, A., Puntervold, T., and Strand, S. (2017). Eor by smart water flooding in sandstone reservoirs - effect of sandstone mineralogy on initial wetting and oil recovery. Paper SPE-187839-MS prepared for presentation at SPE Russian Petroleum Technology Conference held in Moscow, Russia, 1618 October 2017. https://doi.org/10.2118/187839-RU.

Mani, G., Fan, Q., Ugbolue, S. C., and M. Eiff, I. (2011). Size reduction of clay particles in nanometer dimensions. *MRS Proceedings*, 740:113–118. https://www.researchgate.net/publication/275787257.

McCabe, W. L., Harriot, P., and Smith, J. C. (2005). *Unit operations of chemical engineering*. McGraw-Hill chemical engineering series. McGraw-Hill, Boston, 7th ed. edition.

micromeritics (2018). Tristar 2. Online resource. http://www.micromeritics.com/Product-Showcase/TriStar-II-Series/TriStar-II-Series2.aspx.

Northern Arizona Meteorite Laboratory (2014). Feldspar ternary diagram. Online resource, retrieved 23. May 2018. https://www.cefns.nau.edu/geology/naml/Meteorite/Book-GlossaryF.html.

Parsons, I. (1994). *Feldspars and their reactions*, volume 421 of *NATO ASI Series*. Springer, Dordecht, softcover reprint of the original 1st ed. 1994. edition.

Piñerez Torrijos, I. (2017). *Enhanced oil recovery from Sandstones and Carbonates with Smart Water*. Doctoral thesis, University of Stavanger.

Piñerez Torrijos, I., Puntervold, T., Strand, S., Austad, T., Tran, V. V., and Olsen, K. (2017). Impact of temperature on the low salinity eor effect for sandstone cores containing reactive plagioclase. *Journal of Petroleum Science and Engineering*, 156:102 – 109. https://doi.org/10.1016/j.petrol.2017.05.014.

Prothero, D. R. and Schwab, F. (2003, c2004). *Sedimentary geology : an introduction to sedimentary rocks and stratigraphy*. Freeman, 2nd ed edition.

Puntervold, T. (2008). *Waterflooding of carbonate reservoirs EOR by wettability alteration*. PhD thesis, University of Stavanger.

Rafferty, J. P. (2018). Beer's law. http://academic.eb.com/levels/collegiate/article/475388.

Reinholdtsen, A., Rezaeidoust, A., Strand, S., and Austad, T. (2011). Why such a small low salinity eor - potential from the snorre formation? pages 748–757. https://doi.org/10.3997/2214-4609.201404796.

Retsch (2018). XRD-mill McCrone. Online resource. https://www.retsch.com/products/milling/ball-mills/mccrone-xrd-mill/function-features/.

RETSCH GmbH (2017). General catalogue. online resource. Retrived 23. May 2018. https://www.retsch.com/dltmp/www/55d3669d-2fa8-4491-8e80-41f7bc282b86-c77541695d35/brochure_catalogue_general_en.pdf.

RETSCH GmbH (2018). Planetary ball mill pm 100. online resource, retrieved 24. April 2018. https://www.retsch.com/products/milling/ball-mills/planetary-ball-mill-pm-100/function-features/.

RezaeiDoust, A., Puntervold, T., and Austad, T. (2011). Chemical verification of the eor mechanism by using low saline/smart water in sandstone. *Energy & Fuels*, 25(5):2151–2162. https://doi.org/10.1021/ef200215y.

Rouquerol, J., Rouquerol, F., Llewellyn, P., Maurin, G., and Sing, K. S. W. (2013). *Adsorption by powders and porous solids : principles, methodology and applications*. Elsevier Science & Technology, 2nd edition. https://ebookcentral-proquest-com.ezproxy.uis.no/lib/uisbib/detail.action?docID=1386474.

Sandengen, K., Kristoffersen, A., Melhuus, K., and Jø sang, L. O. (2016). Osmosis as mechanism for low-salinity enhanced oil recovery. *Journal of Petroleum Science and Engineering*, 21(4):1227–1235. https://www.onepetro.org/journal-paper/SPE-179741-PA.

Sepp, S. (2018). Feldspar. Online resource, retrieved 4. June 2018. http://www.sandatlas.org/feldspar/.

Smith, J. V. (1994). Surface chemistry in feldspars. In Parsons, I., editor, *Feldspars and their reactions*, pages 541 – 580. Springer-Science+Business Media, B.V. https://doi.org/10.1007/978-94-011-1106-5.

Snoeyink, V. L. (1980). *Water chemistry*. Wiley, New York.

Strand, S., Austad, T., Puntervold, T., Aksulu, H., Haaland, B., and RezaeiDoust, A. (2014). Impact of plagioclase on the low salinity eor-effect in sandstone. *Energy & Fuels*, 28(4):2378–2383. https://doi.org/10.1021/ef4024383.

Strand, S., Puntervold, T., and Austad, T. (2016). Water based eor from clastic oil reservoirs by wettability alteration: A review of chemical aspects. *Journal of Petroleum Science and Engineering*, 146:1079 – 1091. https://doi.org/10.1016/j.petrol.2016.08.012.

Strand, S., Standnes, D., and Austad, T. (2006). New wettability test for chalk based on chromatographic separation of SCN^- and SO_4^{2-}. *Journal of Petroleum Science and Engineering*, 52(1):187 – 197. https://doi.org/10.1016/j.petrol.2006.03.021.

Tang, G.-Q. and Morrow, N. R. (1999). Influence of brine composition and fines migration on crude oil/brine/rock interactions and oil recovery. *Journal of Petroleum Science and Engineering*, 24(2):99 – 111. .

Tat, T. (2017). Smart water injection into sandstone reservoirs for enhancing oil recovery influence of anorthite on sandstone wetting. Bachelor thesis, University of Stavanger.

TerraGIS (2007). Particle size fractions. online resource, retrieved 2. June 2018. http://www.terragis.bees.unsw.edu.au/terraGIS_soil/sp_particle_size_fractions.html.

Turner, J. (2012). Liquid assets: Bp deploys reduced salinity water injection. Online resource, Offshore technology. https://www.offshore-technology.com/features/featurereducedsalinitywater-injectionlosaleorclairridge/.

Wolfe, A. L., Liu, R., Stewart, B. W., Capo, R. C., and Dzombak, D. A. (2007). A method for generating uniform size-segregated pyrite particle fractions. *Geochemical transactions*, 8(9). https://geochemicaltransactions.springeropen.com/articles/10.1186/1467-4866-8-9.

Zolotuchin, A. B. (2000). *Introduction to petroleum reservoir engineering*. Høyskoleforlaget, Kristiansand.

A Appendix

A.1 BET surface area measurements

Table A1: BET surface area measurements

Mineral	Milling time ($minutes$)	BET surface area (m^2/g)
Anorthite	1	1.02
Anorthite	2	1.23
Anorthite	3	1.55
Anorthite	5	1.86
Anorthite	7	2.35
Anorthite	7*	2.23
Microcline	1	1.10
Microcline	2	1.59
Microcline	3	2.27
Microcline	5	3.07
Microcline	7	3.54
Microcline	7*	4.03

* the sample has been settled after milling

A.2 Density measurements

Table A2: Density measurements

Brine	Density (g/cm^3)
HS Brine	1.01987
HS Brine	1.01987
HS Brine	1.01989
Average value	1.0199
LS Brine	0.99861
LS Brine	0.99860
LS Brine	0.99861
Average value	0.9986
0.07 Quinoline	0.99940
0.07 Quinoline	0.99941
0.07 Quinoline	0.99942
Average value	0.9994
DI pH 3	0.99771
DI pH 3	0.99770
DI pH 3	0.99771
Average value	0.9977

A.3 Calibration data

Table A3: Preparation of 0.01 M HSQ and 0.01 M LSQ

0.01 M HSQ: 1.3 Q + 7.8 HS			0.01 M LSQ: 1.3 Q + 7.8 LS		
number of the sample	1	10.00	number of the sample	1	10.00
Quinoline, g	1.30	12.99	Quinoline, g	1.30	12.99
HS, g	7.96	79.55	LS, g	7.79	77.89
Total, g	9.25	92.54	Total, g	9.09	90.88
Density HSQ, g/cm^3	1.0165		Density LSQ, g/cm^3	0.9985	
Total, ml	9.10	91.04	Total, ml	9.10	91.02

Table A4: Preparation of Reference HS and Reference LS

Reference HS: 1.3 DI + 7.8 HS			Reference LS: 1.3 DI + 7.8 LS		
number of the sample	1	5.00	number of the sample	1	5.00
DI (pH 3), g	1.30	6.49	DI (pH 3), g	1.30	6.49
HS, g	7.96	39.78	LS, g	7.79	38.95
Total, g	9.25	46.26	Total, g	9.09	45.43

Table A5: Calibration data calculation for HSQ and LSQ

Calibration data for HSQ												
Total $[ml]$	Dilution rate	HSQ $[ml]$	HSQ $[\mu l]$	DI pH3 desired $[g]$	DI pH3 real $[g]$	HSQ real $[g]$	Total $[g]$	ABS	Real dilution rate	pH	Desired concentration $[mM]$	Real concentration $[mM]$
5	1000	0.005	5	4.9950	4.9950	0.0063	5.0013	0.061	793.9	3.04	0.01	0.013
5	500	0.010	10	4.9900	4.9900	0.0116	5.0016	0.178	431.2	2.99	0.02	0.023
5	200	0.025	25	4.9750	4.9751	0.0287	5.0038	0.385	174.3	3.05	0.05	0.057
5	100	0.050	50	4.9500	4.9502	0.0516	5.0018	0.707	96.6	3.00	0.10	0.103
Calibration data for LSQ												
Total $[ml]$	Dilution rate	LSQ $[ml]$	LSQ $[\mu l]$	DI pH3 desired $[g]$	DI pH3 real $[g]$	LSQ real $[g]$	Total $[g]$	ABS	Real dilution rate	pH	Desired concentration $[mM]$	Real concentration $[mM]$
5	1000	0.005	5	4.9950	4.9945	0.0057	5.0002	0.089	877.2	3.06	0.01	0.011
5	500	0.010	10	4.9900	4.9894	0.0116	5.0010	0.168	431.1	3.08	0.02	0.023
5	200	0.025	25	4.9750	4.9746	0.0258	5.0004	0.363	193.8	3.04	0.05	0.052
5	100	0.050	50	4.9500	4.9503	0.0504	5.0007	0.714	99.2	3.08	0.10	0.101

A.4 Adsorption data

Table A6: Adsorption vs pH data, ambient temperature, HS Test #1 anorthite, 200 dilution

Type	Sample	Anorthite	Brine	Q	Total (Anorthite**+B/Q)
		[g]	[g]	[g]	[g]
HS	1	1.0004	7.9597	1.3000	10.2601
HS	2	1.0005	7.9605	1.2995	10.2605
HS	3	1.0008	7.9602	1.2999	10.2609

HCl*	NaOH*	Total liquid	Q	wt% An	pH	pH after	pH after
[g]	[g]	[g]	[M]	[%]	adjusted	24 hours	24 +24 hours
0.090	-	9.3497	0.0099	9.67	2.68	2.71	3.76
0.030	-	9.2900	0.0100	9.72	4.15	3.91	4.43
-	-	9.2601	0.0100	9.75	7.24	5.60	5.91

Total	Dilution rate	Desired B/Q	DI pH3 desired	DI pH3 real	B/Q real
[ml]		[µl]	[g]	[g]	[g]
5	200	25	4.9750	4.9753	0.0265
5	200	25	4.9750	4.9753	0.0264
5	200	25	4.9750	4.9752	0.0264

Total real	ABS	Real dilution rate	Q in diluted solution***	Q in real solution***
[g]			[mM]	[M]
5.0018	0.353	188.7	0.052006	0.0098160
5.0017	0.332	189.5	0.048974	0.0092786
5.0016	0.289	189.5	0.042766	0.0081022

Base in water	Q adsorbed	Initial Q****	Final Q*****	Mole ads	Adsorption
[%]	[%]	[mole]	[mole]	[mole]	[mg base/g An]
99.13	0.87	9.1055E-05	9.0260E-05	5.3764E-07	0.07
93.13	6.87	9.1020E-05	8.4764E-05	6.2557E-06	0.81
81.03	18.97	9.1048E-05	7.3775E-05	1.7273E-05	2.23

*Under assumption that density of HCl/NaOH solution is 1 g/ml. **Anorthite. ***Q in diluted solution taken from centrifuged An+B/Q sample after 24 hours. ***Q in solution after centrifuged An+B/Q sample after 24 hours. ****Number of moles in initial solution (before rotation). *****Number of moles in solution after 24 hours rotation. An - Anorthite

Table A7: Adsorption vs pH data, ambient temperature, HS Test #2 anorthite, 200 dilution

Type	Sample	Anorthite	Brine	Q	Total (Anorthite**+B/Q)
		[g]	[g]	[g]	[g]
HS	1	1.0000	7.9599	1.2996	10.2595
HS	2	1.0002	7.9603	1.3002	10.2607
HS	3	1.0002	7.9602	1.3001	10.2605

HCl*	NaOH*	Total liquid	Q	wt% An	pH	pH after	pH after
[g]	[g]	[g]	[M]	[%]	adjusted	24 hours	24 +24 hours
0.050	-	9.3095	0.0099	9.70	2.92	3.07	3.78
0.025	-	9.2855	0.0100	9.72	4.93	5.08	5.24
0.040	0.055	9.3553	0.0099	9.66	6.60	6.91	6.86

Total	Dilution rate	Desired B/Q	DI pH3 desired	DI pH3 real	B/Q real
[ml]		[µl]	[g]	[g]	[g]
5	200	25	4.9750	4.9750	0.0262
5	200	25	4.9750	4.9753	0.0260
5	200	25	4.9750	4.9748	0.0260

Total real	ABS	Real dilution rate	Q in diluted solution***	Q in real solution***
[g]			[mM]	[M]
5.0012	0.354	190.9	0.052151	0.0099548
5.0013	0.331	192.4	0.048830	0.0093928
5.0008	0.343	192.3	0.050562	0.0079251

Base in water	Q adsorbed	Initial Q****	Final Q*****	Mole ads	Adsorption
[%]	[%]	[mole]	[mole]	[mole]	[mg base/g An]
100.12	-0.12	9.1027E-05	9.1136E-05	-1.0914E-07	0.00
94.18	5.82	9.1069E-05	8.5765E-05	5.2025E-06	0.68
98.26	1.74	9.1062E-05	8.9478E-05	1.5824E-06	0.20

*Under assumption that density of HCl/NaOH solution is 1 g/ml. **Anorthite. ***Q in diluted solution taken from centrifuged An+B/Q sample after 24 hours. ***Q in solution after centrifuged An+B/Q sample after 24 hours. ****Number of moles in initial solution (before rotation). *****Number of moles in solution after 24 hours rotation. An - Anorthite

Table A8: Adsorption vs pH data, ambient temperature, LS Test #1 anorthite, 200 dilution

Type	Sample	Anorthite	Brine	Q	Total (Anorthite**+B/Q)
		[g]	[g]	[g]	[g]
LS	1	1.0000	7.7898	1.3003	10.0901
LS	2	1.0003	7.7899	1.3000	10.0902
LS	3	1.0000	7.7904	1.3002	10.0906

HCl*	NaOH*	Total liquid	Q	wt% An	pH	pH after	pH after
[g]	[g]	[g]	[M]	[%]	adjusted	24 hours	24 +24 hours
0.102	-	9.1021	0.0099	9.81	2.86	2.67	3.81
0.040	-	9.1299	0.0100	9.87	4.15	3.91	4.37
0.005	-	9.0956	0.0100	9.91	6.10	5.62	5.72

Total	Dilution rate	Desired B/Q	DI pH3 desired	DI pH3 real	B/Q real
[ml]		[µl]	[g]	[g]	[g]
5	200	25	4.9750	4.9747	0.0266
5	200	25	4.9750	4.9749	0.0263
5	200	25	4.9750	4.9753	0.0268

Total real	ABS	Real dilution rate	Q in diluted solution***	Q in real solution***
[g]			[mM]	[M]
5.0013	0.368	188.0	0.051669	0.0097148
5.0012	0.348	190.2	0.048813	0.0092823
5.0021	0.335	186.6	0.046957	0.0087643

Base in water	Q adsorbed	Initial Q****	Final Q*****	Mole ads	Adsorption
[%]	[%]	[mole]	[mole]	[mole]	[mg base/g An]
98.17	1.83	9.1076E-05	8.9413E-05	1.6623E-06	0.21
93.19	6.81	9.1055E-05	8.4855E-05	6.1995E-06	0.80
87.65	12.35	9.1069E-05	7.9819E-05	1.1250E-05	1.45

*Under assumption that density of HCl/NaOH solution is 1 g/ml. **Anorthite. ***Q in diluted solution taken from centrifuged An+B/Q sample after 24 hours. ***Q in solution after centrifuged An+B/Q sample after 24 hours. ****Number of moles in initial solution (before rotation). *****Number of moles in solution after 24 hours rotation. An - Anorthite

Table A9: Adsorption vs pH data, ambient temperature, LS Test #2 anorthite, 200 dilution

Type	Sample	Anorthite	Brine	Q	Total (Anorthite**+B/Q)
		[g]	[g]	[g]	[g]
LS	1	1.0001	7.7898	1.3002	10.0901
LS	2	1.0000	7.7902	1.2998	10.0900
LS	3	0.9999	7.7900	1.3353	10.1252

HCl*	NaOH*	Total liquid	Q	wt% An	pH	pH after	pH after
[g]	[g]	[g]	[M]	[%]	adjusted	24 hours	24 +24 hours
0.040	-	9.1300	0.0100	9.87	3.12	2.98	3.86
0.020	0.005	9.1150	0.0100	9.98	4.72	4.96	5.06
0.028	0.045	9.1983	0.0102	9.80	7.22	7.17	7.13

Total	Dilution rate	Desired B/Q	DI pH3 desired	DI pH3 real	B/Q real
[ml]		[µl]	[g]	[g]	[g]
5	200	25	4.9750	4.9748	0.0256
5	200	25	4.9750	4.9750	0.0257
5	200	25	4.9750	4.9754	0.0255

Total real	ABS	Real dilution rate	Q in diluted solution***	Q in real solution***
[g]			[mM]	[M]
5.0004	0.358	195.3	0.050241	0.0098135
5.0007	0.352	194.6	0.049384	0.0096092
5.0009	0.343	196.1	0.048099	0.0094329

Base in water	Q adsorbed	Initial Q****	Final Q*****	Mole ads	Adsorption
[%]	[%]	[mole]	[mole]	[mole]	[mg base/g An]
98.51	1.49	9.1069E-05	8.9713E-05	1.3561E-06	0.18
96.33	3.67	9.1041E-05	8.7700E-05	3.3401E-06	0.43
92.89	7.11	9.3527E-05	8.6877E-05	6.6498E-06	0.86

*Under assumption that density of HCl/NaOH solution is 1 g/ml. **Anorthite. ***Q in diluted solution taken from centrifuged An+B/Q sample after 24 hours. ***Q in solution after centrifuged An+B/Q sample after 24 hours. ****Number of moles in initial solution (before rotation). *****Number of moles in solution after 24 hours rotation. An - Anorthite

Table A10: Adsorption vs pH data, ambient temperature, HS Test #1 microcline, 200 dilution

Type	Sample	Microcline	Brine	Q	Total (Microcline**+B/Q)
		[g]	[g]	[g]	[g]
HS	1	1.0008	7.9608	1.3000	10.2616
HS	2	1.0002	7.9608	1.3000	10.2610
HS	3	1.0001	7.9605	1.3001	10.2607

HCl*	NaOH*	Total liquid	Q	wt% Mi	pH	pH after	pH after
[g]	[g]	[g]	[M]	[%]	adjusted	24 hours	24 +24 hours
0.080	-	9.3408	0.0991	9.68	1.98	2.12	3.04
0.025	-	9.2858	0.0997	9.72	3.50	3.40	4.07
-	-	9.2606	0.0100	9.75	6.54	5.29	5.49

Total	Dilution rate	Desired B/Q	DI pH3 desired	DI pH3 real	B/Q real
[ml]		[µl]	[g]	[g]	[g]
5	200	25	4.9750	4.9748	0.0264
5	200	25	4.9750	4.9753	0.0264
5	200	25	4.9750	4.9751	0.0266

Total real	ABS	Real dilution rate	Q in diluted solution***	Q in real solution***
[g]			[mM]	[M]
5.0012	0.366	189.4	0.053883	0.010208
5.0017	0.293	189.5	0.043343	0.008212
5.0017	0.368	188.0	0.054172	0.010186

Base in water	Q adsorbed	Initial Q****	Final Q*****	Mole ads	Adsorption
[%]	[%]	[mole]	[mole]	[mole]	[mg base/g Mi]
102.98	-2.98	9.1055E-05	9.3769E-05	-2.7148E-06	0
82.35	17.65	9.1055E-05	7.4984E-05	1.6071E-05	2.08
101.86	-1.86	9.1062E-05	9.2756E-05	-1.6940E-06	0

*Under assumption that density of HCl/NaOH solution is 1 g/ml. **Microcline . ***Q in diluted solution taken from centrifuged Mi+B/Q sample after 24 hours. ***Q in solution after centrifuged Mi+B/Q sample after 24 hours. ****Number of moles in initial solution (before rotation). *****Number of moles in solution after 24 hours rotation. Mi - Microcline

Table A11: Adsorption vs pH data, ambient temperature, HS Test #2 microcline, 200 dilution

Type	Sample	Microcline	Brine	Q	Total (Microcline**+B/Q)
		[g]	[g]	[g]	[g]
HS	1	1.0003	7.9599	1.2996	10.2598
HS	2	0.9996	7.9603	1.3003	10.2602
HS	3	1.0003	7.9603	1.3003	10.2609

HCl*	NaOH*	Total liquid	Q	wt% Mi	pH	pH after	pH after
[g]	[g]	[g]	[M]	[%]	adjusted	24 hours	24 +24 hours
0.025	0.020	9.3045	0.0995	9.71	3.16	3.01	3.53
0.015	-	9.2756	0.0999	9.73	4.62	5.00	5.11
0.074	0.096	9.4306	0.0982	9.59	7.30	6.72	6.70

Total	Dilution rate	Desired B/Q	DI pH3 desired	DI pH3 real	B/Q real
[ml]		[µl]	[g]	[g]	[g]
5	200	25	4.9750	4.9750	0.0262
5	200	25	4.9750	4.9751	0.0262
5	200	25	4.9750	4.9751	0.0264

Total real	ABS	Real dilution rate	Q in diluted solution***	Q in real solution***
[g]			[mM]	[M]
5.0012	0.351	190.9	0.051717	0.0098721
5.0013	0.338	190.9	0.049840	0.0095140
5.0015	0.283	189.5	0.041899	0.0079379

Base in water	Q adsorbed	Initial Q****	Final Q*****	Mole ads	Adsorption
[%]	[%]	[mole]	[mole]	[mole]	[mg base/g Mi]
99.23	0.77	9.1027E-05	9.0329E-05	6.9716E-07	0.09
95.28	4.72	9.1076E-05	8.6778E-05	4.2978E-06	0.56
80.85	19.15	9.1076E-05	7.3632E-05	1.7443E-05	2.25

*Under assumption that density of HCl/NaOH solution is 1 g/ml. **Microcline. ***Q in diluted solution taken from centrifuged Mi+B/Q sample after 24 hours. ***Q in solution after centrifuged Mi+B/Q sample after 24 hours. ****Number of moles in initial solution (before rotation). *****Number of moles in solution after 24 hours rotation. Mi - Microcline

Table A12: Adsorption vs pH data, ambient temperature, LS Test #1 microcline, 200 dilution

Type	Sample	Microcline	Brine	Q	Total (Microcline**+B/Q)
		[g]	[g]	[g]	[g]
LS	1	1.0002	7.7903	1.3003	10.0908
LS	2	1.0001	7.7901	1.3005	10.0907
LS	3	1.0003	7.7901	1.2996	10.0900

HCl*	NaOH*	Total liquid	Q	wt% Mi	pH	pH after	pH after
[g]	[g]	[g]	[M]	[%]	adjusted	24 hours	24 +24 hours
0.075	-	9.1656	0.00993	9.84	2.55	2.18	3.10
0.020	-	9.1106	0.00999	9.89	3.63	3.52	4.13
-	-	9.0897	0.01001	9.91	7.27	5.39	6.01

Total	Dilution rate	Desired B/Q	DI pH3 desired	DI pH3 real	B/Q real
[ml]		[µl]	[g]	[g]	[g]
5	200	25	4.9750	4.9751	0.0262
5	200	25	4.9750	4.9749	0.0246
5	200	25	4.9750	4.9752	0.0266

Total real	ABS	Real dilution rate	Q in diluted solution***	Q in real solution***
[g]			[mM]	[M]
5.0013	0.345	190.9	0.048385	0.0092361
4.9995	0.245	203.2	0.034104	0.0069309
5.0018	0.348	188.0	0.048813	0.0091787

Base in water	Q adsorbed	Initial Q****	Final Q*****	Mole ads	Adsorption
[%]	[%]	[mole]	[mole]	[mole]	[mg base/g Mi]
93.00	7.00	9.1076E-05	8.4763E-05	6.3128E-06	0.82
69.36	30.64	9.1090E-05	6.3226E-05	2.7864E-05	3.60
91.71	8.29	9.1027E-05	8.3539E-05	7.4874E-06	0.97

*Under assumption that density of HCl/NaOH solution is 1 g/ml. **Microcline. ***Q in diluted solution taken from centrifuged Mi+B/Q sample after 24 hours. ***Q in solution after centrifuged Mi+B/Q sample after 24 hours. ****Number of moles in initial solution (before rotation). *****Number of moles in solution after 24 hours rotation. Mi - Microcline

Table A13: Adsorption vs pH data, ambient temperature, LS Test #2 microcline, 200 dilution

Type	Sample	Microcline	Brine	Q	Total (Microcline**+B/Q)
		[g]	[g]	[g]	[g]
LS	1	0.9999	7.7897	1.3000	10.0896
LS	2	1.0000	7.7902	1.3002	10.0904
LS	3	1.0003	7.7897	1.3003	10.0903

HCl*	NaOH*	Total liquid	Q	wt% Mi	pH	pH after	pH after
[g]	[g]	[g]	[M]	[%]	adjusted	24 hours	24 +24 hours
0.020	0.010	9.1197	0.00998	9.88	3.01	3.04	3.83
0.015	-	9.1054	0.01000	9.90	4.59	5.12	5.30
0.015	0.034	91390	0.00996	9.87	7.11	6.78	6.78

Total	Dilution rate	Desired B/Q	DI pH3 desired	DI pH3 real	B/Q real
[ml]		[µl]	[g]	[g]	[g]
5	200	25	4.9750	4.9748	0.0255
5	200	25	4.9750	4.9751	0.0258
5	200	25	4.9750	4.9748	0.0261

Total real	**ABS**	Real dilution rate	Q in diluted solution***	Q in real solution***
[g]			[mM]	[M]
5.0003	0.366	196.1	0.051384	0.010076
5.0009	0.344	193.8	0.048242	0.009351
5.0009	0.345	191.6	0.048385	0.009271

Base in water	Q adsorbed	Initial Q****	Final Q*****	Mole ads	Adsorption
[%]	[%]	[mole]	[mole]	[mole]	[mg base/g Mi]
100.97	-0.97	9.1055E-05	9.2007E-05	-9.5217E-07	0
93.54	6.46	9.1069E-05	8.5253E-05	5.8155E-06	0.75
93.08	6.92	9.1076E-05	8.4834E-05	6.2415E-06	0.81

*Under assumption that density of HCl/NaOH solution is 1 g/ml. **Microcline. ***Q in diluted solution taken from centrifuged Mi+B/Q sample after 24 hours. ***Q in solution after centrifuged Mi+B/Q sample after 24 hours. ****Number of moles in initial solution (before rotation). *****Number of moles in solution after 24 hours rotation. Mi - Microcline

A.5 IC data

Table A14: IC data

Injection number	Injection name Selected peak	Natrium Area ($\mu S{\cdot}min$)	Potassium Area ($\mu S{\cdot}min$)	Calcium Area ($\mu S{\cdot}min$)
1	DW	0.0386	0.0071	0.0065
2	DW	0.0034	n.a.	0.001
3	FW (100000 NaCl) dx500	15.1542	0.0008	0.0056
4	LS (1000 NaCl) dx500	0.1386	0.001	0.0022
5	LScal	0.1952	0.0941	0.1596
6	HScal	4.4369	0.1016	0.178
7	DI Test	1.3007	0.5753	0.0865
8	5000 Test	0.7106	0.0013	0.0035
9	30000 Test	6.3497	0.0012	0.0037
10	50000 Test	7.2231	0.0009	0.0025
11	100000 Test	14.719	0.0015	0.0034
12	FW (100000 NaCl) dx500	15.3496	0.0005	0.0018
13	LS (1000 NaCl) dx500	0.1452	0.0016	0.002
14	LScal	0.2005	0.0961	0.1646
15	HScal	4.5031	0.1042	0.1825
16	DW	0.0409	0.0022	0.0017
17	DW	0.0044	0.0007	n.a.
Maximum		15.3496	0,5753	0.1825
Average		4.1479	0.0619	0.0503
Minimum		0.0034	0.0005	0.001
Standard Deviation		5.7239	0.1435	0.0751
Relative Standard Deviation		138.00 %	231.99 %	149.30 %

A.6 Calculations

A.6.1 Calculate size of settled particles

An estimate of the settled particle size can be calculated from Stokes law. Settling time $t = 3600s$, height of watercolumn $h = 0.20m$, DI water viscosity at ambient temperature $\mu_w = 0.001kg/(m \cdot s)$, Average mass density for K-feldspars $\rho_p = 2560kg/m^3$, Average mass density for Ca-feldspars $\rho_p = 2780kg/m^3$ (Sepp, 2018), Average mass density of DI water $\rho_f = 998kg/m^3$, Gravitational acceleration constant $g = 9.81m/s^2$.
Stokes law:

$$v = \frac{2 \cdot r^2 \cdot g \cdot (\rho_p - \rho_f)}{9 \cdot \mu}$$

Using that $v = h/t$ and replacing this into stokes law. Solving for r:

$$r = \sqrt{\frac{h \cdot 9 \cdot \mu}{2 \cdot t \cdot g \cdot (\rho_p - \rho_f)}}$$

Calculate for microcline which gives:

$$r = \sqrt{\frac{0.20m \cdot 9 \cdot 0.001kg/m^3}{2 \cdot 3600s \cdot 9.81m/s^2 \cdot (2560kg/m^3 - 998kg/m^3)}}$$

microcline:

$$r = 4.0 \cdot 10^{-6}m$$

using same calculation for anorthite, which gives:

$$r = 3.8 \cdot 10^{-6}m$$

Feldspar particles with a radius below 3.8 μm should be removed by a sedimentation procedure.

A.6.2 Adsorption calculations

Calculations for Anorthite HS Test #1, Sample 1, adsorption data given in table A6:

Initial values (before dilution):
Mass anorthite, $m_{An} = 1.0004g$
Mass quinoline, $m_q = 1.3000g$
Initial concentration quinoline sample, $C_{qi} = 0.07$
Density $Q_{0.07}$, $\rho_{Q_{0.07}} = 0.9994g/cm^3$ from table A2
Density HS, $\rho_{HS} = 1.0199g/cm^3$ from table A2
Density LS, $\rho_{LS} = 0.9986g/cm^3$ from table A2
Molar mass quinoline, $Mm_q = 129.16g/mole$
Mass HS, $m_{HS} = 7.9597g$
Mass HCl, $m_{HCl} = 0.090g$
Mass total liquid, $m_{totliq} = m_q + m_{HS} + m_{HCl} + m_{NaCl} = 9.3497g$
Total mass, $m_{tot_i} = m_{An} + m_{totliq} = 10.2601g$
Concentration quinoline in B/Q sample (theoretical), $C_q = \frac{n_{qi}}{V_{totliq}} = 0.010M$

Samples diluted 200 times:
Density HSQ, $\rho_{HSQ} = 1.0165g/cm^3$ from table A5
Mass DI water pH 3, $m_{DI} = 4.9753g$
Mass brine / quinoline, $m_{b/q} = 0.0265g$
Mass total amount of liquid, $m_{tot} = m_{DI} + m_{b/q} = 5.0018g$
Dilution rate=200

Calibration curve, HS, from figure 18

$$y = 6.9261x - 0.0072$$

where

y is measured absorbance, ABS

x is concentration of quinoline in solution

Insert for $y = ABS$ and $x = C_{qi}$ and solve for C_{qi}:

$$C_{qi} = \frac{ABS}{6.9261} + 0.0072$$

Measured $ABS = 0.353$

Calculations:
Real dilution rate, RDR:

$$RDR = \frac{m_{tot}}{m_{tot} - m_{DI}} = 188.7$$

Concentration of quinoline in diluted solution, C_{qd}:

$$C_{qd} = \frac{ABS}{6.9261} + 0.0072 = 0.052006mM$$

Concentration of quinoline in real solution, C_{qr}:

$$C_{qr} = \frac{C_{qd} \cdot RDR}{1000} = 0.0098160M$$

% Base in water:

$$\%Base\ in\ water = \frac{C_{qr}}{C_q} \cdot 100 = 99.13\%$$

% Q adsorbed:

$$\%Q\ adsorbed = 100 - \%Base\ in\ water = 0.87\%$$

Using that volume $(V) = mass\ (m)/density\ (\rho)$ and mole $(n) = Volume\ (V) \cdot Concenrtration\ (C)$, $1\ liter = 1000cm^3$ to calculate moles of quinoline in the sample.
Mole quinoline initial in sample before rotation, n_i. :

$$n_i = \frac{\frac{m_q}{\rho_q}}{1000} \cdot C_{qi} = 9.1055 \cdot 10^{-5}mole$$

Mole quinoline final in sample after rotation, n_f:

$$n_f = \frac{\frac{m_{HS}}{\rho_{HS}} + \frac{m_q}{\rho_q} + \frac{m_{HCl}}{1} + \frac{m_{NaOH}}{1}}{1000} \cdot C_{qr} = 9.0260 \cdot 10^{-5}mole$$

Mole quinoline adsorbed onto the anorthite surface, n_{ads} is given by the difference between initial moles of quinoline and final moles of quinoline:

$$n_{ads} = n_i - n_f = 5.3764 \cdot 10^{-7}mole$$

Using that mass $(m) = moles(n) \cdot Molarmass(Mm)$
Adsorption of quinoline onto the anorthite surface, Ads:

$$Ads = \frac{n_{ads} \cdot Mm_q \cdot 1000}{m_{An}} = 0.07mg\ base/g\ An$$

$M = mole/liter$

A.7 SEM pictures

A.7.1 Anorthite unmilled

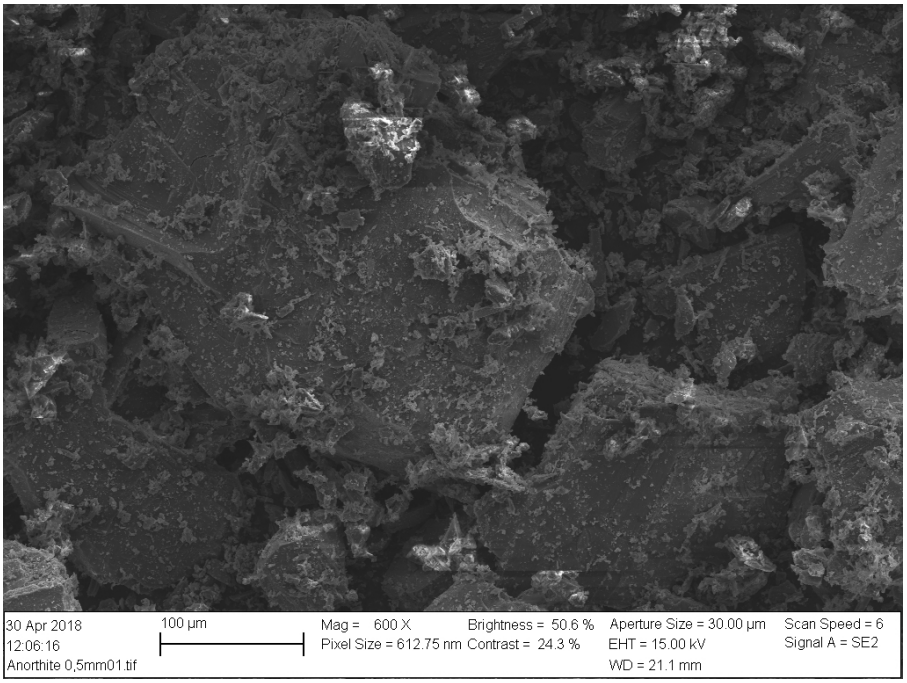

Figure A1: SEM image of anorthite sieved through 0.5 mm mesh, unmilled

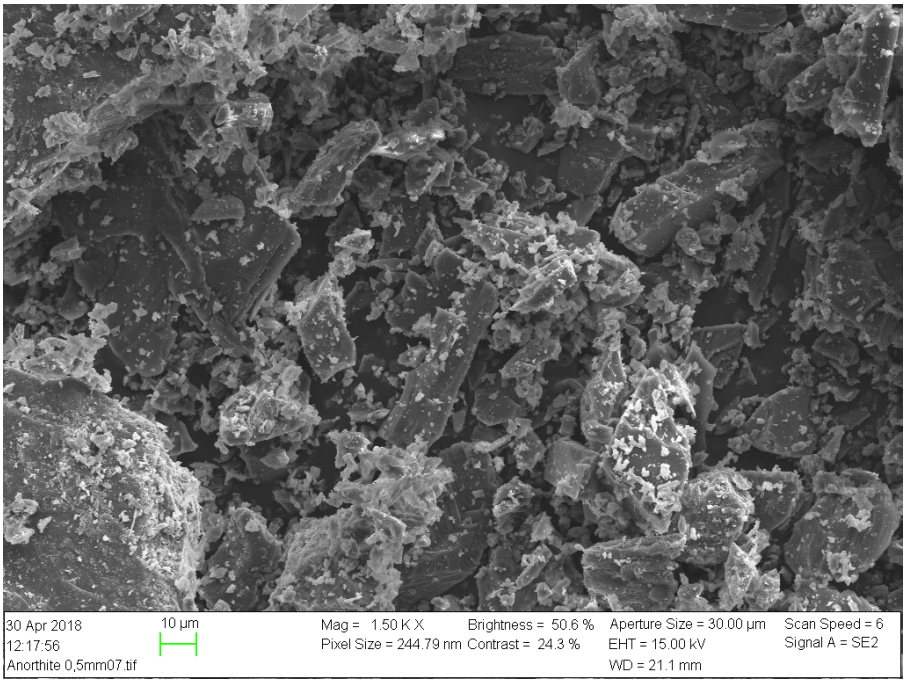

Figure A2: SEM image of anorthite sieved through 0.5 mm mesh, unmilled

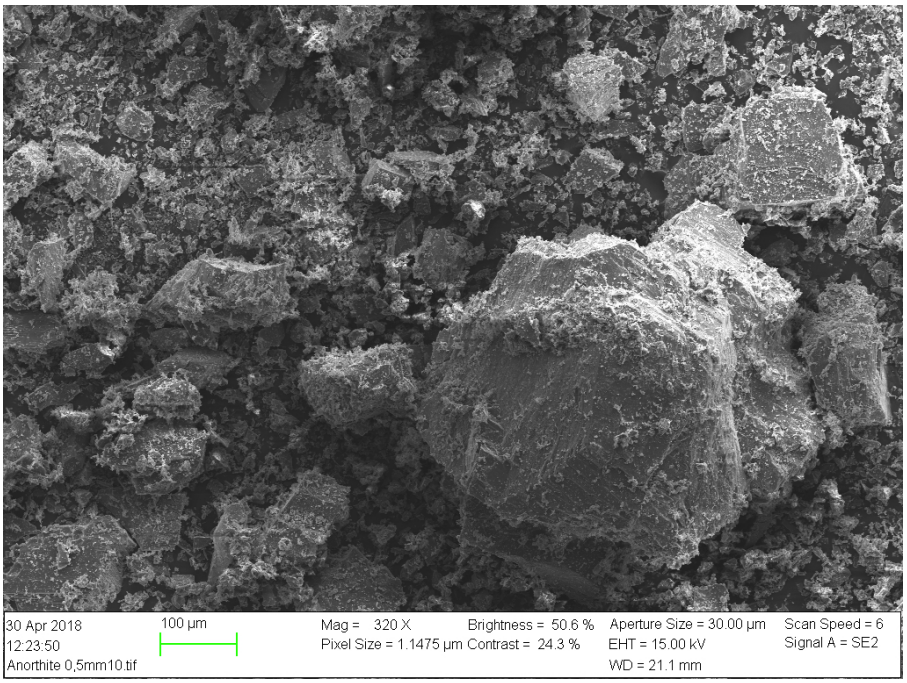

Figure A3: SEM image of anorthite sieved through 0.5 mm mesh, unmilled

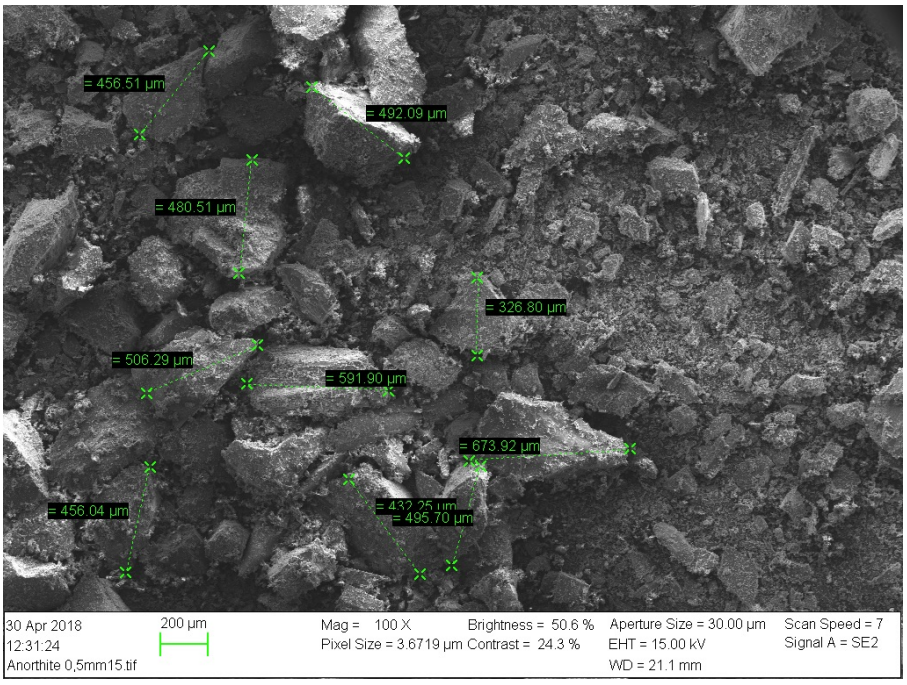

Figure A4: SEM image of anorthite sieved through 0.5 mm mesh, unmilled

A.7.2 Anorthite milled 1 min

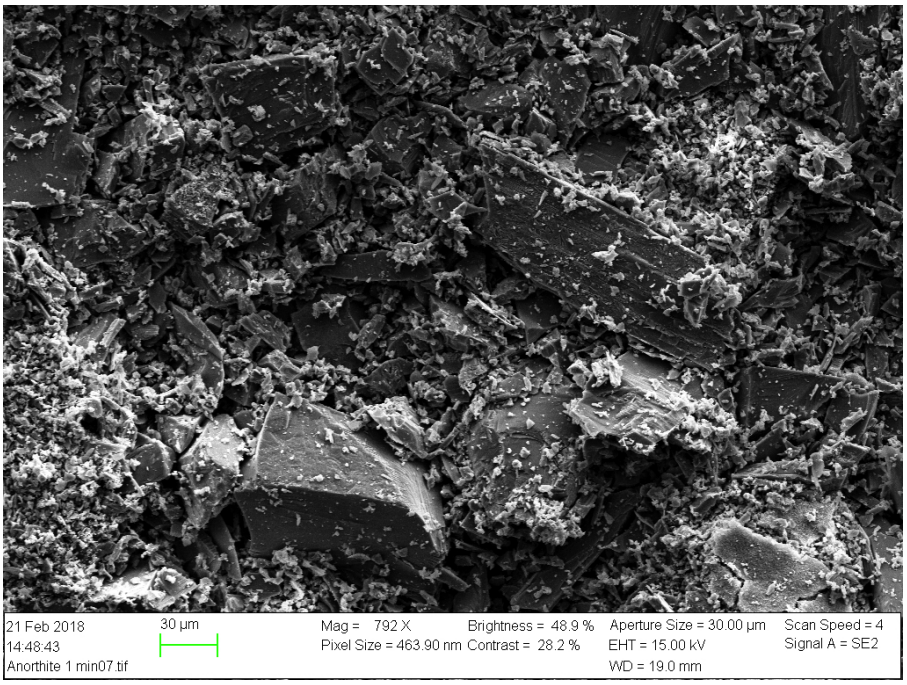

Figure A5: SEM image of anorthite milled 1 minute

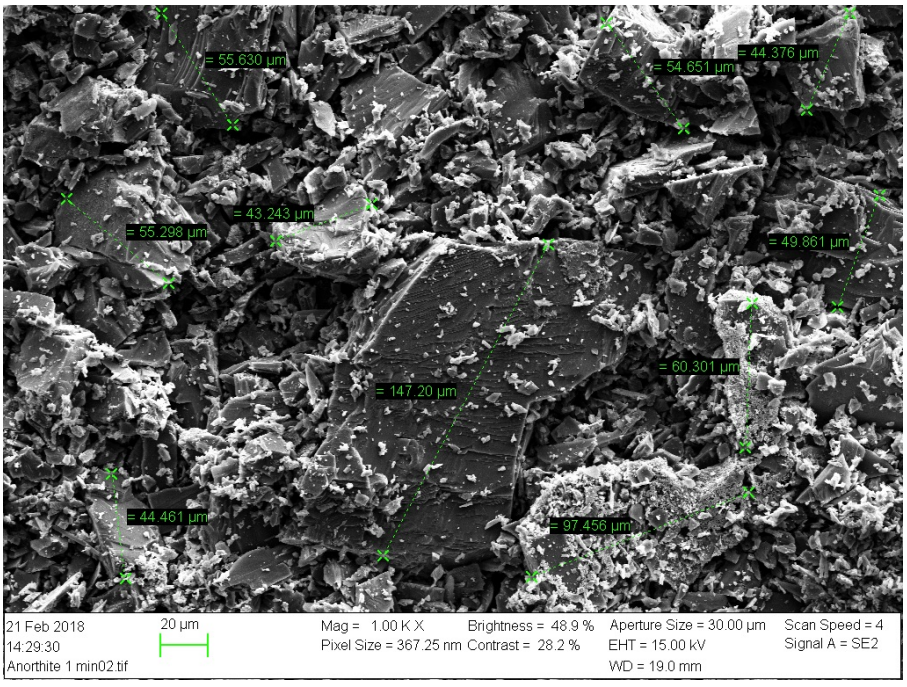

Figure A6: SEM image of anorthite milled 1 minute

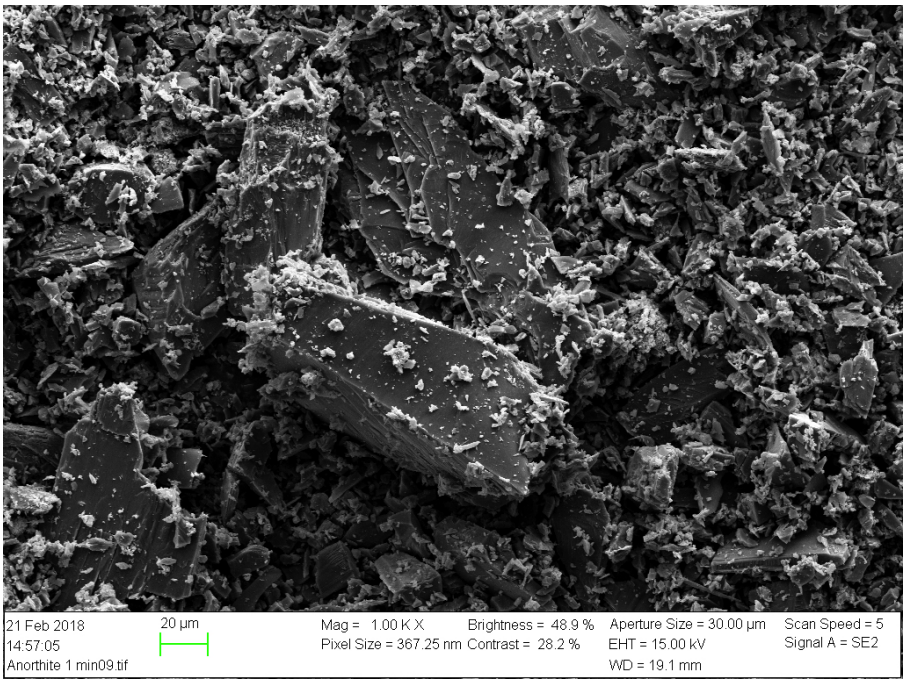

Figure A7: SEM image of anorthite milled 1 minute

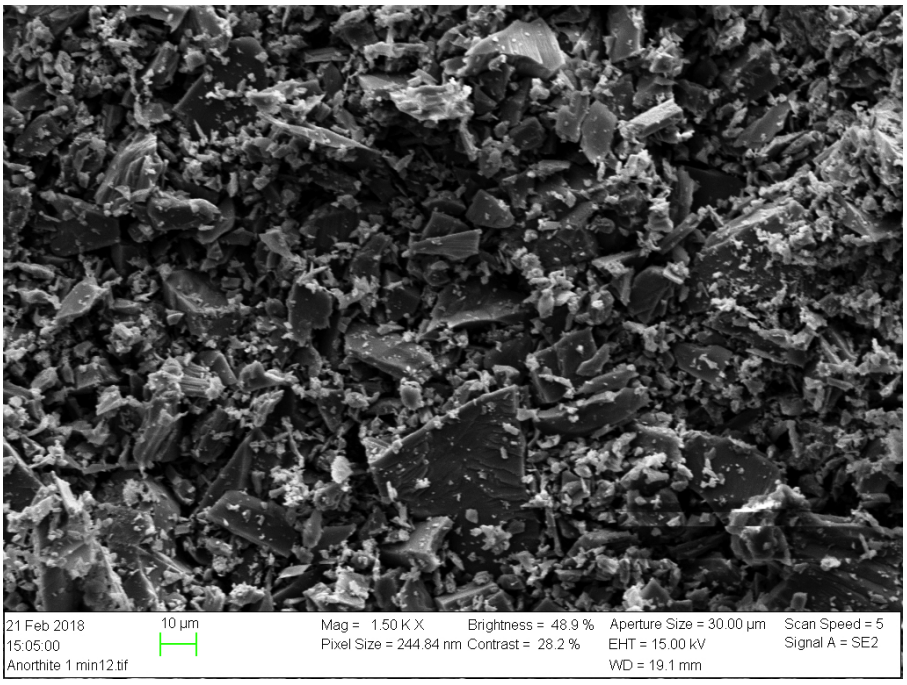

Figure A8: SEM image of anorthite milled 1 minute

A.7.3 Anorthite milled 2 minutes

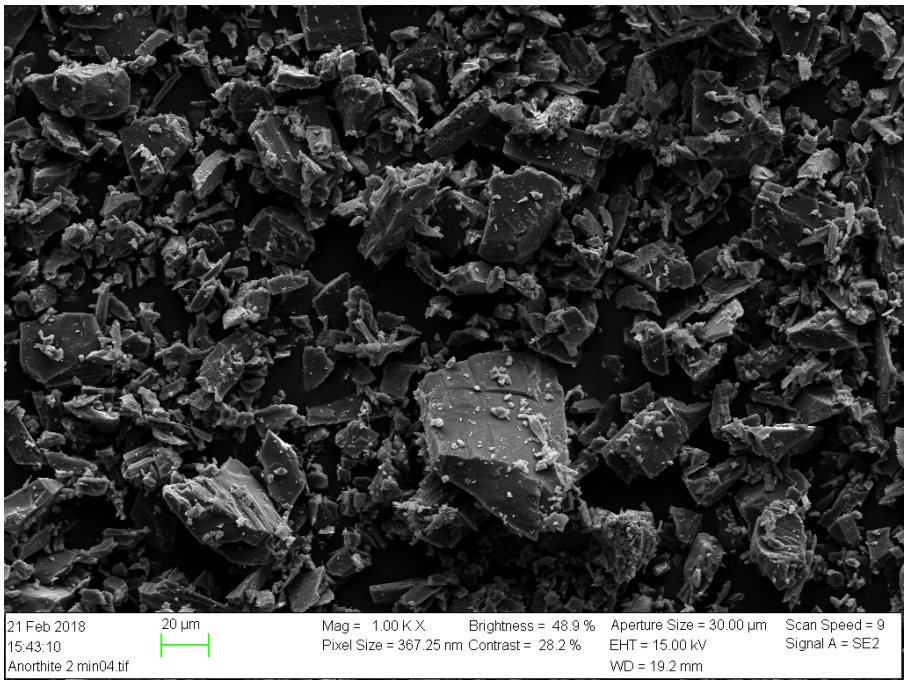

Figure A9: SEM image of anorthite milled 2 minutes

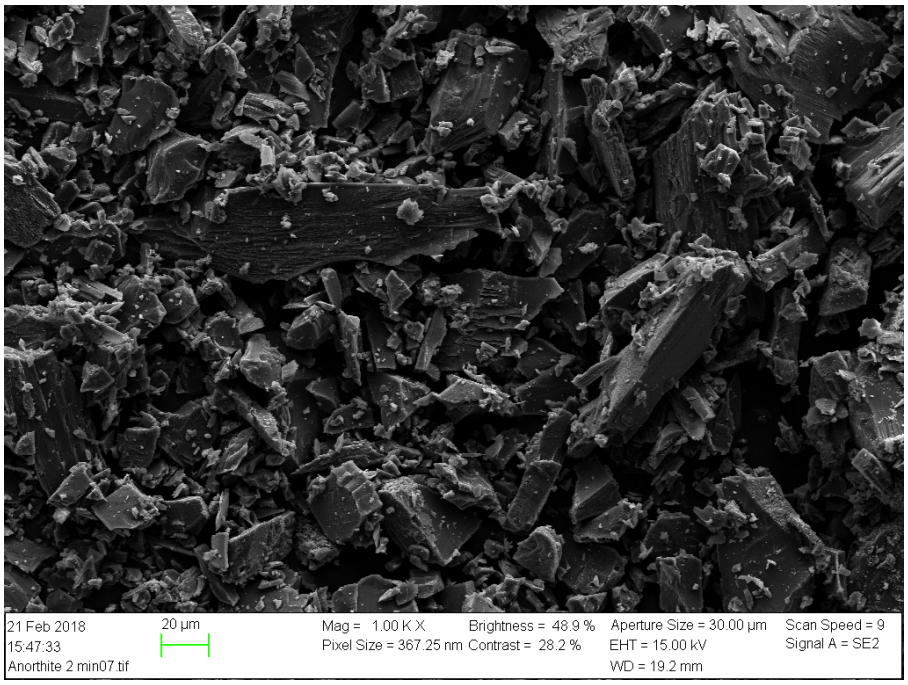

Figure A10: SEM image of anorthite milled 2 minutes

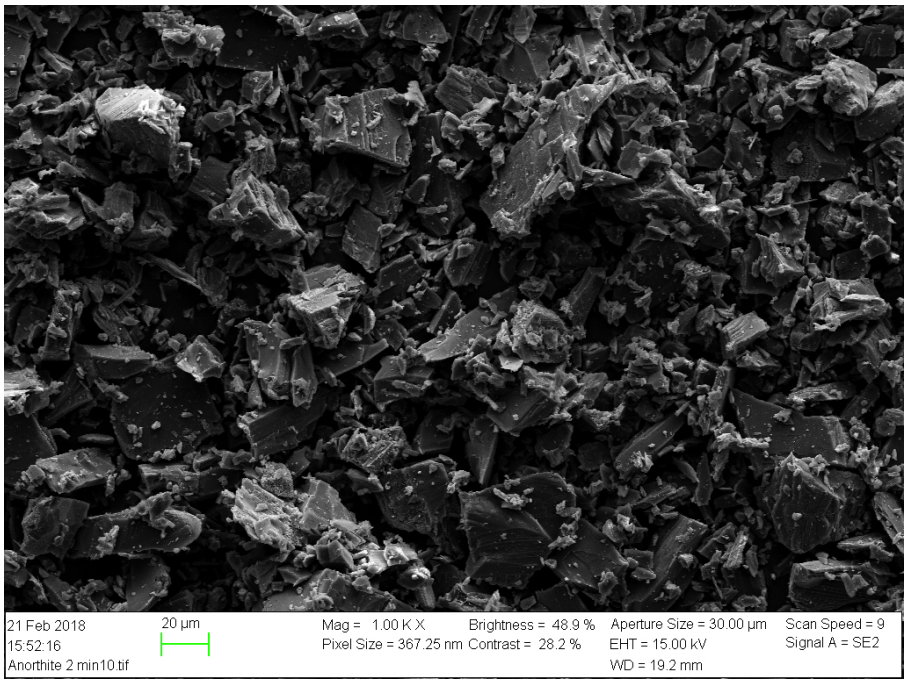

Figure A11: SEM image of anorthite milled 2 minutes

A.7.4 Anorthite milled 3 minutes

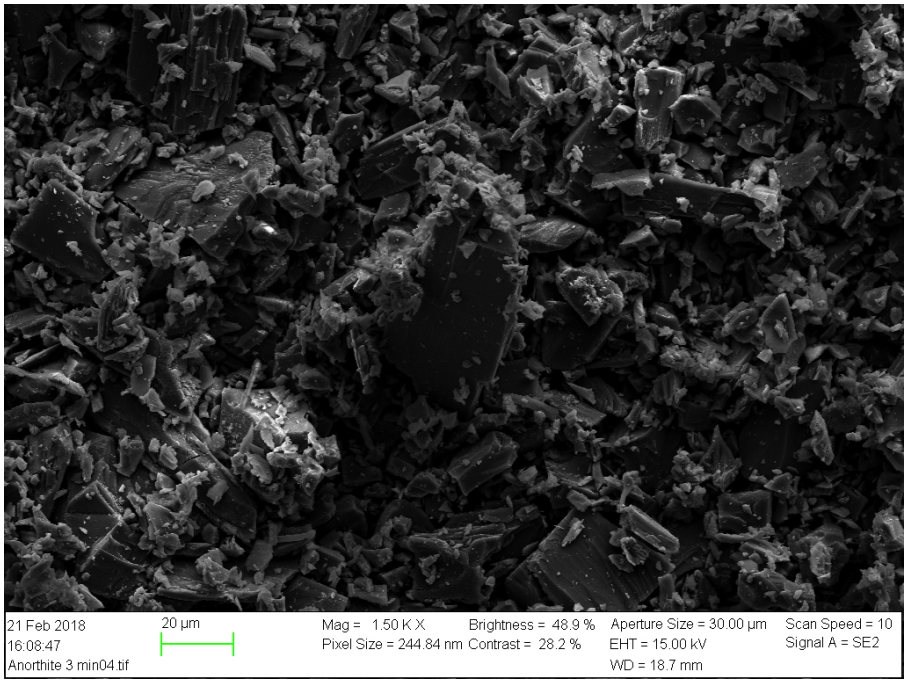

Figure A12: SEM image of anorthite milled 3 minutes

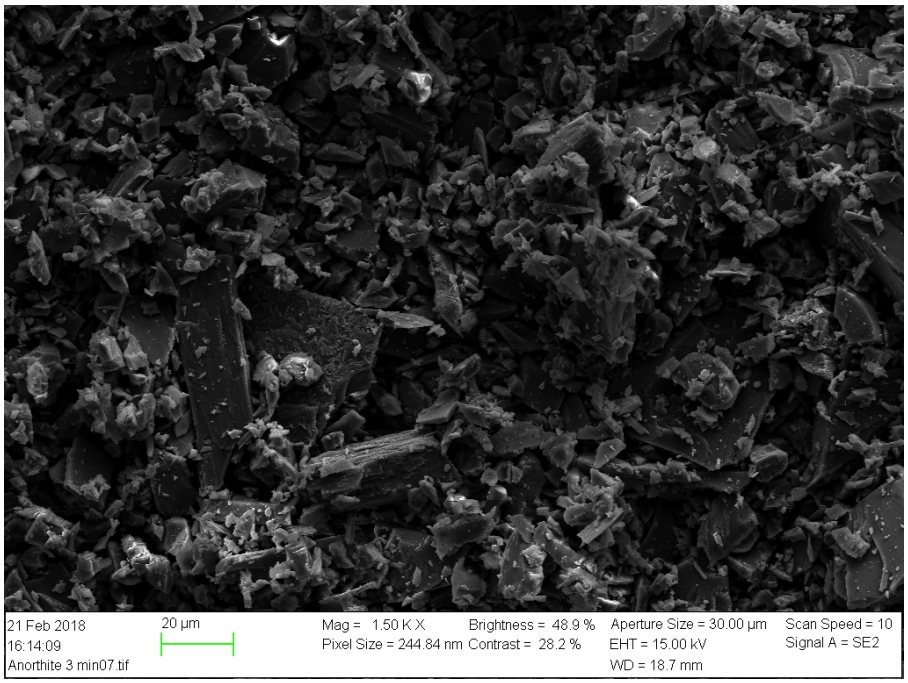

Figure A13: SEM image of anorthite milled 3 minutes

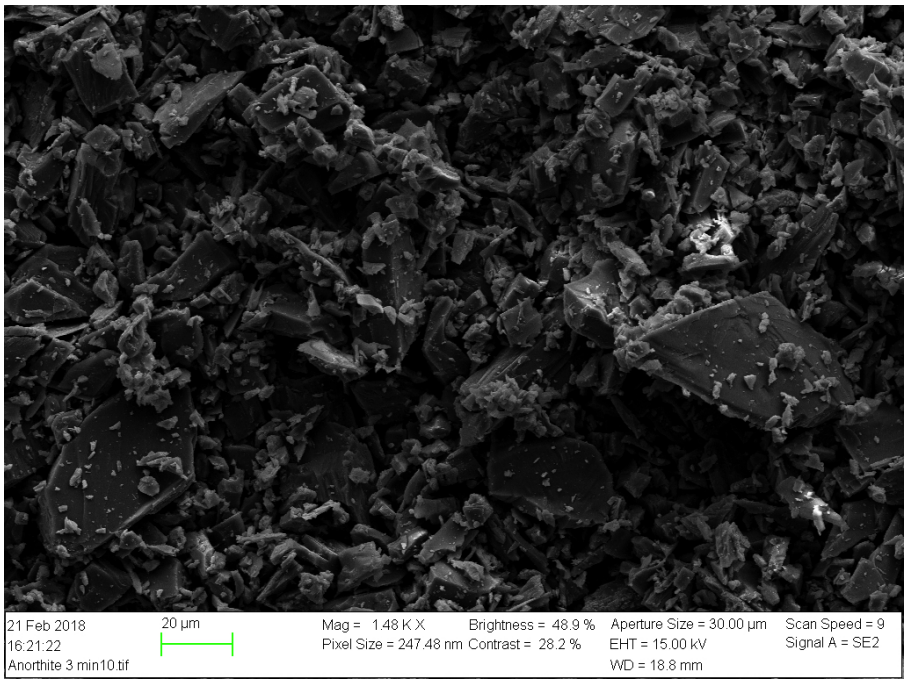

Figure A14: SEM image of anorthite milled 3 minutes

A.7.5 Anorthite milled 5 minutes

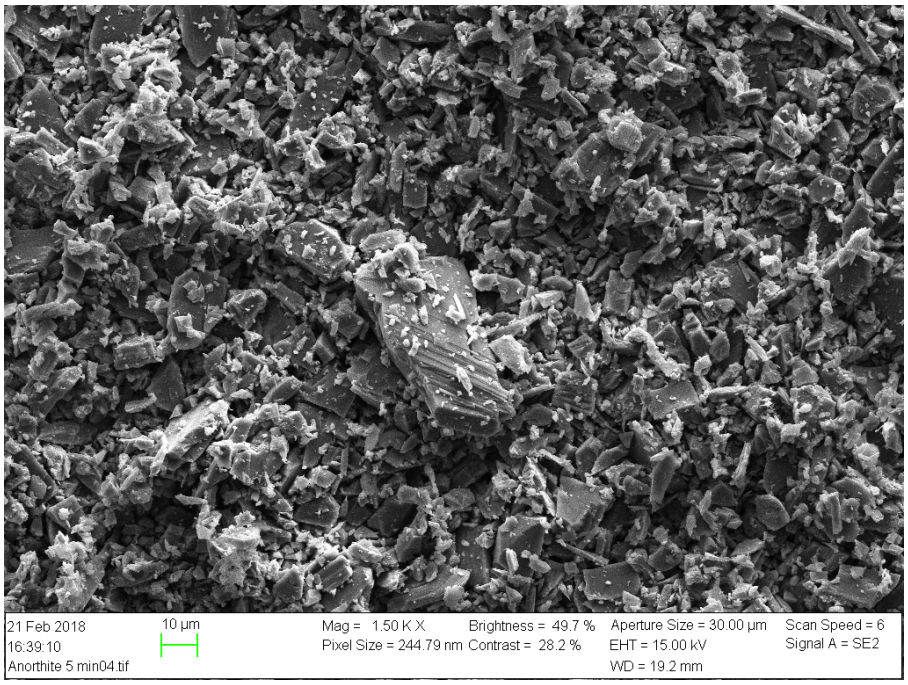

Figure A15: SEM image of anorthite milled 5 minutes

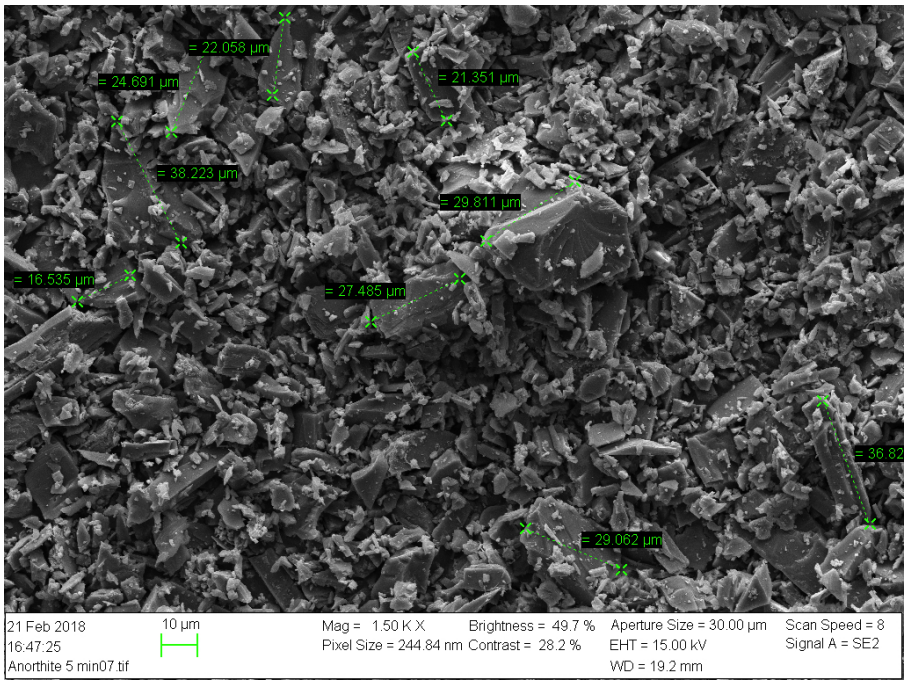

Figure A16: SEM image of anorthite milled 5 minutes

A.7.6 Anorthite milled 7 minutes

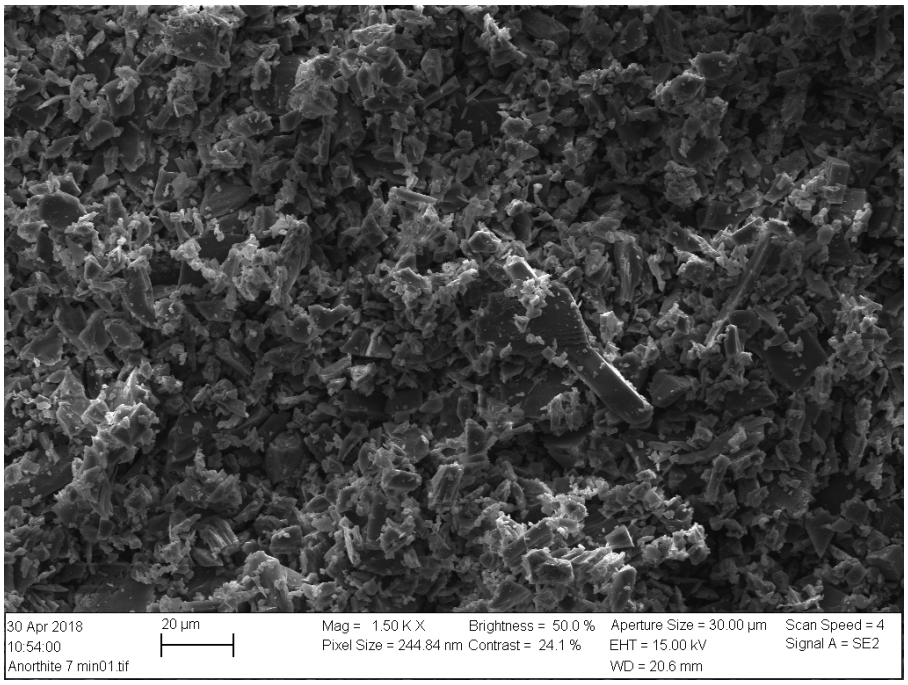

Figure A17: SEM image of anorthite milled 7 minutes

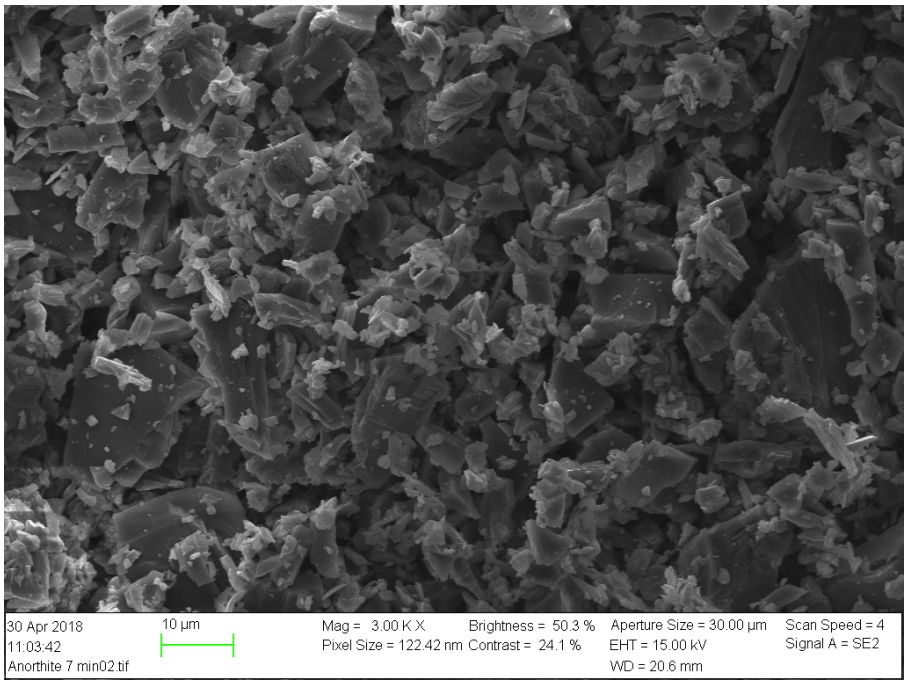

Figure A18: SEM image of anorthite milled 7 minutes

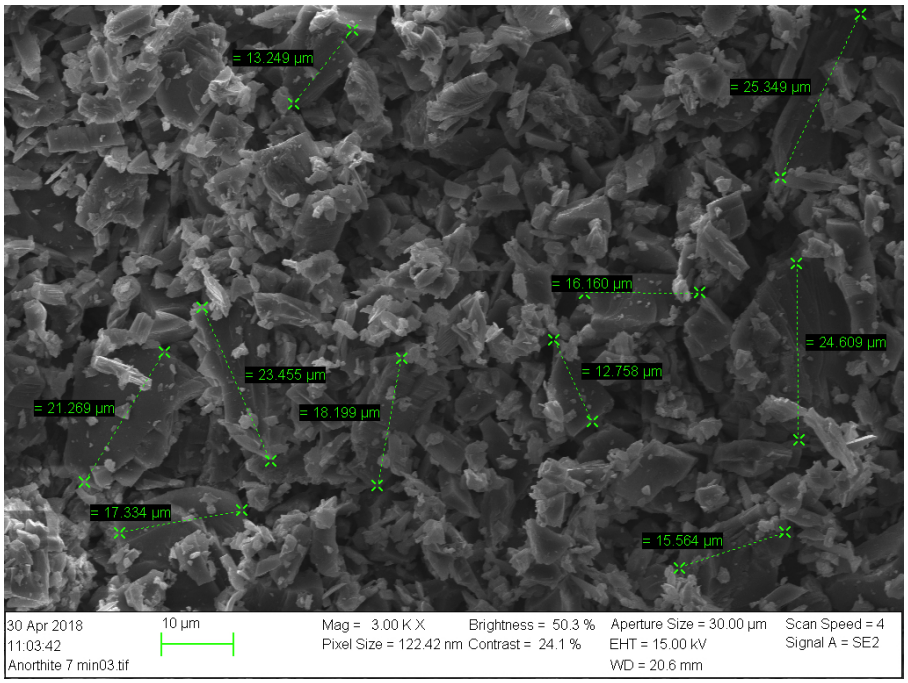

Figure A19: SEM image of anorthite milled 7 minutes

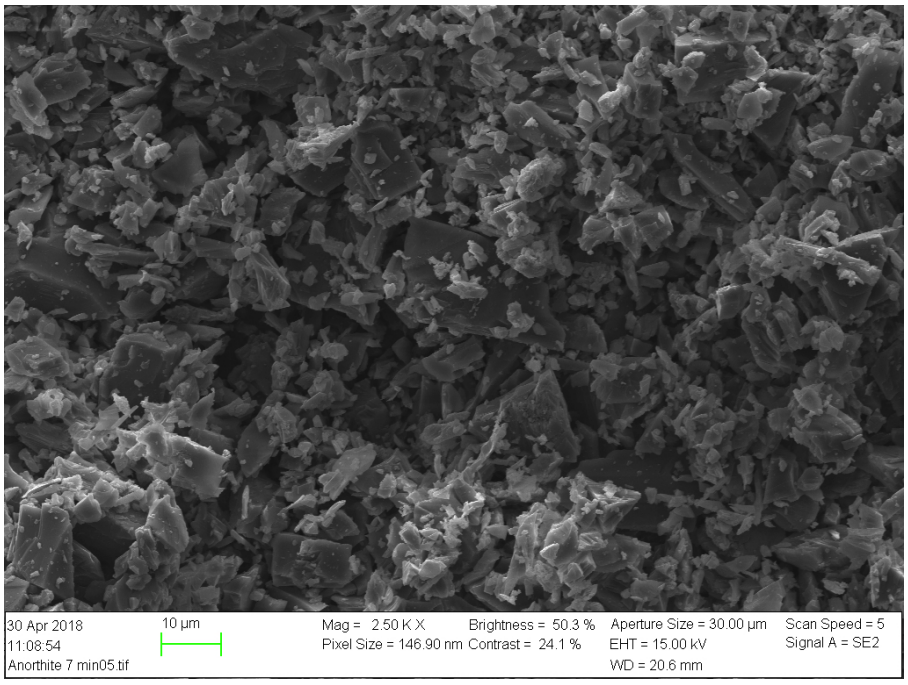

Figure A20: SEM image of anorthite milled 7 minutes

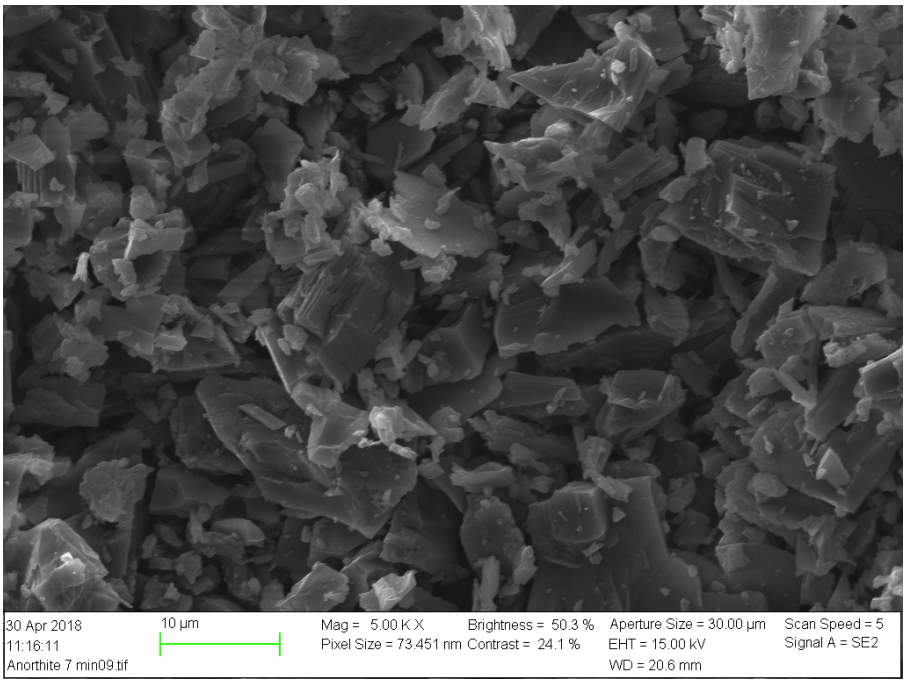

Figure A21: SEM image of anorthite milled 7 minutes

A.7.7 Anorthite milled 7 minutes and settled

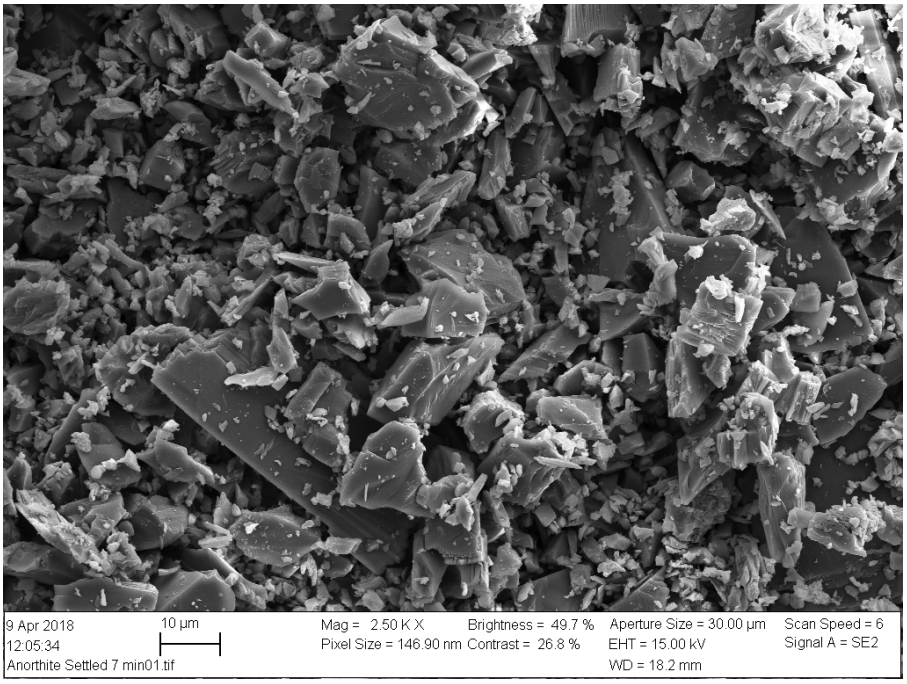

Figure A22: SEM image of anorthite milled 7 minutes and settled

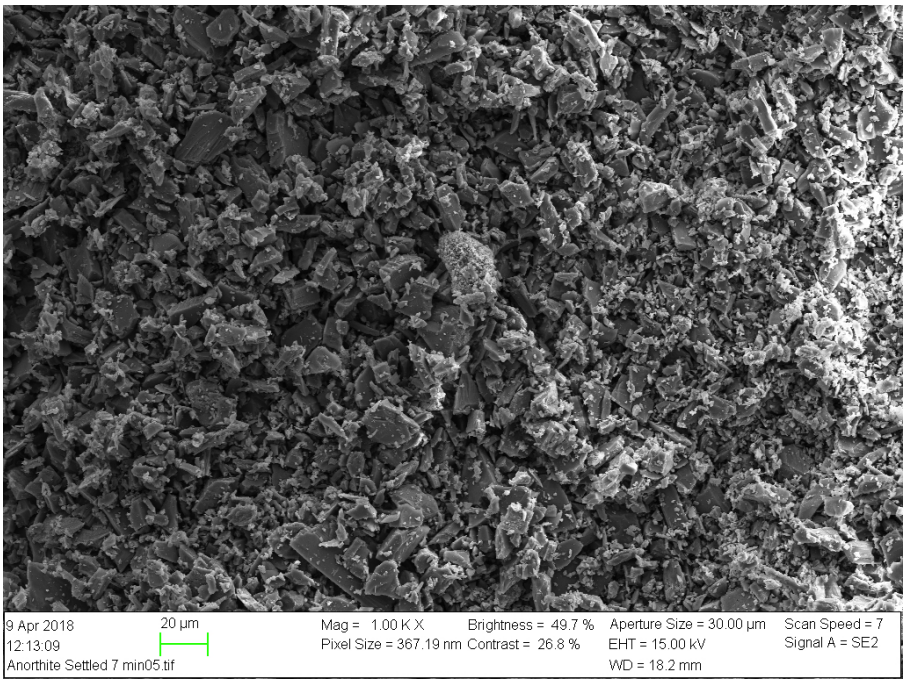

Figure A23: SEM image of anorthite milled 7 minutes and settled

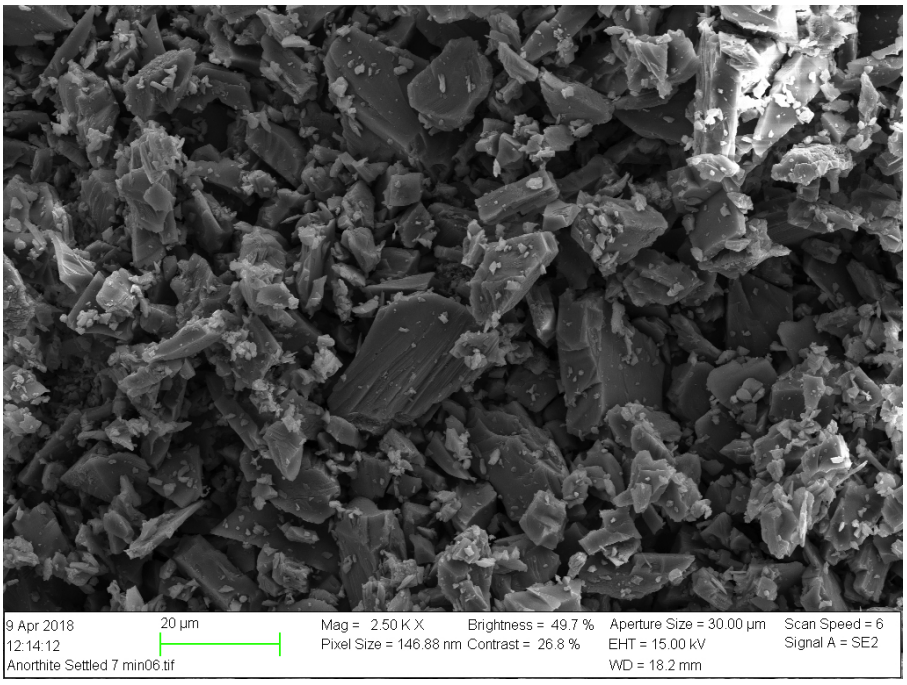

Figure A24: SEM image of anorthite milled 7 minutes and settled

A.7.8 Microcline unmilled

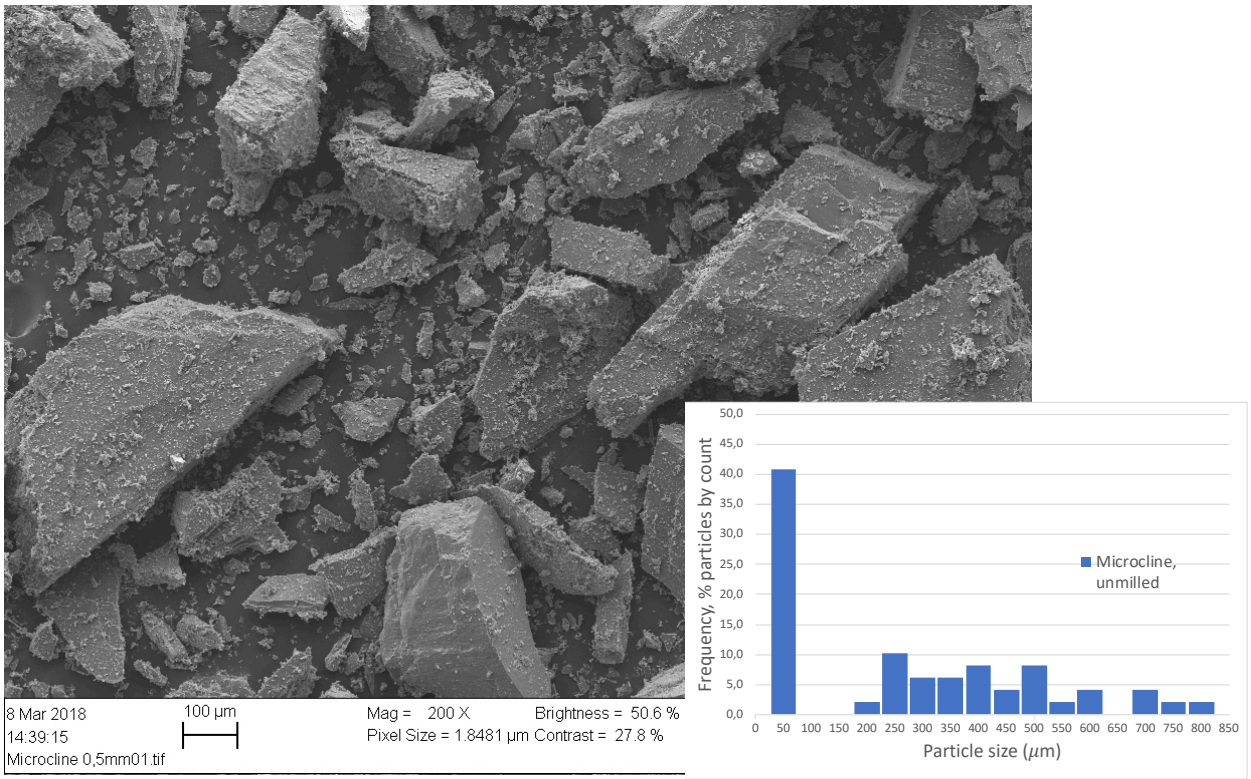

Figure A25: SEM image and PSD range of an unmilled microcline sample which has been crushed and sieved through 0.5 mm mesh using the milling preparation set.

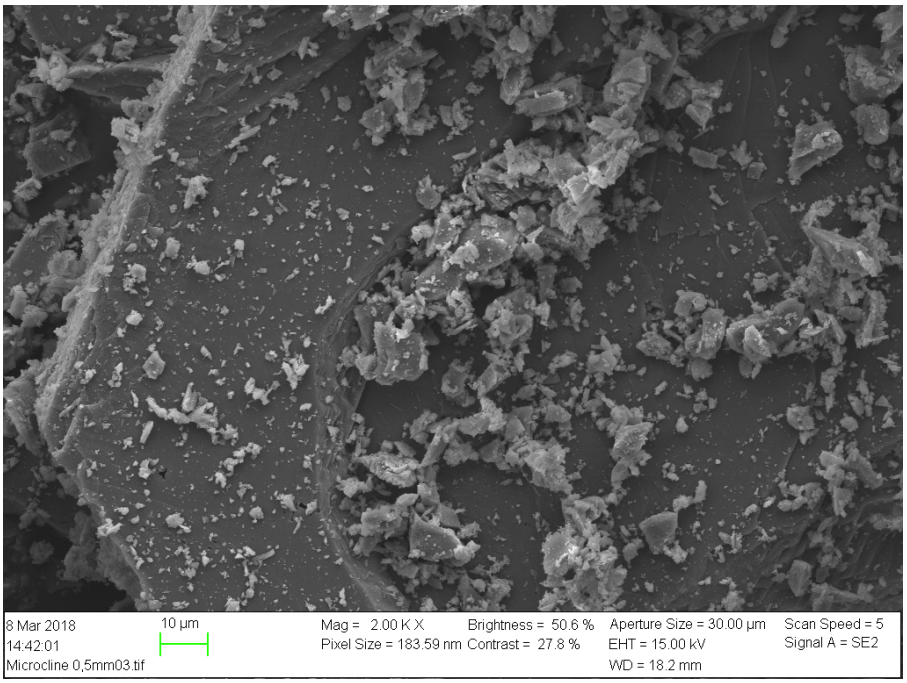

Figure A26: SEM image of microcline sieved through 0.5 mm mesh, unmilled

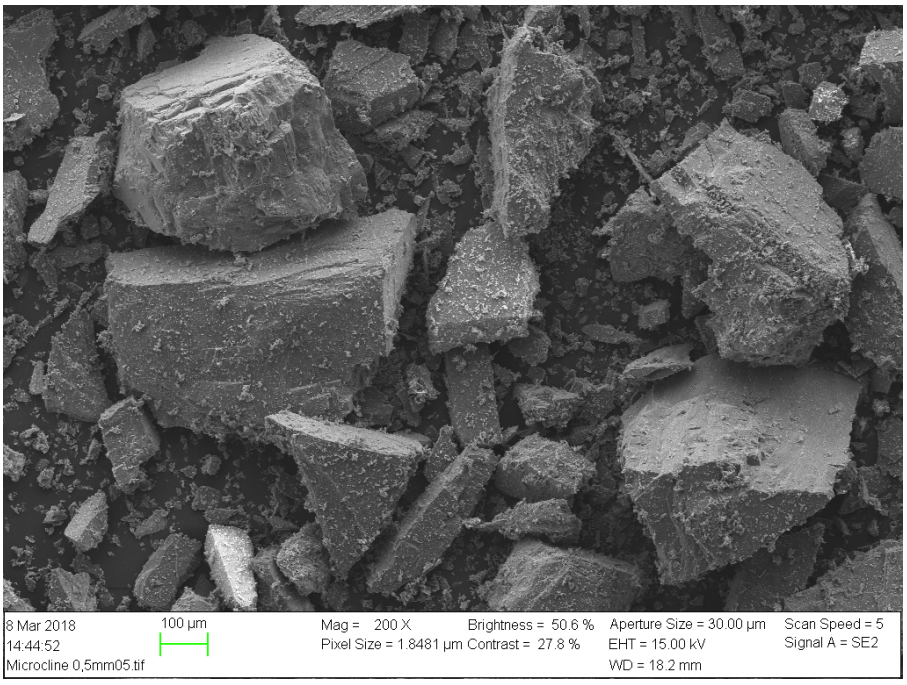

Figure A27: SEM image of microcline sieved through 0.5 mm mesh, unmilled

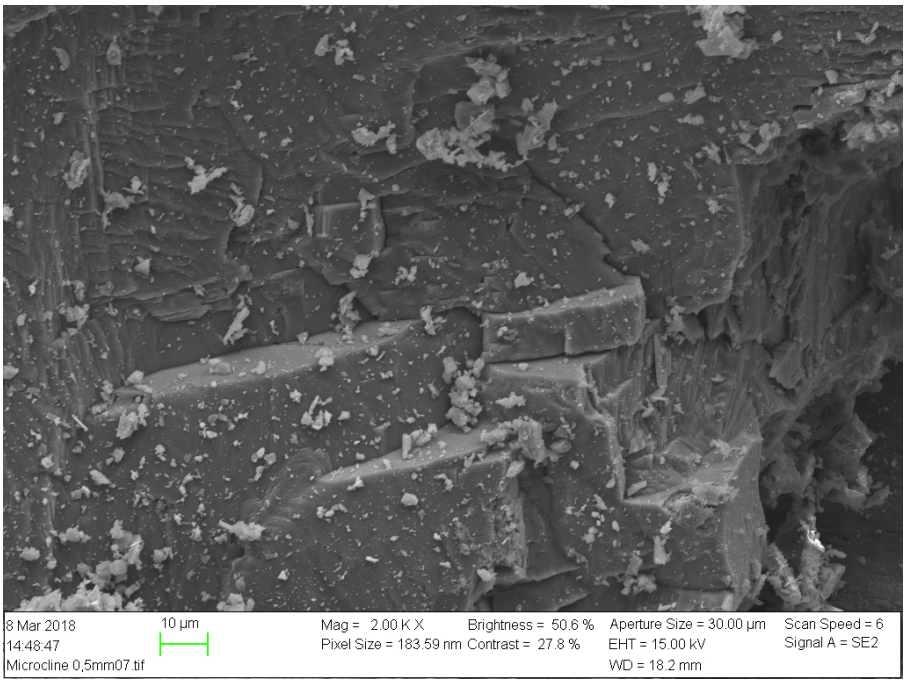

Figure A28: SEM image of microcline sieved through 0.5 mm mesh, unmilled

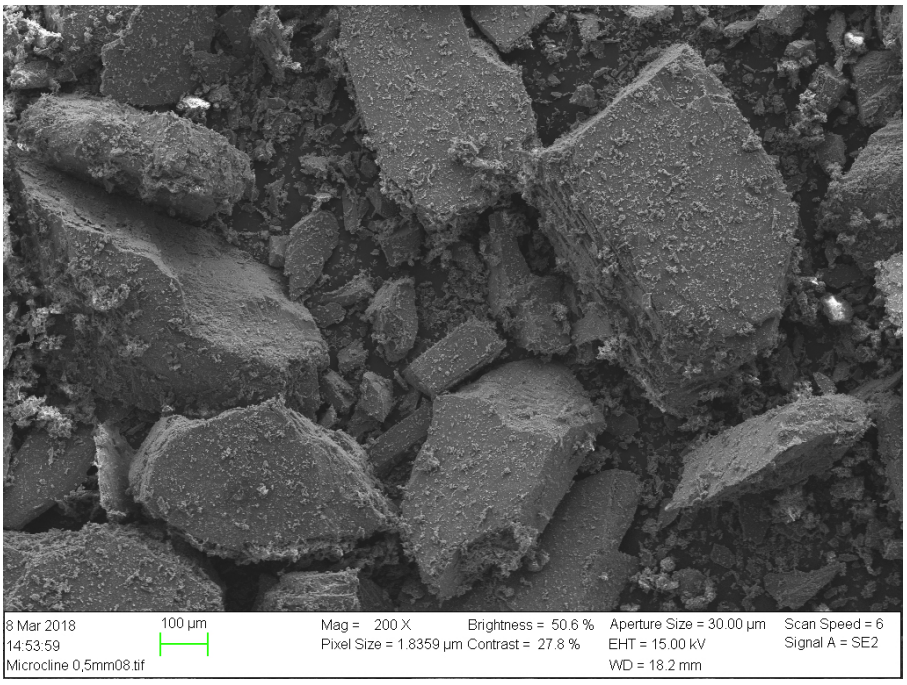

Figure A29: SEM image of microcline sieved through 0.5 mm mesh, unmilled

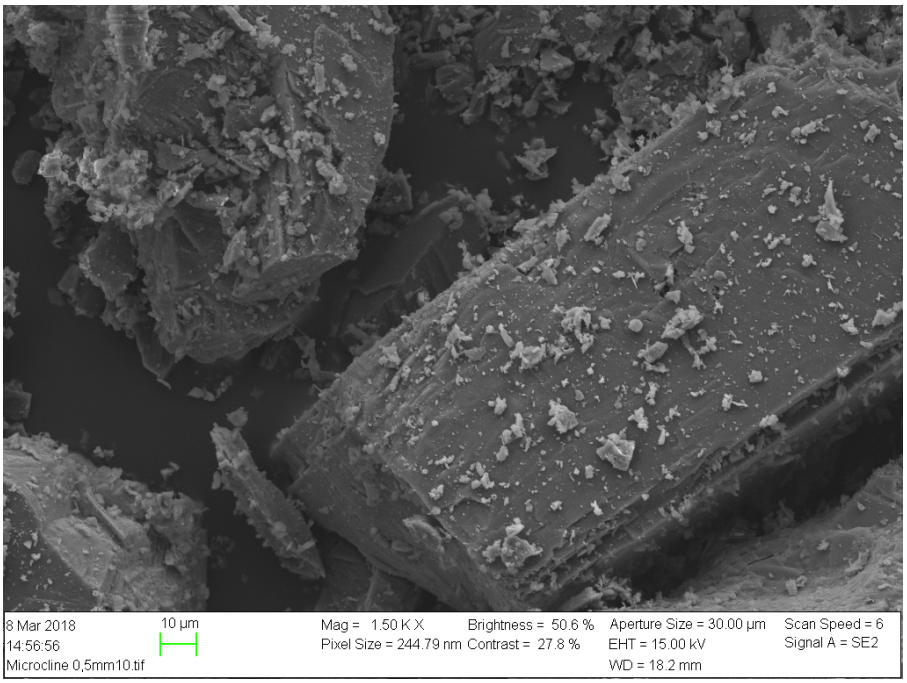

Figure A30: SEM image of microcline sieved through 0.5 mm mesh, unmilled

A.7.9 Microcline milled 1 minute

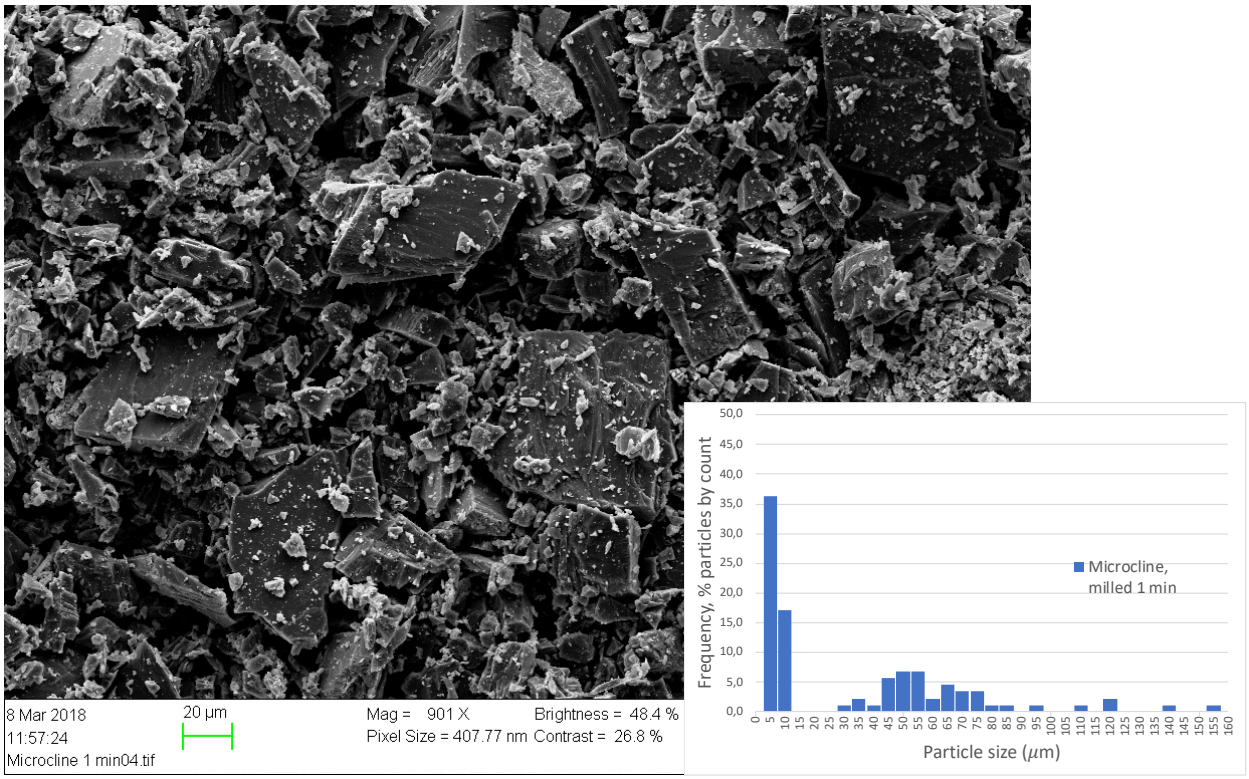

Figure A31: SEM image and PSD range of microcline sample, milled 1 minute

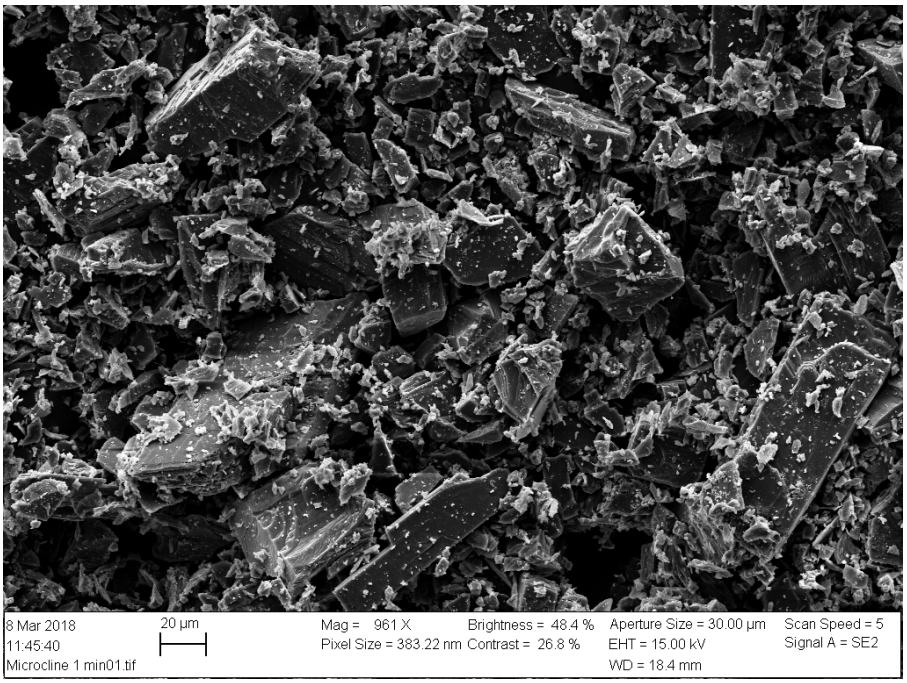

Figure A32: SEM image of microcline milled 1 minute

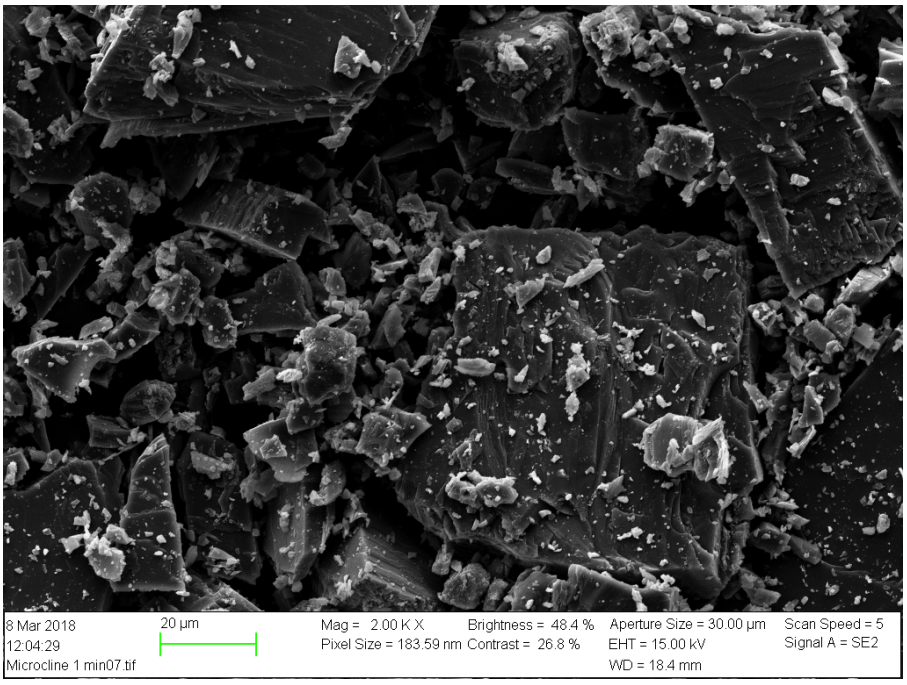

Figure A33: SEM image of microcline milled 1 minute

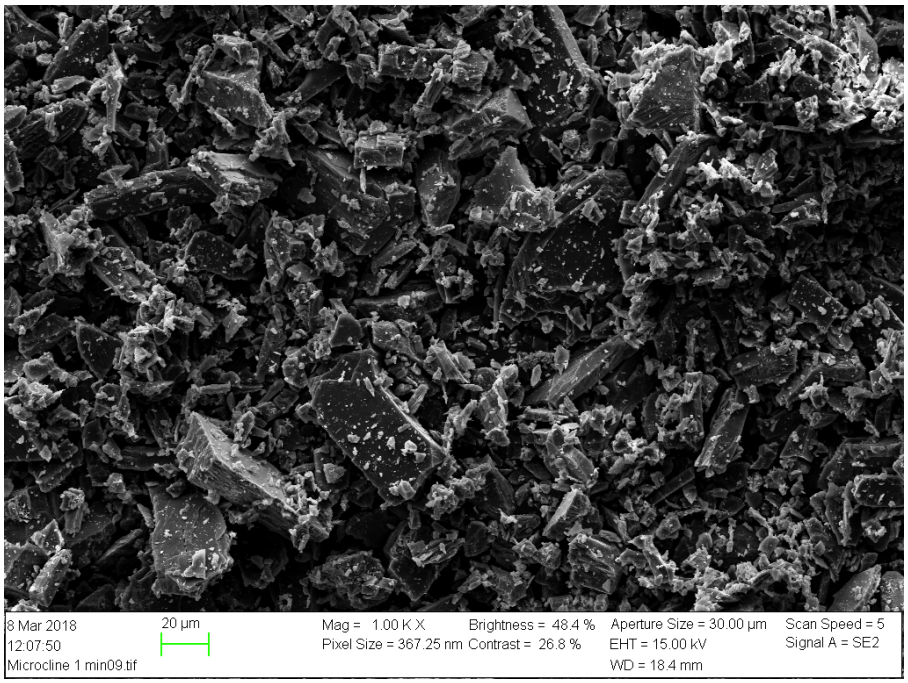

Figure A34: SEM image of microcline milled 1 minute

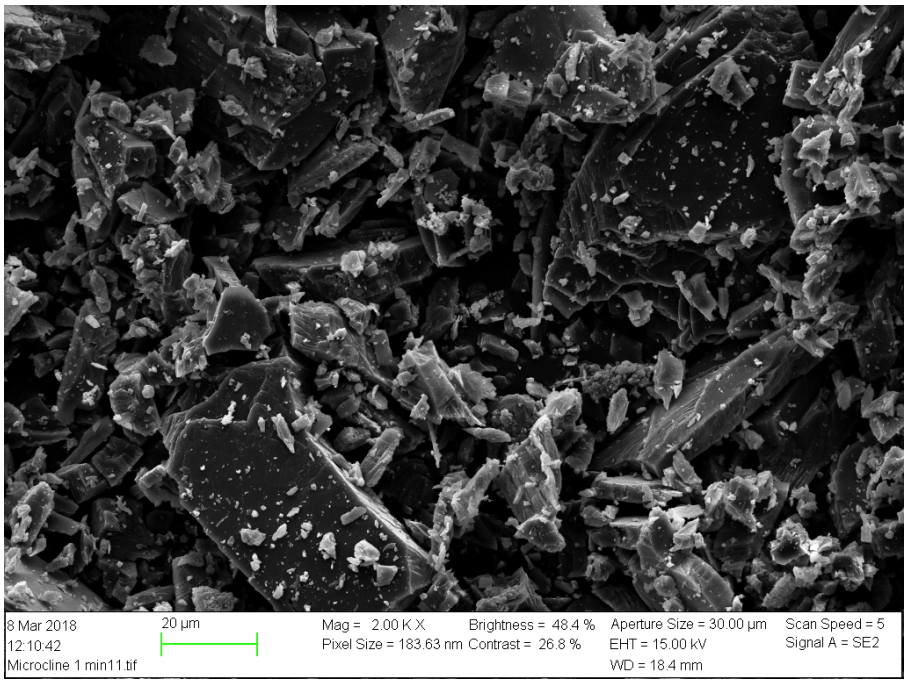

Figure A35: SEM image of microcline milled 1 minute

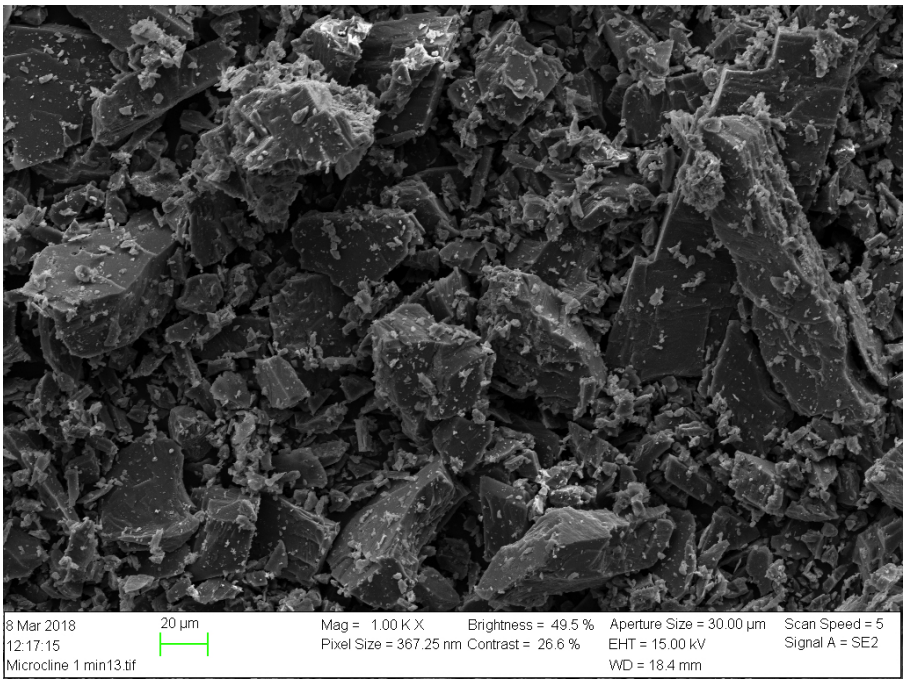

Figure A36: SEM image of microcline milled 1 minute

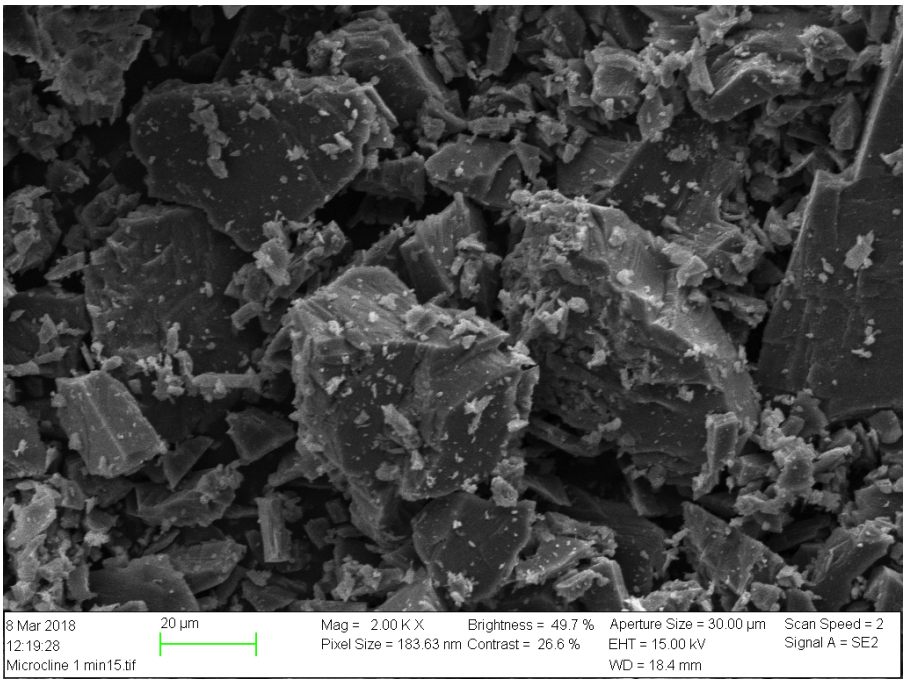

Figure A37: SEM image of microcline milled 1 minute

A.7.10 Microcline milled 2 minutes

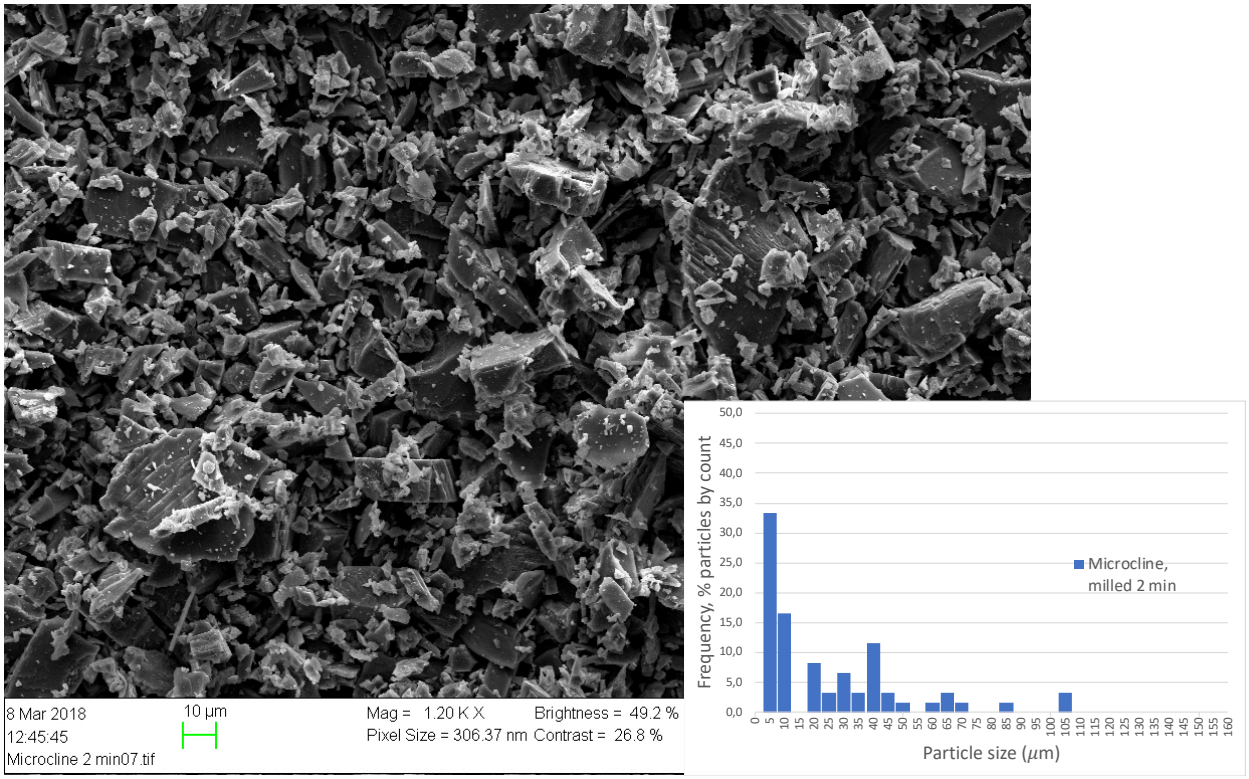

Figure A38: SEM image and PSD range of microcline milled 2 minutes

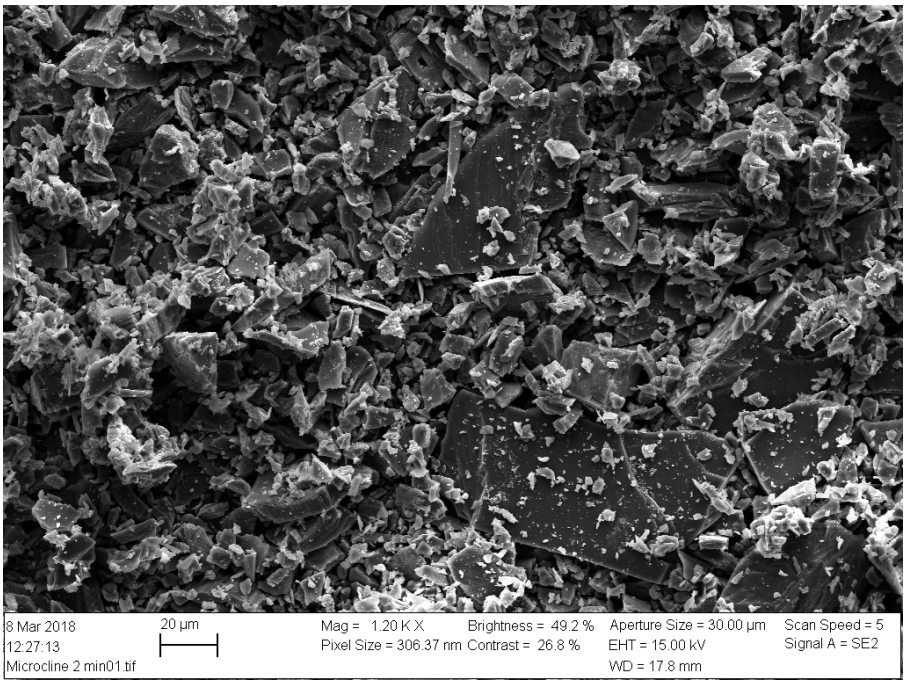

Figure A39: SEM image of microcline milled 2 minutes

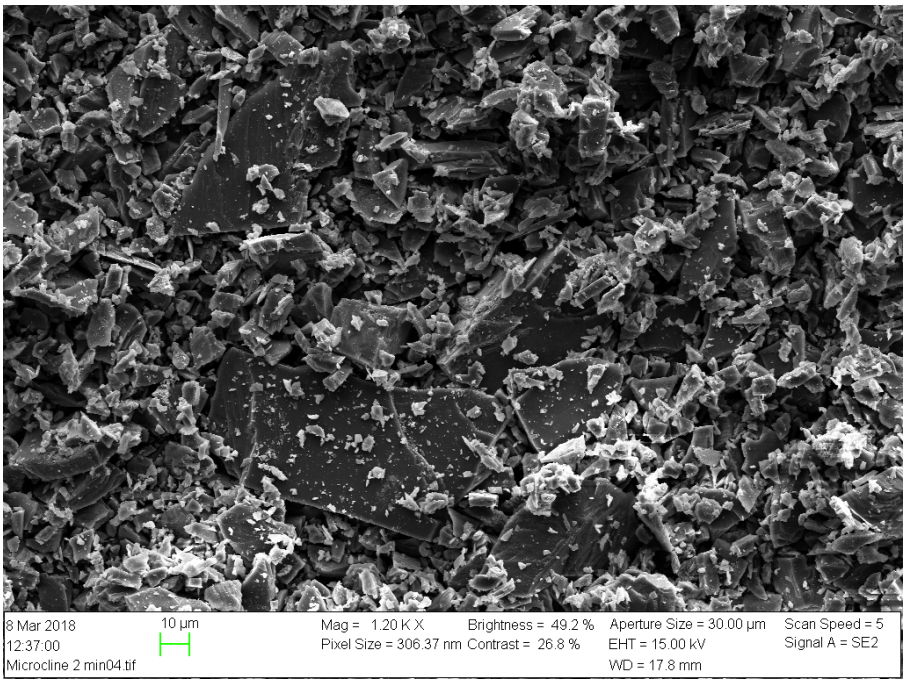

Figure A40: SEM image of microcline milled 2 minutes

A.7.11 Microcline milled 3 minutes

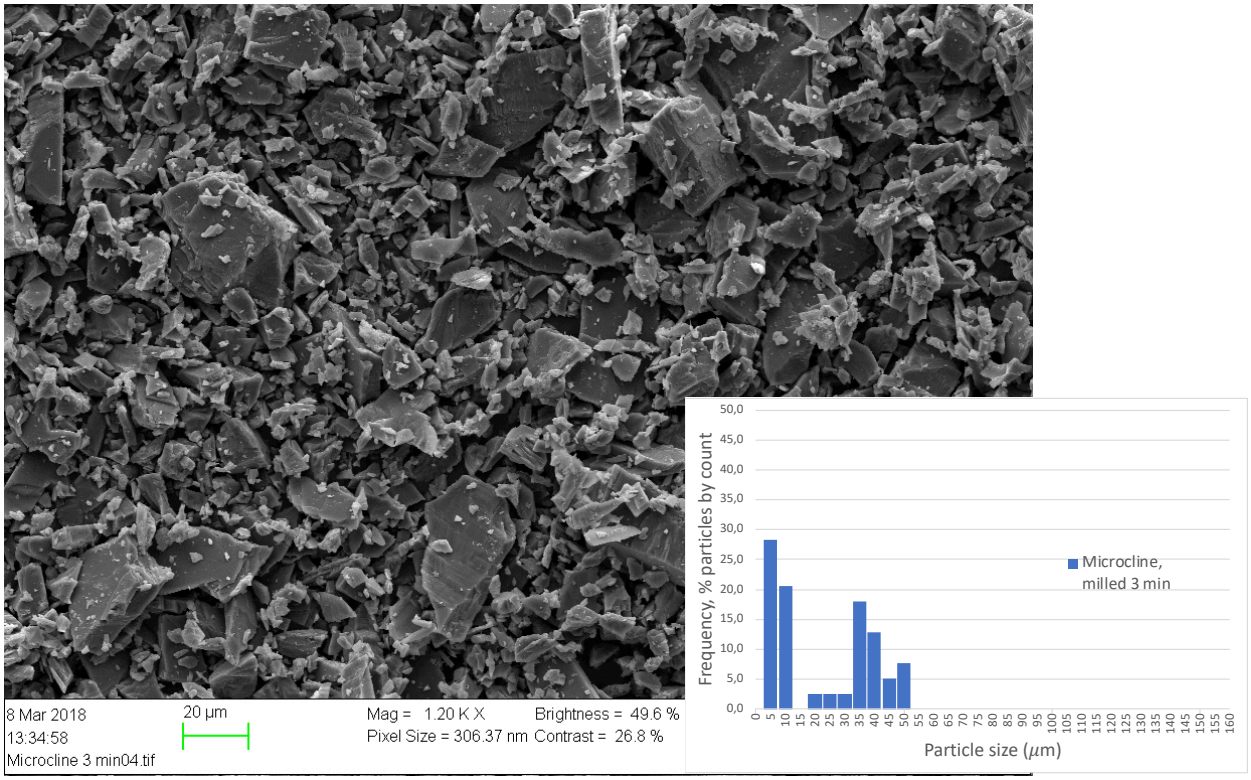

Figure A41: SEM image and PSD range of microcline sample, milled 3 minutes

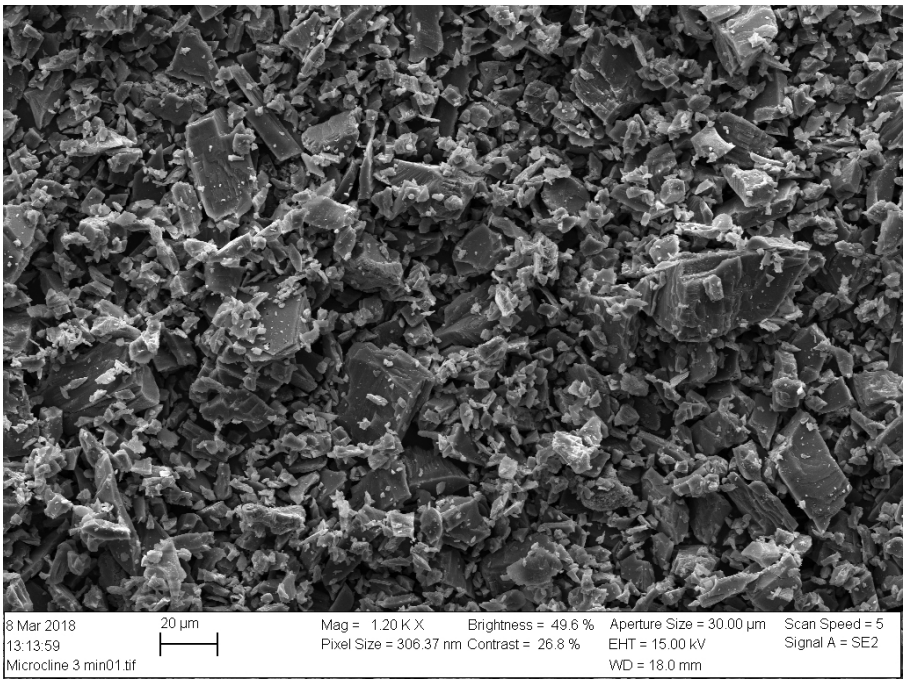

Figure A42: SEM image of microcline milled 3 minutes

A.7.12 Microcline milled 5 minutes

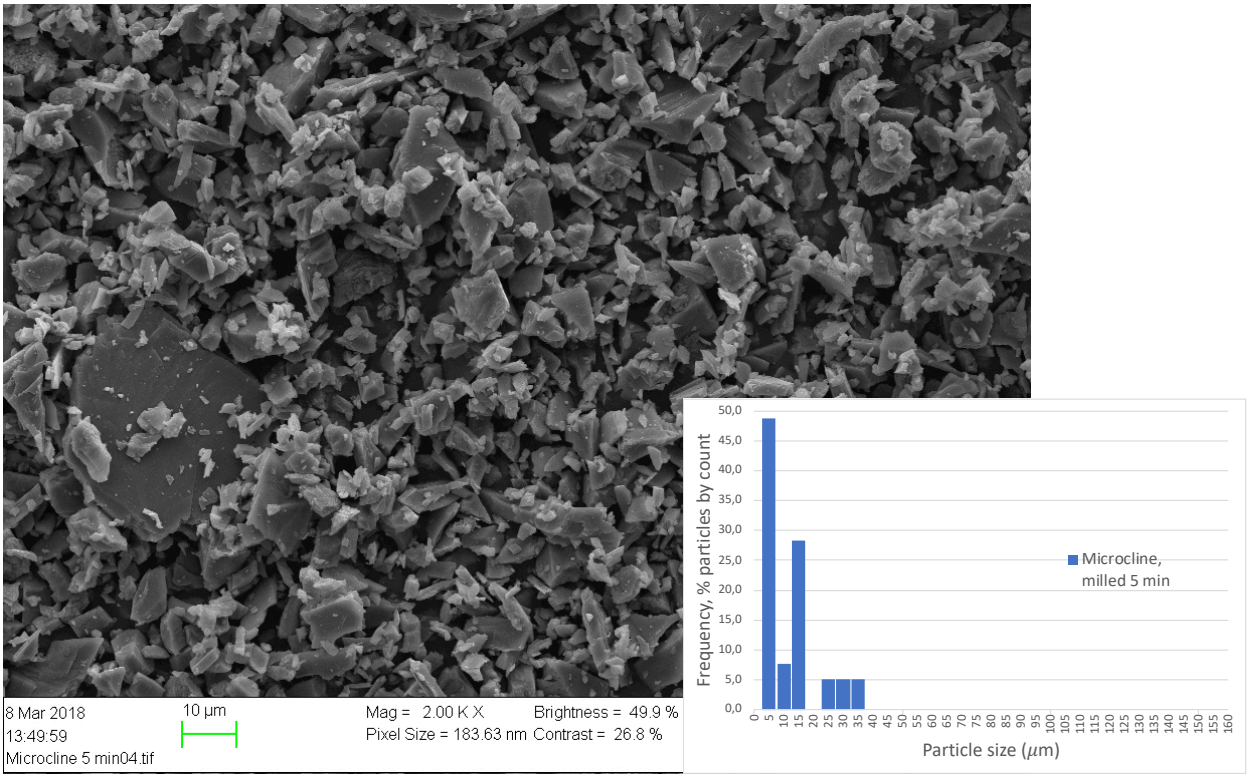

Figure A43: SEM image and PSD range of microcline sample, milled 5 minutes

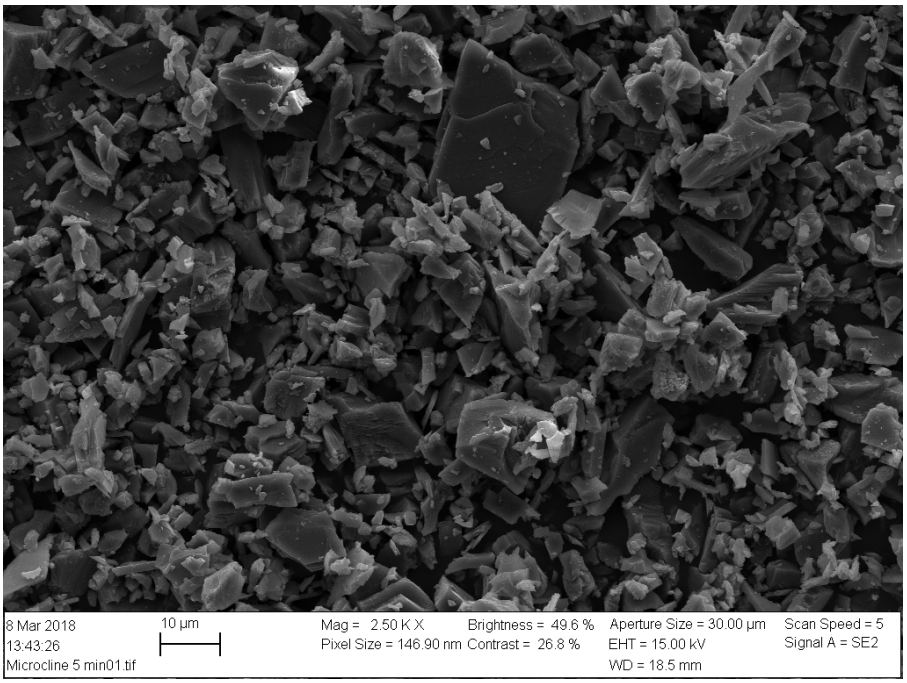

Figure A44: SEM image of microcline milled 5 minutes

A.7.13 Microcline milled 7 minutes

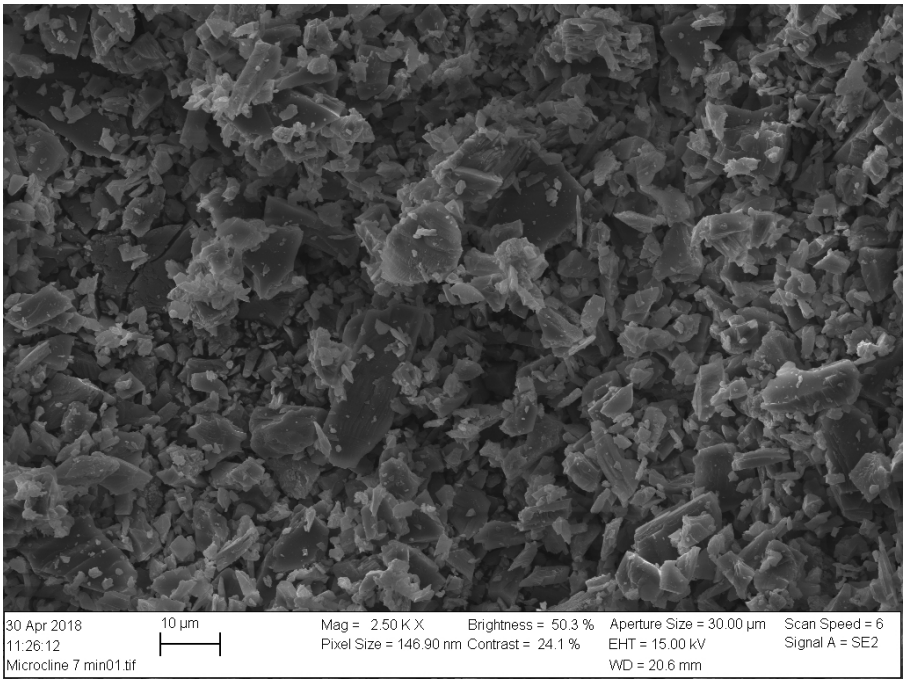

Figure A45: SEM image of microcline milled 7 minutes

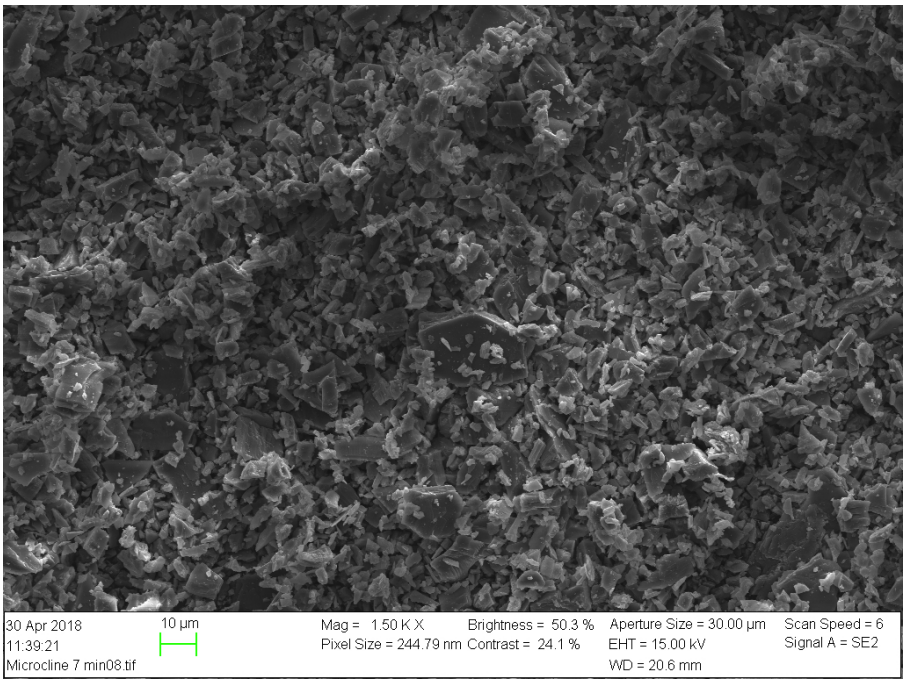

Figure A46: SEM image of microcline milled 7 minutes

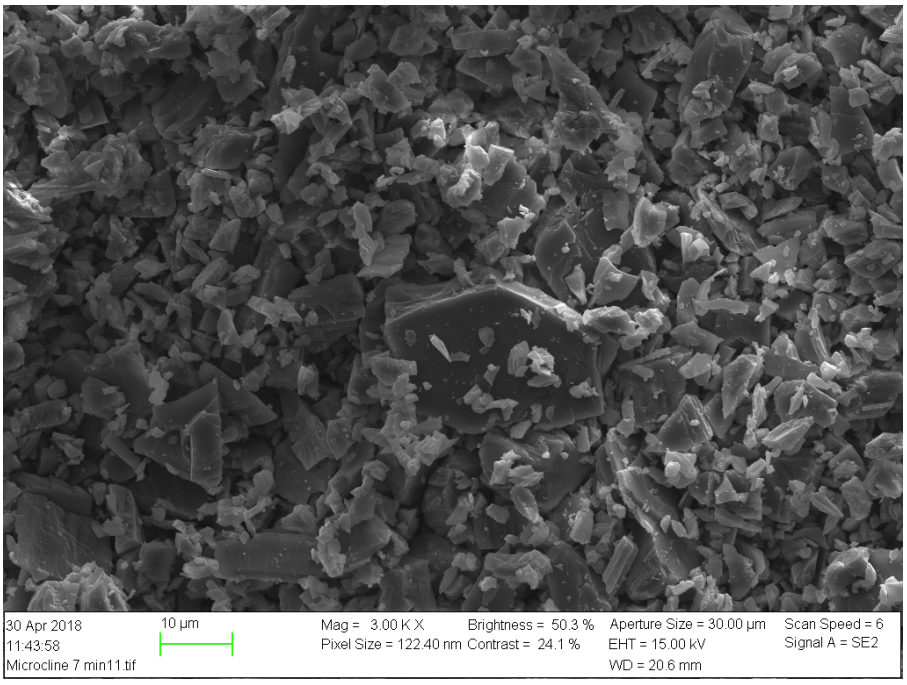

Figure A47: SEM image of microcline milled 7 minutes

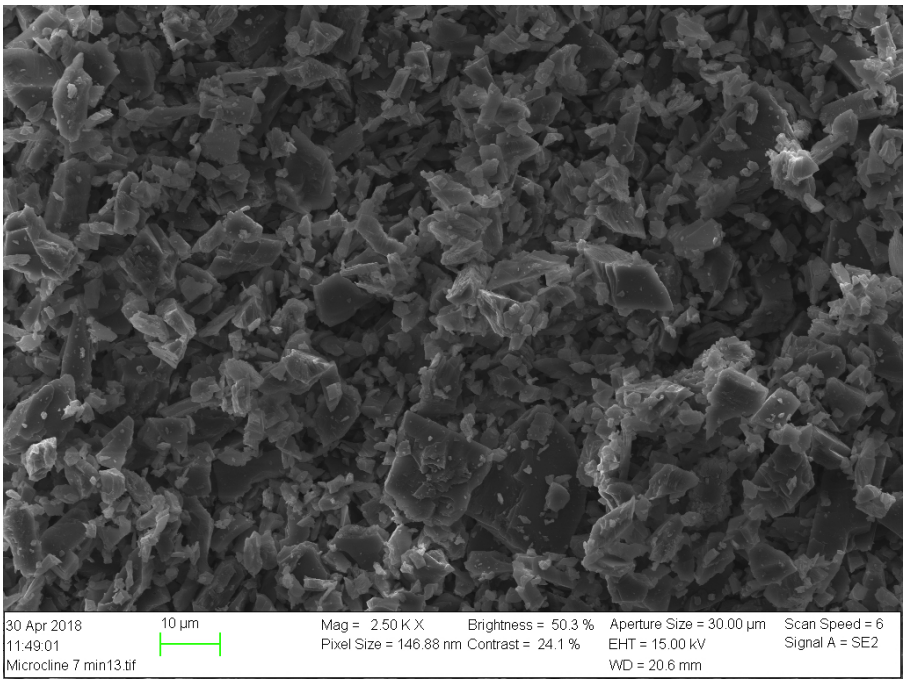

Figure A48: SEM image of microcline milled 7 minutes

A.7.14 Microcline milled 7 minutes and settled

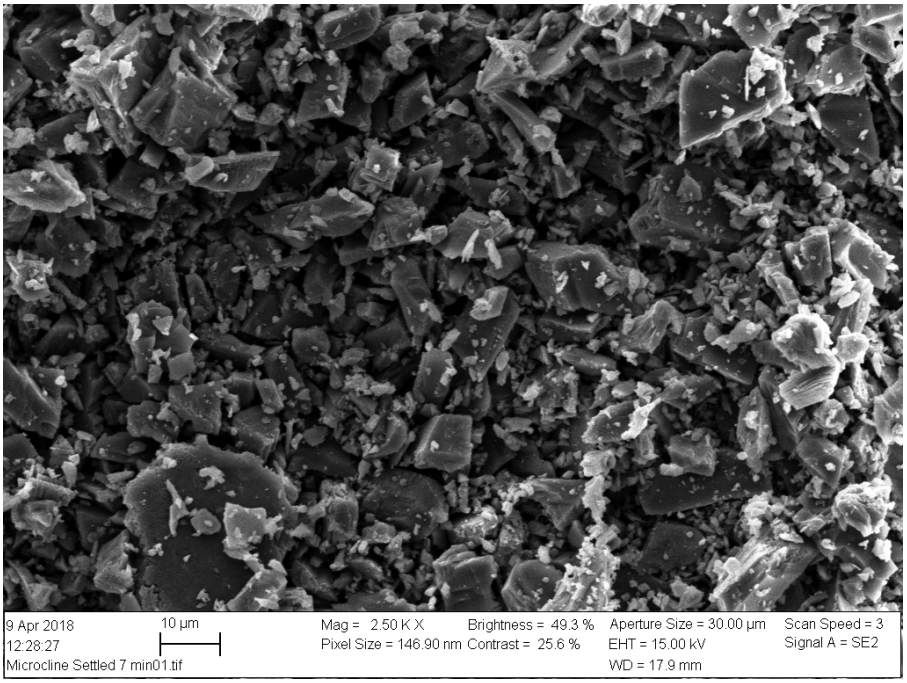

Figure A49: SEM image of microcline milled 7 minutes and settled

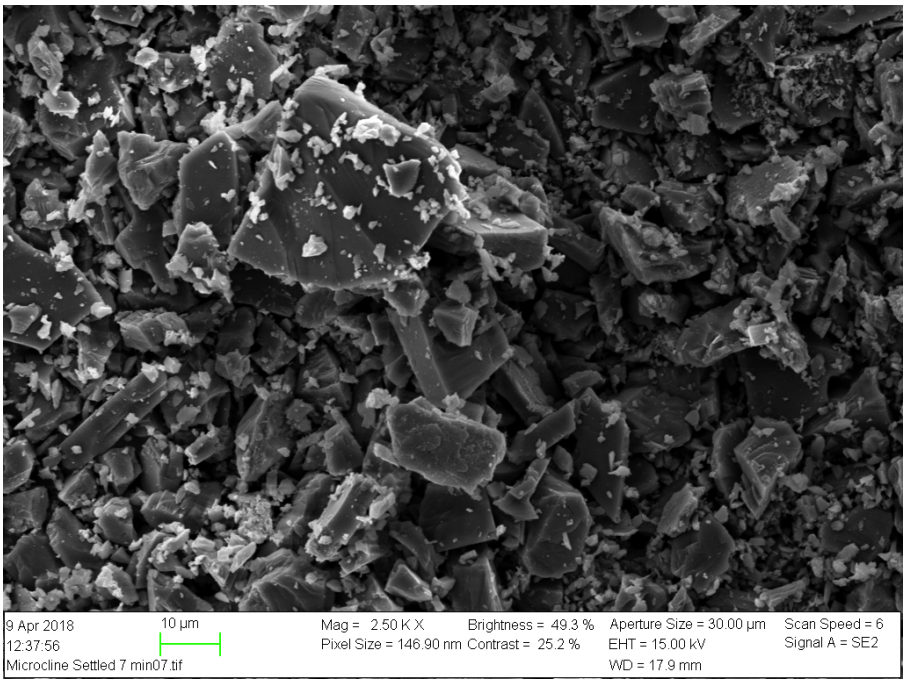

Figure A50: SEM image of microcline milled 7 minutes and settled